TECHNISCHE UNIVERSITÄT MÜNCHEN
Fachgebiet für Entwicklungsbiologie der Pflanzen

The Function of the *Arabidopsis* Receptor-Like Kinase *SRF4* in Growth Regulation

Christine Skornia

Vollständiger Abdruck der von der Fakultät Wissenschaftszentrum Weihenstephan für Ernährung, Landnutzung und Umwelt der Technischen Universität München zur Erlangung des akademischen Grades eines

Doktors der Naturwissenschaften

genehmigten Dissertation.

Vorsitzender		Univ.-Prof. Dr. C. Schwechheimer
Prüfer der Dissertation:	1.	Univ.-Prof. Dr. K. Schneitz
	2.	Priv.-Doz. Dr. E. J. Glawischnig

Die Dissertation wurde am 22.12.2011 bei der Technischen Universität München eingereicht und durch die Fakultät Wissenschaftszentrum Weihenstephan für Ernährung, Landnutzung und Umwelt am 09.02.2012 angenommen.

Für meine Eltern

Contents

List of Abbreviations

Abbreviation	Description
cDNA	Complementary DNA
CLSM	Confocal Laser Scanning Microscopy
DLG	Däumling
ΔDLG	Sequence part of DLG used for Y2H screen
EGFP	Enhanced Green Fluroescent Protein
ePK	Eukaryotic Protein Kinase
GST	Glutathione-S-Transferase
GUS	β-glucuronidase
HRP	Horse Radish Peroxidase
IPTG	Isopropyl-β-D-Thiogalactopyranosid
KD	Kinase Domain
LB	T-DNA Left Border
LRR	Leucine-Rich Repeat
MBP	Myelin Basic Protein
PCR	Polymerase Chain Reaction
PEST	Peptide sequence rich in proline (P), glutamic acid (E), serine (S) and threonin (T)
qRT-PCR	quantitative Real Time-PCR
RB	T-DNA Right Border
RLK	Receptor-Like Kinase
RTK	Receptor Tyrosine Kinase
RT	Room Temperature
RT-PCR	Reverse Transcriptase-PCR
SDS-PAGE	Sodium Dodecyl Sulfate Polyacrylamide Gel Electrophoresis
Ser/Thr	Serine/Threonine

Abbreviation	Description
SRF	Strubbelig Receptor Family
$SRF4_{i}$	Intracellular sequence part of SRF4
$SRF4_{KD}$	Kinase dead mutated version of SRF4
SUB	STRUBBELIG
TAE	Tris-acetate EDTA buffer
T-DNA	Transferred DNA
TM	Transmembrane Domain
WIZ	Winzling
ΔWIZ	Sequence part of WIZ used for Y2H screen
WIZL	Winzling Like
Y2H	Yeast Two-Hybrid

Summary

The regulation of plant size is a field of high interest with enormous relevance for agriculture. To allow proper organ growth, cells have to communicate. Molecular components involved in cell-cell communication are promising targets for the investigation of the regulation of organ size. Receptor-Like Kinases (RLK) connect the intra- and the extracellular matrix thereby mediating cell-cell communication. The Leucine-Rich Repeat (LRR) RLK SRF4 was shown to be a positive regulator of leaf size. SRF4 belongs to the Strubbelig Receptor Family (SRF), which comprises of nine members. All members carry a kinase domain. However, the well-established protein STRUBBELIG (SUB, SRF9) could be shown to be an atypical kinase.

The aim of this thesis was to further investigate the influence of *SRF4* on organ size control, its molecular characterization and to identify potential downstream components of the SRF4 signaling mechanism.

On this account two potential downstream targets of SRF4, previously identified in a Y2H screen, were investigated. One is the cytosolic hydroxy-pyruvate reductase DÄUMLING (DLG) or HPR2. The other one is WINZLING (WIZ), a WD40 domain containing protein of unknown function. Phenotypic characterization was performed. In addition transcript an protein expression patterns were investigated with the help of transgenic plants carrying GUS and EGFP-based reporter constructs. Interaction studies *in vitro*, in yeast and *in planta* were also carried out. For the RLK SRF4 an *in vitro* kinase assay was done. All three genes were analysed in the context of evolution in *Viridiplantae*.

SRF4 did not show any kinase activity *in vitro*. The phenotypic characterization of the loss-of-function mutant *srf4-8* and gain-of-function transgenic *UBQ::SRF4* lines verified the function of *SRF4* as a positive growth regulator. A similar role is suggested for *DLG*, as *dlg-6* shows smaller and *UBQ::DLG* bigger

plants. SRF4 and DLG interaction could be confirmed *in vitro*. Thus the data supports the view that SRF4 mediates its effect on organ size through DLG. The translational fusion of SRF4 with EGFP could be detected at the plasma membrane whereas DLG:EGFP could be located in the cytosol. The reporter GUS analysis suggests a broad expression pattern for SRF4, including leaves, pollen and roots. For DLG also a strong expression throughout the whole plant body could be observed. SRF4 does not appear to act exclusively through DLG as *dlg-6* plants, transformed with *UBQ::SRF4*, showed wildtype phenotype.

The loss-of-function mutant *wiz-1* shows small, bleached plants, while its overexpression *wiz-2* exhibits smaller, semi-sterile plants with roundish, dark green leaves. The interaction with SRF4 in yeast could be reproduced. The reporter GUS expression demonstrated a strong staining in all plant organs. Double mutant analysis between *srf4-8*, *dlg-6*, *wiz-1* and *wiz-2* revealed a complex connection between the three genes *SRF4*, *DLG* and *WIZ*.

Taken together, the results presented in this thesis are compatible with the notion that SRF4 and DLG are positive regulators of leaf size. In addition SRF4 may control this process in part through the direct interaction with DLG.

Zusammenfassung

Die Regulierung der Pflanzengröße ist ein höchst interessantes Feld das enorme Bedeutung für die Agrarwirtschaft hat. Für ein korrektes Wachstum der Pflanzenorgane müssen Zellen miteinander kommunizieren. Molekulare Bauteile, die an der Zell-Zell Kommunikation beteiligt sind, sind vielversprechende Ziele bei der Erforschung der Regulation der Organgröße von Pflanzen. Rezeptor Kinasen verbinden die intra- und extrazelluläre Matrix und vermitteln so Zell-Zell Kommunikation. Die leucin-reiche Rezeptor Kinase SRF4 ist ein positiver Regulator der Blattgröße. SRF4 gehört der Strubbelig Rezeptor Familie (SRF) an, die aus neun Mitgliedern besteht. Alle Mitglieder besitzen eine Kinase Domäne. Für das bekannte Protein STRUBBELIG (SUB, SRF9) konnte jedoch gezeigt werden, dass es sich dabei um eine atypische Kinase handelt.

Das Ziel dieser Arbeit war die genauere Erforschung der Auswirkungen von *SRF4* auf die Organgröße, seine molekulare Charakterisierung sowie die Identifizierung möglicher nachgelagerter Interaktionspartner des SRF4 Signal Mechanismus.

Aus diesem Grund wurden zwei potentielle nachgelagerte Zielobjekte von *SRF4*, die in einem vorangegangenen Y2H Screen identifiziert wurden, untersucht. Eines ist die zytosolische Hydroxy-Pyruvat Reduktase DÄUMLING (DLG) oder HPR2. Bei dem anderen handelt es sich um WINZLING (WIZ), einem Protein mit einer WD40 Domäne von unbekannter Funktion. Eine phänotypische Charakterisierung wurde durchgeführt. Zusätzlich wurden die Transkript- und Protein-Expressionsmuster mit Hilfe von transgenen Pflanzen, die mit auf GUS und EGFP basierenden Reporter-Konstrukten transformiert wurden, untersucht. Interaktionsstudien *in vitro*, in Hefen und in Pflanzen wurden ebenfalls ausgeführt. Für die Rezeptor Kinase SRF4 wurde ein *in vitro* Kinase Assay durchgeführt. Alle drei Gene wurden auf Ihre Evolution in *Viridiplantae* hin

untersucht.

SRF4 zeigte keine Kinase Aktivität *in vitro*. Die phänotypische Charakterisierung der Verlustmutante *srf4-8* und der Überexpressionslinie *UBQ::SRF4* verifizierten die Funktion von *SRF4* als positiver Größenregulator. Eine ähnliche Rolle scheint DLG zuzukommen, da *dlg-6* kleinere und *UBQ::DLG* größere Blätter zeigt. Die Interaktion von SRF4 und DLG *in vitro* konnte nachgewiesen werden. Die Daten unterstützen somit die Annahme, dass SRF4 seinen Effekt auf die Pflanzengröße durch DLG steuert. Das translationale Fusionsprotein von SRF4 mit EGFP konnte an der Plasmamembran detektiert werden, während DLG:EGFP im Zytosol lokalisiert ist. Die Reporter GUS Analyse lässt eine weitreichende Expression von SRF4, inklusive Blätter, Pollen und Wurzeln, vermuten. Für DLG konnte ebenfalls eine starke Expression in der ganzen Pflanze beobachtet werden. SRF4 scheint nicht exklusiv durch DLG zu agieren, da *dlg-6* Pflanzen, die mit *UBQ::SRF4* transformiert wurden, Wildtyp Phänotyp zeigten.

Die Verlustmutante *wiz-1* zeigt kleine, gebleichte Pflanzen, während seine Überexpressionslinie *wiz-2* kleinere, semi-sterile Pflanzen mit runden, dunkelgrünen Blättern aufweist. Die Interaktion mit SRF4 in Hefe war reproduzierbar. Mit einer GUS Reportergen Analyse konnte eine starke Färbung in allen Pflanzenorganen beobachtet werden. Die Analyse der Doppelmutanten zwischen *srf4-8*, *dlg-6*, *wiz-1* und *wiz-2* lässt eine komplexe Verbindung zwischen den drei Genen *SRF4*, *DLG* und *WIZ* erkennen.

Zusammengenommen gehen die Ergebnisse, die in dieser Arbeit präsentiert werden, mit der Ansicht konform, dass SRF4 und DLG positive Regulatoren der Blattgröße sind. Des Weiteren ist es möglich, dass SRF4 diesen Prozess teilweise durch die direkte Interaktion mit DLG kontrolliert.

Chapter 1

Introduction

1.1 Plant receptor-like kinases

For each living organism it is crucial to sense environmental conditions and control the adjustments to be made in the smallest unit of the organism, the cell. In animals this sensing is done by receptor tyrosine kinases (RTKs) and receptor serine/threonine kinases (RSKs) which are composed of three main parts: an extracellular domain (ECD) and an intracellular kinase domain (KD) which are connected via a plasma-membrane spanning transmembrane domain (TM). The extracellular domain is capable of binding ligands which can be small peptides or hormones. The kinase domain is able to phosphorylate tyrosine or serine/threonine residues of other proteins and can thus transfer a signal to the inner part of the cell. They serve therefore as the connection between the extracellular matrix and the cytoplasm and its organelles and help the organism to keep in touch with its environment.

Compared to animals plants are thought to depend much more on environmental conditions, as they are usually tied to a certain place and cannot move on their own. Therefore they have a strong need of interaction with their surrounding environment. The sensing of temperature, water resources, pathogens, nutrients etc., and the according adjustments are crucial for the plant to survive. Receptor-like kinases (RLKs) contribute to this process. RLKs mimic the same structurally build-up as animal RTKs, but whereas animal receptor kinases phosphorylate mostly tyrosine residues, the known plant receptor kinases phosphorylate exclusively serine/threonine residues. The amount of receptor kinases in plants is much higher than in any other organism. Sequence

analysis showed that more than 600 proteins of *Arabidopsis thaliana* belong to the RLK/Pelle family, one of the biggest plant protein families. 417 code for a RLK which is therefore the largest class of transmembrane sensors in plants. With 216 members the biggest subgroup are the leucine-rich repeat (LRR) RLKs [Shiu and Bleecker, 2001]. One important reason for the massive evolution of the RLK/Pelle protein family seems to be the lack of an active immune system in plants [Afzal et al., 2008] and consequently a high demand to deal with biotic stress. It could be shown, by grouping the different ECD *Arabidopsis* sequences, that they build 21 structural classes [Shiu and Bleecker, 2001]. The large variety of ECDs, fused with different KDs, makes RLKs an excellent signal transduction system which can react on a big amount of different ligands and initiate a diversity of defense strategies.

The analysis of the *Arabidopsis* kinome showed that around 13 % of all proteins lack the specific residues needed for kinase activity. Looking only onto the RLK/Pelle protein family, a large protein family where the RLKs belong to, even around 20 % are found to be atypical kinases [Castells and Casacuberta, 2007]. So RLKs do not only play a huge role in signal transduction via phosphorylation, but also phosphorylation-independent signaling seems to be important for plant cell communication.

The functions of RLKs are diverse and range from hormone signaling via bacterial plant defense to meristem and leaf development. An overview of RLK evolution, structures, functions, ligands and mechanisms of signal transduction is given in the following sections.

1.1.1 Evolution of receptor-like kinases

The first RLK was identified in maize [Walker and Zhang, 1990] [Shiu et al., 2004] and revealed the striking similarity between plant RLKs and animal RTKs which are able to phosphorylate proteins by control of an extracellular signal. The powerful mechanism of phosphorylation evolved before the divergence of the animal and plant kingdom. This could be shown by a phylogenetic analysis of kinase domain sequences including representative *Arabidopsis* RLKs, animal RTKs/RSKs and other *Human* and *Arabidopsis* eukaryotic protein kinases (ePKs). The phylogenetic tree (see figure 1.1) revealed that plant and animal receptor kinases (including RLKs, RTKs, RSKs, Raf and Pelle) share a monophyletic origin compared with other ePKs. Three divergence events led

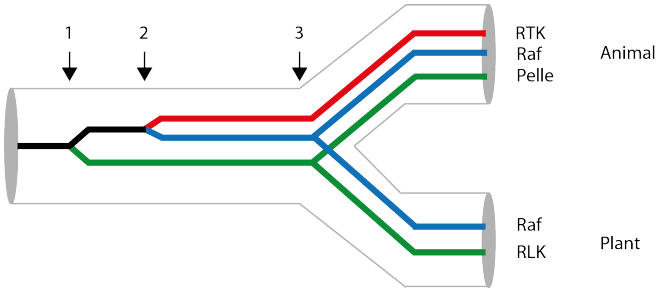

Figure 1.1: Sequence alignments revealed the illustrated evolution of plant and animal receptor kinase families: two duplication events (see arrow 1 and 2) were first dividing the RLK Pelle from the RTK Raf and afterwards the RTK from Raf. The third divergence event ended up in the animal and plant lineage. (Adapted from [Shiu and Bleecker, 2001], Copyright © 2001, The National Academy of Sciences)

to the evolution of the different Receptor Kinases. A first duplication event caused the junction between RLK/Pelle and RTK/Raf proteins, and the second duplication led to an independent evolution of RTK and Raf. The third junction was finally the division between animals and plants leading to an independent evolution of receptor kinases in both kingdoms. Pelle kinases are consequently the animal homologs of the plant RLKs [Shiu and Bleecker, 2001] .

After the divergence of plant and animal receptor kinases the evolution of the RLK/Pelle family went on separately in both lineages. While the protein family in animals stayed small, plants evolved a much higher amount of RLKs. For example, *Drosophila melanogaster* has 1 Pelle kinase and the human RLK/Pelle family consists of four members, the interleukin-1 receptor-associated kinases (*IRAK*). Another interesting fact, despite the amount of receptor kinases, is that RLK/Pelle family members in plants include two subgroups: RLKs and receptor-like cytoplasmic kinases (RLCK) which lack an extracellular domain. In animals only RLCKs could be found. The history of the evolution of the RLK/Pelle family in plants could be followed by sequence analysis of different species including algae, moss, rice, poplar and *Arabidopsis*. The bottom rule of this study was that the receptor configuration, including the ECD and TM, has evolved before the divergence between algae and land plants and that all 21 RLK ECD subclasses have developed before the divergence of vascular plants and moss. When looking at the 37 subfamilies, gained by grouping receptor kinases in a phylogenetic study of their KDs, the same holds true. An interesting finding appears to be the fact that ECDs in the same subfamily tend to have the same configuration. It could also be shown that during evolution of rice, poplar and *Arabidopsis* different fusion events of known ECDs with KDs of other subfamilies

occurred, and that the enormous diversity of RLKs in land plants seems to be achieved by these domain fusions rather than changes in RLK configuration itself [Lehti-Shiu et al., 2009]. Taken together with the fact that the amount of kinases not belonging to the RLK/Pelle family in algae and land plants is stable one comes to the conclusion that this protein family contributed the most to the variety of plant kinases [Lehti-Shiu et al., 2009].

But why did the RLK/Pelle family expand in such an enormous way? One reasonable answer relates to the fact that plants lack an active immune system. Facing many different pathogens they are in need of an alternative defense mechanism [Afzal et al., 2008]. With their ability to detect ligands and sending signals to the intracellular part, RLKs are perfectly shaped to help to defend plants against diverse illnesses. With their big expansion during land plant evolution, RLKs gained big diversity. And indeed, it could be shown that subfamilies, including members important for stress and defense mechanisms, have expanded much stronger. Also the earlier described ECDs, which got bound during evolution to new KDs to form new RLKs, were found to be part of proteins important for pathogen defense. In addition, it could be shown that RLKs were overrepresented when checking for upregulation under stress conditions (biotic and abiotic) in publicly available AtGenExpress microarray data [Kilian et al., 2007]. Accordingly, several RLKs could be shown to function in basal plant immunity. FLAGELLIN SENSITIVE 2 (FLS2) and EF-Tu receptor (EFR) are a part of the defense pathway of bacterial perception [Gomez-Gomez and Boller, 2000] [Zipfel et al., 2006]. The LRR-RLK BAK1, which is known to be involved in brassinosteroid signaling (see section 1.1.4), can interact with FLS2 by forming heterodimers. The flagellin triggered response in *bak1* mutants is disturbed indicating BAK1 to be a positive regulator of flagellin signaling [Chinchilla et al., 2007] [Heese et al., 2007]. The LRR-RLK Xa21 of *Oryza sativa* confers pathogen resistance to rice plants [Song et al., 1995]. These results support the theory that RLKs are involved in stress responses and that their fast expansion was a consequence of adaption to evolving pathogens [Lehti-Shiu et al., 2009].

Evolution of RLKs involved in stress response seems to be driven by tandem duplication. As tandem duplications can happen in short time periods organisms can adapt to new situations fast [Lehti-Shiu et al., 2009]. It could be shown that tandem repeats correlate positively with recombination rates [Zhang and Gaut, 2003] and that recombination rates enlarge under stress con-

ditions [Molinier et al., 2006]. With these facts in mind, stress seems to drive the evolution of genes organized in tandem repeats. Indeed, it could be shown that RLKs are significantly more often organized in tandem repeats than other genes in *Arabidopsis*. Additionally, RLKs organized in tandem repeats are more likely to be upregulated due to biotic stress. Downregulated RLKs are more likely to sit in non-tandem regions [Lehti-Shiu et al., 2009]. For example, for the RLK DUF26 subfamily, which is strongly involved in biotic stress response [Lehti-Shiu et al., 2009], 35 out of 40 members in *Arabidopsis* are located on the same chromosome and 34 of them are organized in tandem repeats [Shiu and Bleecker, 2001].

For the LRR-RLK subfamilies, which are known to be part of plant developmental processes, the evolutionary development seems to be different. The 51 genes of the LRR subfamilies X, XI and XIII are distributed all over the five *Arabidopsis* chromosomes. This distribution implies an early development of the LRR-RLK subfamilies, followed by polyploidization and chromosome rearrangements or some early local duplication events which cannot be followed anymore [Shiu and Bleecker, 2001]. Indeed, all 20 LRR-RLK subfamilies were already present in mosses while the DUF26 RLK subfamily could not be detected [Lehti-Shiu et al., 2009], which supports the early evolution theory. More on LRR-RLKs can be found in section 1.1.2.

Plant RLKs and animal RTKs share the same structural organisation with an extracellular ligand binding domain, a membrane spanning transmembrane domain and an intracellular kinase domain. As it was discussed on page 3, the divergence of these two linages happend before animals and plants split (see figure 1.1). As the members of the plant and animal RLK/Pelle family revealed, the receptor build-up including the ECD developed in plants also not until the split of the two kingdoms. Therefore, RLKs and RTKs seemed to evolve convergently, which is supported by the facts that their ECDs are completely different and also their interaction partners are mostly non homologous proteins. Nevertheless, they do reveal mechanistic similarities in ligand binding and signal transduction, the assembly of receptor complexes and activation control by autoactivation and downregulation due to phosphatase activity. These similarities reflect the adaption of the two kingdoms to same molecular problems by convergent evolution [Cock et al., 2002].

1.1.2 Leucine-rich repeat receptor-like kinases

The biggest group within the plant RLK/Pelle family are the LRR-RLKs. Their name arises from a certain amount of leucine-rich repeats in the ECD. LRRs are 20-29 amino acid long motifs with a conserved 11-residue stretch with the consensus sequence LxxLxLxxN/CxL (whereas x is a spacer for any amino acid and L can be also possessed by valine, isoleucine or phenylalanine). LRRs are known to be involved in different kinds of protein-protein interactions, by serving as a structural framework [Kobe and Kajava, 2001].

When clustered by their ECD sequence, 8 different structural LRR classes could be distinguished [Shiu and Bleecker, 2001]. Out of the 37 arising RLK subfamilies, 20 belonged exclusively to LRR-RLKs. All of them developed in early land plant evolution and can be found already in mosses. While further evolution and family expansion none of the LRR subfamilies gave rise to new ECD/KD fusions [Lehti-Shiu et al., 2009]. The reason might be that LRRs are already well adapted for ligand sensing and a wide range of LRR-RLK subfamilies are already adjusted well so that modifications within the subfamilies did not show any advantage to the plants. The LRR-RLK subfamilies are known to be involved in various biological processes, like e.g. in hormone signaling where BRASSINOSTEROID INSENSITIVE 1 (BRI1) gets activated by the plant hormone brassinosteroid [Li and Chory, 1997] [Gish and Clark, 2011], in pathogen recognition by FLAGELLIN SENSITIVE 2 (FLS2), where pathogens get recognized by flagellin perception [Gomez-Gomez and Boller, 2000] [Gomez-Gomez and Boller, 2002], in meristem control where CLAVATA 1(CLV1) gets activated by the polypeptide CLAVATA 3 (CLV3) [Clark et al., 1997] [Trotochaud et al., 2000] or organ development by *STRUBBELIG* (*SUB*) which might function via a so far unknown ligand [Chevalier et al., 2005] [Kwak et al., 2005]. The well studied signal transduction pathways of BRI1 and CLV1 are explained in detail in section 1.1.4.

1.1.3 Atypical receptor-like kinases

The kinase domains of receptor kinases persist mostly of 250-300 residues and can be subdivided in 12 subdomains with conserved amino acids throughout the sequence. This indicates that they play an important role in signaling via phosphorylation [Hanks and Hunter, 1995]. The subdomains form two lobes of which the small N-terminal lobe is responsible for binding and adjusting the ATP

molecule, whereas the big C-terminal lobe binds the substrate and launches its phosphorylation. RLKs function mostly in two steps: (1) binding of the ligand and oligomerization followed by KD activation and (2) binding and activation of downstream proteins. An interesting finding was made when checking for the conserved residues in the KD sequences of animals and plants. Out of 518 genes belonging to the human kinome, 10 % lack crucial conserved residues needed for kinase activity indicating them to be enzymatically inactive. Similarly, 13 % of the *Arabidopsis* kinome, containing 911 genes, revealed the lack of important conserved residues. When restricting the set of sequences only to RLKs the amount of atypical kinases increased to 20 %, which indicates that phosphor-independent signaling plays a crucial role in plant receptor signal transduction [Castells and Casacuberta, 2007]. Indeed, in animals atypical RTKs could be observed, e.g. the human COLON CARCINOMA KINASE-4 (CCK-4) [Mossie et al., 1995] and ErbB-3 [Sierke et al., 1997] or the Drosophila Doughnut (DNT) [Savant-Bhonsale et al., 1999]. But also for plant RLKs the evidence for phosphorylation independent mechanisms is supplied by the MAIZE ATYPICAL RECEPTOR KINASE (MARK) [Llompart et al., 2003] and SUB [Chevalier et al., 2005].

In the following section 1.1.4 examples for signal transduction of functional and atypical kinases are presented and explained.

1.1.4 The mechanism of signal transduction of typical and atypical receptor-like kinases

RLKs are membrane bound receptors with an extracellular ligand binding domain and an intracellular kinase domain which phosphorylates downstream signaling proteins. But also signaling without phosphorylation is a common instrument of signal transduction in plants and animals. The functional RLKs BRI1 and CLV1 and their way of activation is described here, as well as the signaling pathway of the atypical RKs ErbB-3 and MARK [Gish and Clark, 2011].

BRI1 signaling pathway The brassinosteroids are plant hormones which influence plant growth and development. One global player in brassinosteroid signal transduction is *BRASSINOSTEROID INSENSITIVE 1 (BRI1)*. The mutant phenotype of *bri1* shows a strong dwarfism and was fished in a forward genetic screen [Li and Chory, 1997]. *BRI1* is a LRR-RLK with 25 LRRs in the ECD.

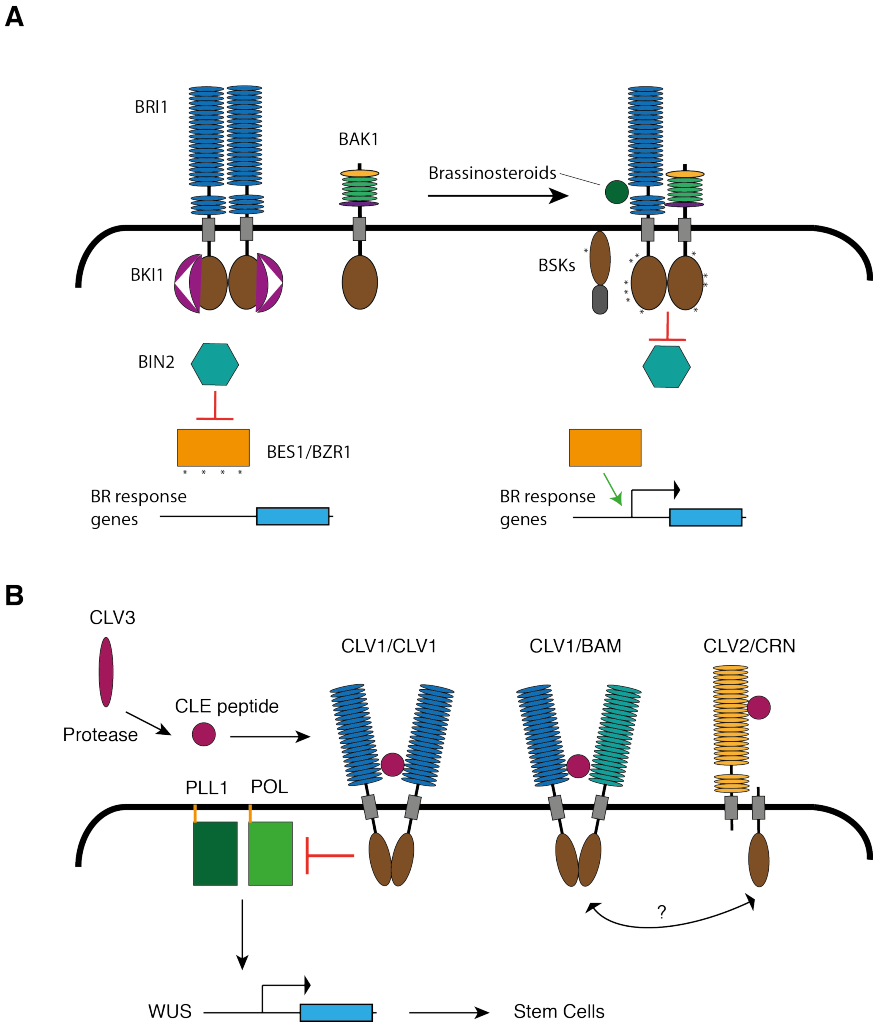

Figure 1.2: Signal transduction of the RLKs BRI1 and CLV1. A: BRI1 builds homodimers which get inhibited by BKI1 and BRI1 itself, while BES1 and BZR1 get repressed by BIN2. When the ligand brassinosteriod binds to BRI1, BRI1 and BAK1 can interact and transphosphorylate due to the release of BKI1 inhibition. BSK favors the repression of BIN2 by BRI1, which releases BES1 and BZR1 and grants therefore the transcription of brassinosteroid-response genes. Asterisks show phosphorylation sites. B: Processing of the signal peptide CLV3 by a serine protease enables it to bind to CLV1, BAM and CLV2. CLV1 and CLV2 might interact. By activation of CLV1, the phosphatases POL and PLL1, which regulate WUS transcription, get repressed. (Adapted from [Gish and Clark, 2011], © 2011 The Authors. The Plant Journal © 2011 Blackwell Publishing Ltd.)

While being inactive, BRI1 forms a homodimer which is controlled by BKI1 and the BRI1 autoinhibitory domain. The phosphorylation status of this domain restricts its function [Wang et al., 2005] [Wang and Chory, 2006]. During that stage the kinase BIN2 represses actively the transcription factors BES1/BZR1 by phosphorylation. When brassinosteroids bind to BRI1, BKI1 gets phosphorylated by BRI1, BRI1 is relieved and the monodimer is ready to interact with another LRR-RLK, namely BAK1 [Li et al., 2002]. Subsequently, sequential transphosphorylation between BRI1 and BAK1, which makes signal transduction possible, takes place. Other membrane associated cytoplasmic kinases, BSK1, 2 and 3, support the BRI1/BAK1 receptor complex to actively repress BIN2 and therefore release BES1 and BZR1 [Li and Nam, 2002] [Tang et al., 2008]. BES1/BZR1 accumulate in the nucleus where they trigger brassinosteroid response [He et al., 2002] [Yin et al., 2002] [Zhao et al., 2002]. An illustration of the BRI1 signal transduction mechanism can be seen in figure 1.2 (A).

CLV1 signaling pathway The maintenance of the shoot apical meristem, which gives rise to above ground organs of plants, is a crucial and sensitive task. Up to date many players in this pathway have been identified. The first one was the LRR-RLK *CLAVATA1 (CLV1)* with 21 LRRs in its ECD. *clv1* mutant phenotype exhibits plants with enlarged shoot and floral meristem [Clark et al., 1997]. A closer look at the other components of stem cell regulation around CLV1 is given in the following paragraph.

CLV1 is able to homodimerize and to build multiheterodimers with its homolog LRR-RLKs BARELY ANY MERISTEM (BAM) [Kondo et al., 2008] [Ogawa et al., 2008] [Bleckmann et al., 2010] [Guo et al., 2010] [Zhu et al., 2010]. CLV1 as well as BAM are able to bind its ligand CLAVATA3 (CLV3). Before being functional the polypeptide CLV3 needs to be processed by a serine protease [Ito et al., 2006] [Ni et al., 2011]. The signaling via CLV1 happens by repressing the activity of the membrane bound phosphatases POLTERGEIST (POL) and PLL1 [Yu et al., 2003] [Song and Clark, 2005] [Song et al., 2006] . No direct interaction between the receptor complex and the phosphatases could be shown so far. But POL/PLL1 control the expression of WUSCHEL (WUS), a transcription factor which facilitates stem cell specification [Mayer et al., 1998] [Schoof et al., 2000]. One characteristic feature of CLV signaling is the fact that CLV3 also binds to CLV2, a receptor like protein which lacks a kinase domain [Kayes and Clark, 1998]. Signaling seems to happen through the transmembrane

putative kinase CORYNE (CRN) [Muller et al., 2008] [Bleckmann et al., 2010] [Guo et al., 2010] [Zhu et al., 2010]. The knock-outs of CLV1 and CLV2 show severe phenotypes so that it is argued that both receptor complexes are needed for stem cell control in vivo. In figure 1.2 (B) an outline of the pathway is shown.

MARK signaling pathway The Maize Atypical Receptor Kinase (MARK) is an atypical kinase found in a screen for genes important for maize embryogenesis control, with 6 imperfect LRRs in its ECD. The kinase domain is similar to other serine/threonine kinases, but some conserved amino acids are missing. Also *in vitro* no auto- or transphosphorylation could be shown. MARK interacts downstream with the GCK-like kinase MIK. As the interaction induces MIK kinase activity in a strong way, a mechanism for signal transduction through an atypical kinase was found [Llompart et al., 2003]. As MIK is autoinhibiting its own kinase activity, it is likely that the interaction with MARK causes some conformational changes which activate MIK [Castells et al., 2006]. In figure 1.3 (C) a sketch of the signal transduction mechanism can be seen.

ErbB-3 signaling pathway The RTK ErbB-3 is part of the epidermal-growth-factor-receptor family [Guy et al., 1994] [Sierke et al., 1997] [Stein and Staros, 2000]. The kinase domain exhibits amino acid substitutions on, in functional kinases, highly conserved residues and it was shown that its kinase activity is strongly disturbed [Kim et al., 1998b]. Nevertheless, ErbB3 is an active protein as in mutant mice it caused embryo lethality [Riethmacher et al., 1997]. Signaling through ErbB-3 is possible by its interaction with other EGFR family members which phosphorylate ErbB-3 and create therefore a docking site for other proteins. Interaction partners of ErbB-3 are the phosphatidyl-inositol 3-kinase and SHC [Prigent and Gullick, 1994] which are known to be effector proteins important for the mitogen-activated protein kinase (MAPK) cascade activation [Citri et al., 2003]. In figure 1.3 (B) a sketch of the signal transduction mechanism can be seen.

Description of the BRI1 and CLV1 pathway in [Gish and Clark, 2011] was followed. For revealing MARK and ErbB-3 signaling cascade the paper [Castells and Casacuberta, 2007] was used.

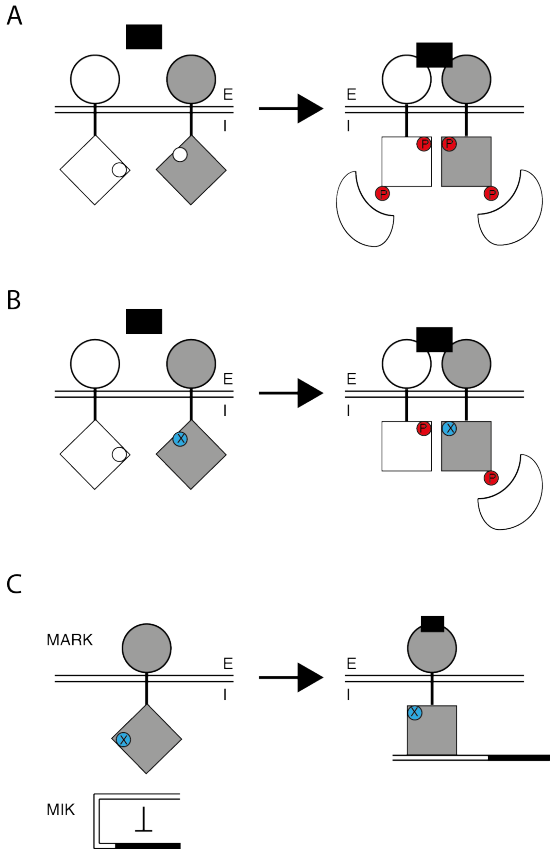

Figure 1.3: Signal transduction of the atypical kinases ErbB-3 and MARK. A: Typical signal transduction through RLKs. The ligand (filled square) binds to the extracellular domains of the receptor (open and grey circles). By autophosphorylation (open small circle indicate the activation loops, red circles indicate phosphorylation) the receptor gets activated and can form homo- or heterodimers, which might give rise to other phosphorylation sites. Those residues can serve as interaction sites for other downstream signaling proteins. B: Atypical kinase signaling by ErbB3. The binding of the ligand by the ErbB3 heterodimer, consisting of ErbB3 (grey) and another member of the EGFR family, causes the phosphorylation of the unfunctional kinase domain (indicated by an blue small circle) of ErbB3 by the EGFR partner kinase, which becomes therefore a docking site for other proteins. C: Signaling through the atypical kinase MARK. Ligand binding might cause a conformational change. Therefore the unfunctional kinase domain can bind to MIK. MIK kinase activity is inhibited by its own C-terminal domain (open rectangle). The interaction with MARK causes a conformational change of MIK which activates its kinase activity. E indicates the extracellular matrix, while I represents the intracellular part. The plasma membrane is marked by a double line. (Adapted from [Castells and Casacuberta, 2007], Copyright © 2007, Oxford University Press)

1.1.5 The *Strubbelig Receptor Family*

The *STRUBBELIG RECEPTOR FAMILY (SRF)* is a monophyletic group of LRR-RLKs which build the LRR-V subfamily. It comprises of nine members *SRF1-8* and *STRUBBELIG (SUB)* where *SUB* is *SRF9*. The SRF members correlate to the *ltk* gene family in maize which might be involved in seed development but their exact function remained unknown so far [Li and Wurtzel, 1998] [Eyuboglu et al., 2007].

STRUBBELIG The whole subfamily gained its name from the well studied *SUB* gene. *SUB* was identified in an EMS mutant screen for plants with impaired ovule development [Schneitz et al., 1997]. The outer integument development is affected by protrusions and can even end in failing to encapsulate the inner integument. At late stage 2-III/early stage 2-IV the difference becomes aberrant. Additional to the ovule phenotype, *sub* plants exhibit severe problems in morphology. They show reduced overall height and twisted organs like stems, carpels and petal pedicels [Chevalier et al., 2005]. A reduction of epidermal, cortex and pith cells was noted. Periclinal cell divisions in the L2 layer of the apical meristem of 30 day old plants and in the young floral meristem could be observed. *SUB* was proven to be an atypical kinase. It could be shown that its kinase activity is not needed for its function, but the kinase domain is still needed for signaling [Chevalier et al., 2005] [Vaddepalli et al., 2011]. The identification of the STRUBBELIG LIKE MUTANTS (SLMs) QUIRKY, ZERZAUST and DETORQUEO [Fulton et al., 2009] might give a new insight in atypical receptor kinase signaling *in planta*. An extensive structure function analysis of *SUB* confirmed the importance of the STRUBBELIG N-capping domain (see figure 1.4) and revealed the stability of the gene against several sequence variations [Vaddepalli et al., 2011]. *SUB* undergoes quality control at the endoplasmic reticulum and its stability gets regulated by a MG132-sensitive process. Furthermore, *SUB* seems to mediate inter-cell-layer signaling in floral organ development in a non cell-autonomous fashion [Yadav et al., 2008]. It could be shown that *SUB/SCRAMBLED (SCM)* is needed for the patterning of post-embryonic epidermis root cells [Kwak and Schiefelbein, 2007]. *WEREWOLF (WER)* [Lee and Schiefelbein, 1999], an important player in epidermal cell patterning, is negatively regulated by SUB/SCM [Kwak and Schiefelbein, 2007].

The *SUB* phenotype suggests a role in floral organ formation and shaping as well as in root hair patterning by controlling cell morphogenesis and the

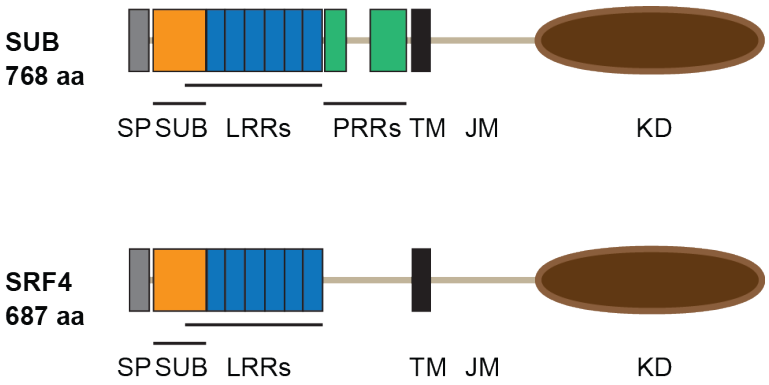

Figure 1.4: Overview of the domain structure of SUB and SRF4. Abbreviations: SP: signal peptide, SUB: SUB-domain, LRR: leucine-richt repeat, PRR: proline-richt repeat, TM: transmembrane domain, JM: juxtamembrane domain, KD: kinase domain, aa: amino acid. (Adapted from [Vaddepalli et al., 2011])

Figure 1.5: Phylogenetic tree of the *SRFs*. The coding sequences were used for the Alignment.

adjustment of the division plane.

SRF4 The analysis of the loss-of-function mutant plants of *SRF4* showed a clear growth reduction phenotype. In contrary its gain of function mutant developed bigger leaves. Therefore *SRF4* is believed to be a positive regulator of leaf size [Eyuboglu et al., 2007]. *SRF4* exhibits the same domains as *SUB* except of the proline-rich repeats (PRRs) (see figure 1.4). The closest homologue of *SRF4* is *SRF5* (see phylogenetic tree in figure 1.5). As well as *SUB*, *SRF4* is believed to be an inactive kinase, as important amino acid residues in the kinase domain are mutated (see section below for detailed information).

SRF3 Recently it could be shown that *SRF3* drives incompatibilities between *Arabidopsis thaliana* L*er* and diverse Asian accessions. The geographic separation of incompatible SRF3 alleles fits to incompatibility events. Those incompatibilities seem to be immune-triggered. The fact that the receptiveness for

diseases related to compatible and incompatible *SRF3* alleles mirrors different MAMP-triggered immunity (MTI) responses, gives rise to the assumption that this might lead to a selective advantage during pathogen attack when lowering the activation threshold of MTI [Alcazar et al., 2010].

Structure and Function of the *SRFs* Like all RLKs, the *SRFs* consist of an extracellular domain, a transmembrane domain and a kinase domain. The *SRFs* contain six LRR in their ECD which are likely to maintain protein-protein interactions [Kobe and Kajava, 2001]. The LRRs among the family members are not highly conserved which indicates different interaction partners and therefore different functions of the single receptors [Eyuboglu, 2008]. N-terminal to the LRRs a stretch of unique, conserved residues among the LRR-V family was found. This domain is called the SUB domain and its purpose is unknown even though it is needed for STRUBBELIG function [Chevalier et al., 2005]. *SUB, SRF1A* and *B, SRF6* and *7* contain a proline-rich region (PRR) in front of the transmembrane domain. *SRF3* exhibits this domain intracellular, between the TM and the kinase domain. PRRs are known to be involved in protein-protein interactions [Anggono and Robinson, 2007]. All *SRFs* have a kinase domain except for the splice variant of *SRF1*, *SRF1B*. This gene seems to code for a receptor like protein which lacks the kinase domain. Its way of signaling might be similar to CLV2 (see section 1.1.4). *SUB, SRF2* and *SRF8* developed characteristic activation segments, which are part of the kinase domain and which are important for substrate binding [Huse and Kuriyan, 2002] [Johnson et al., 1996], while the phylogenetic closest relative pairs *SRF1/SRF3*, *SRF6/7* and *SRF4/5* are also dissimilar to each other in this region (see figure 1.1). Within the pairs the similarity is higher. This results might give insights into different substrate bindings and consequently different functions of the *SRFs* [Eyuboglu et al., 2007].

The *SRF* members are likely to encode for atypical kinases. For *SUB* it could be already shown that its kinase domain is not functional [Chevalier et al., 2005]. A sequence analysis of the other family members revealed amino acid substitutions at critical, conserved residues in the kinase domain. Sequence analysis of all *SRF* members showed a substitution in kinase subdomain VIb from aspartic acid to asparagine at position 625 in *SUB*, except for *SRF2* [Chevalier et al., 2005] [Eyuboglu, 2008]. But also other conserved motifs have undergone substitutions. In subdomain VII the highly conserved DFG motif, at position 643-645 in *SUB*, is altered to DSG in *SUB, SRF6* and *7*, to DCG in *SRF1, 2*

and *3* and to DYG in *SRF4* and *5*. Furthermore the GT/SxxY/FxAPE motif in subdomain VII is not maintained among the *SRFs* [Carrera et al., 1994] [Eyuboglu, 2008]. The exchange of the amino acids in subdomain VIb and VII seem to be crucial as these residues are still conserved in active kinases like *BRI* and *AtCRR1*. In the atypical kinases *MARK* and *TMKL1* this residues are also mutated in a similar way which indicates that *SRF* kinase domains are no longer active [Castells and Casacuberta, 2007]. Subdomain VIb and VII are known to be important for autophosphorylation of the receptor, mostly the aspartic acid in subdomain VIb serves as the substrates proton acceptor. The aspartic acid in the DFG motif in subdomain VII is important for ATP positioning [Meylan and Tschopp, 2008]. Consequently, some characteristic features of an functional Ser/Thr kinase seem to be missing in the *SRF* members sequences which gives rise to further investigation. Maybe the *SRFs* signal transduction is similar to ErBB-3 or MARK which was explained in section 1.1.4.

An additional feature of the LRR-V RLK family is the fact that certain members bear PEST signals. Those signals are involved in protein degradation [Rechsteiner and Rogers, 1996], but it could also be shown that in human CYSTIC FIBROSIS TRANSMEMBRANE CONDUCTANCE REGULATOR (CFTR) the PEST signal might play a role in protein maturation [Chen and Clarke, 2002]. *SUB, SRF1A* and *B, SRF3, SRF5* and *SRF6* have PEST sequences in the ECD between the LRRs and the TM. *SRF4* exhibits an intracellular PEST signal. Nevertheless, an alignment of the PEST motifs within the *SRF* members did not reveal striking conservation. So far, any function of the PEST regions could not be proven.

Unfortunately, no ligand of the STRUBBELIG RECEPTOR FAMILY could be detected. So far it remains unclear what activates the *SRFs* and where the ligand might bind in the ECD.

Another interesting aspect of the LRR-V RLK family is the fact that, when applying biotic or abiotic stress, the family has a concentrated amount of downregulated members which can be seen in [Lehti-Shiu et al., 2009]. As it was already shown for *SUB* and *SRF4*, the whole family might be involved in developmental processes. The downregulation in stress situation might be a consequence of limited resources while fighting deseases or environmental changes [Lehti-Shiu et al., 2009].

Except for *SUB*, *SRF4* and *SRF3* no function of the *SRF* members was identified so far. For all *SRF* members T-DNA lines were ordered and analysed as

well as the gain-of-function mutants *35S::SRF1-8*. None of the mutants showed any obvious phenotype, except for *srf4*. The ectopic expression lines *35S::SRF1-8* showed various phenotypes. *35S::SRF2, 3, 4, 5, 7* showed male sterility, *35S::SRF1A* and *35S::SRF8* showed seedling lethality and *35S::SRF4* bigger leaves. *35S::SRF1B* and *35S::SRF6* did not show any obvious phenotypes. Taken together with the loss-of-function mutants, it cannot be told whether the observed defects under 35S promoter correspond to the wildtype function of the *SRFs*, but *SRF4* seemed to be an exciting candidate to investigate further [Eyuboglu et al., 2007].

1.2 Photorespiration in general and hydroxypyruvate-reductases in particular

One of the most fascinating features about plants is the fact that they use light energy, CO_2 and water to produce carbohydrates and oxygen. This process is called photosynthesis and consists of two phases: light reaction and carbon linked reactions (Calvin cycle). Photosynthesis takes place in chloroplasts where light gets absorbed by the pigment chlorophyll. During the light reaction O_2, ATP and NADPH are produced, whereas ATP and NADPH are consumed during the conversion of CO_2 to sugar in the Calvin cycle. One problem during the uptake of CO_2 is the fact that the responsible enzyme RuBisCO (Ribulose-1,5-bisphosphat-carboxylase/oxygenase) is not specific enough for CO_2 under recent atmospheric conditions, where it is also capable of binding O_2. This rises the need of an additional pathway to avoid the poisoning of the plant with intermediate products. This light-dependent pathway is called photorespiration and uses energy to recycle as much as possible of the lost carbon due to oxygenase activity of RuBisCO. Photorespiration consumes energy and looses carbon by CO_2 release. To avoid those losses some plants, namely C4 and CAM, have evolved strategies to keep photorespiration as small as possible [Buchanan et al., 2000]. It was found that the putative interaction partner of *SRF4* is the cytosolic hydroxypyruvate-reductase 2 (HPR2) [Timm et al., 2008], which is responsible for the reduction of hydroxypyruvate to glycerate in the photorespiratory pathway. An overview of this process is given in the following sections.

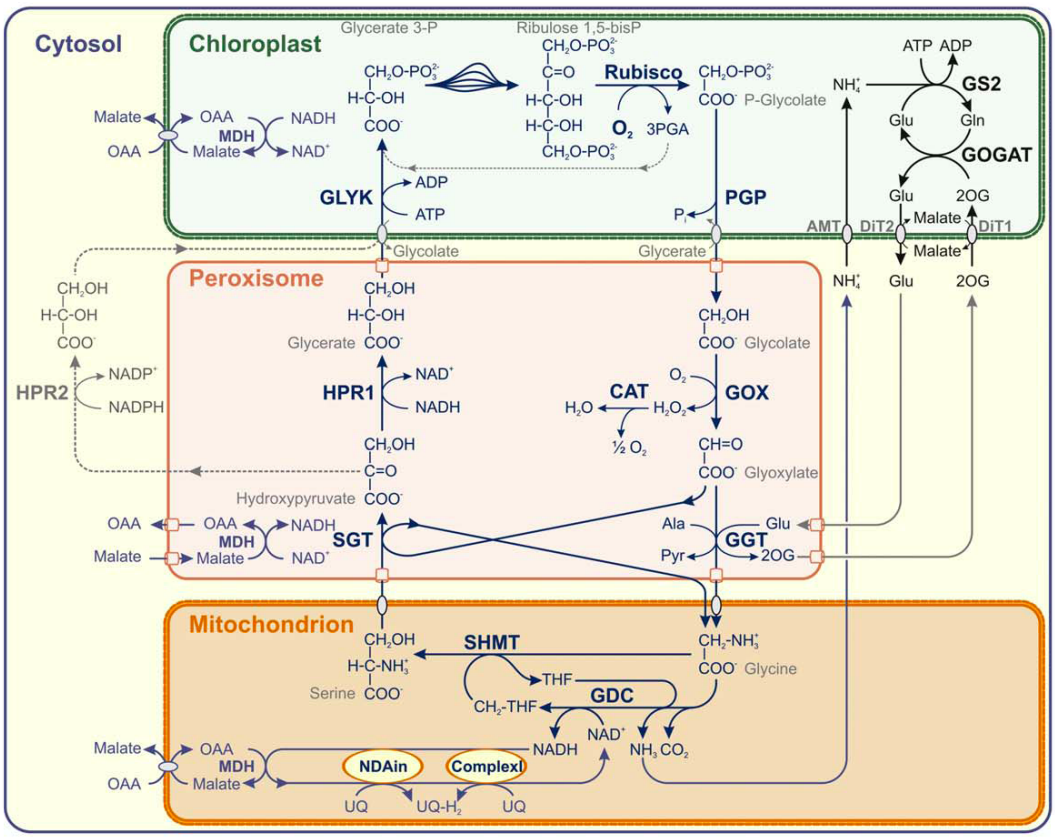

Figure 1.6: Photorespiration takes place in different compartments and is linked to nitrogen metabolism. The C2 cycle is blue, the associated nitrogen cycle black and other reactions are marked in grey and light blue. The Calvin-cycle is shown as repeated arrows between 3PGA and RubP. HPR3 is not yet integrated in this figure. The enzymes are CAT, catalase; ComplexI, NADH:ubiquinone reductase of the mitochondrial electron transport chain; GDC, glycine decarboxylase; GLYK, glycerate 3-kinase; GOGAT, ferredoxin-dependent glutamate synthase; GOX, glycolate oxidase; GGT, glutamate:glyoxylate aminotransferase; GS, glutamine synthetase; HPR1, peroxisomal hydroxypyruvate reductase; HPR2, cytosolic hydroxypyruvate reductase; MDH, malate dehydrogenase; NDAin, internal NADH:ubiquinone reductase; PGP, 2PG phosphatase; SGT, serine:glyoxylate aminotransferase; and SHMT, serine hydroxymethyltransferase. (Copyright © 2010, Elsevier, [Bauwe et al., 2010])

1.2.1 Photorespiration and its purpose

Following photosynthesis, photorespiration is the most important pathway in terms of mass flow [Bauwe et al., 2010]. The photorespiratory pathway is well understood, meaning acting enzymes and required substrates and cofactors. An overview of the pathway, including the compartments, is given in figure 1.6. Even if this picture might not be complete [Peterhansel and Maurino, 2011] the most important players are known.

The origin of photorespiration could be found already in cyanobacteria. Cyanobacteria are likely to be the precursor of todays chloroplasts which ended

up in plants by endosymbiosis. It could be shown that photorespiration co-evolved to photosynthesis in this blue-green algae [Bauwe et al., 2010]. The nonspecific binding of substrates by RuBisCO reflects its evolutionary origin in ancient anaerobic times and organisms. The fact that it did not loose its oxygenase ability till now makes photorespiration look like an evolutionary relict. This is also supported by the fact that C4 and CAM plants try to overcome the problems of energy loss by photorespiration. Nevertheless, photorespiration is essential for all plants which do oxygenic photosynthesis. Disruption of the photorespiratory pathway ends in non viable plants.

RuBisCO is around 100 folds less active with O_2 as substrate compared to CO_2 [Tcherkez et al., 2006]. Taking recent atmospheric conditions and the higher solubility of CO_2 in cytosol and chloroplasts into account [Ku and Edwards, 1977], around 1/4 of RuBisCO activity ends up in oxygenation and therefore photorespiration. While CO_2 uptake by RuBisCO produces two 3-phosphoglycerate (3-PGA), which can be directly used in the C_3 Calvin Cycle, its affinity to O_2 produces one 3-PGA and one 2-phosphoglycolate (2-PG). This component cannot be used any further and is even thought to inhibit chloroplast function [Anderson, 1971a]. Furthermore, it was shown to inhibit enzymes which are needed in the Calvin cycle to recover Ribulose-1,5-bisphosphat (RuBP) [Anderson, 1971b] and in starch breakdown [Kelly and Latzko, 1976]. To get rid of this toxic molecules plants evolved the C_2 oxidative photosynthetic carbon cycle (photorespiration) in which 2-PG gets recycled to one more 3-PGA. But carbon recycling takes its toll. The energy balance of the C2 cycle is as follows:

$$2\ RuBP + 3\ O_2 + 2\ Fdx_{\mathrm{red}} + 2\ ATP \rightleftharpoons$$
$$3\ 3 - PGA + CO_2 + 2\ Fdx_{\mathrm{ox}} + 2\ ADP + 2\ P_{\mathrm{i}}$$

$\mathrm{Fdx_{red}}$ = reduced ferrodoxin, e.g. NAD(P)H [Buchanan et al., 2000]

The loss of carbon (CO_2) and energy by photorespiration is one factor which causes the question for its meaning. When also counting the regeneration of RuBP from 3-PGA in the Calvin Cycle and recapturing the released CO_2 it is clear that O_2 fixation by RuBisCO is quite costly [Buchanan et al., 2000]. Under moderate conditions around 20 % CO_2 gets lost in C_3 plants [Cegelski and Schaefer, 2006].

But why do plants maintain this pathway? The uptake of oxygen by RuBisCO is an evolutionary remainder as in former times the atmosphere comprised of much more CO_2 than O_2. It did not matter to the protein if it was also able to act as an oxygenase. If it is assumed that oxygen uptake is just a tolerated feature of RuBisCO, which would even harm the plant by energy waste, then one would wonder why it was kept during atmospheric changes. Obviously, even under the recent conditions the C2 cycle is needed for plants and their physiology. One interesting fact is that RuBisCOs affinity to CO_2 is shrinking the warmer it gets [Jordan and Ogren, 1984]. Furthermore, under warm conditions plants close their stomata and consequently the amount of carbon dioxide is decreasing in the leaf. Under these high oxygen environment the photorespiratory pathway might make the best of the situation by recovering 75 % of the carbon [Peterhansel and Maurino, 2011]. Maybe, under these conditions the pathway is also needed to keep the electron flux running and preventing therefore the overload of the photosynthetic reaction centres [Campell, 1998].

High oxygen environments stress the plants and stop it from producing energy. CAM and C4 plants, which are known to be able to face also hot and sunny conditions, evolved new strategies for carbon fixation. For C4 plants this includes the reduction of photorespiration by establishing a pump to increase the CO_2 level in chloroplasts which consequently reduces the amount of 2-PG. But even under normal air conditions the enrichment with CO_2 does not prevent the plants, having defects in the C2 cycle, from dying [Zelitch et al., 2009]. The carbon losses might be little, but the toxic intermediates seem to be likely to damage the plant [Peterhansel and Maurino, 2011].

Cyanobacteria *Synechocystis* established 3 pathways for 2-PG conversion and it also has a CO_2 pump which enriches the CO_2 level around RuBisCO [Eisenhut et al., 2008]. Only one homolog of the several additional enzymes in *Synechocystis* could be found in *Arabidopsis* (glycolate dehydrogenase) [Bari et al., 2004]. The very interesting finding about this was the fact that overexpression of the bacterial pathway in *Arabidopsis* chloroplasts resulted in an higher CO_2 level in chloroplasts and therefore a decreased mass flow through the plant photorespiratory pathway, which lead to 30 % more leaf biomass [Kebeish et al., 2007]. Also the identification of natural accuring tabacco plants, favoring less photorespiration, showed more photosynthesis and enhanced growth; unfortunately the effect could not be maintained in following generations [Zelitch, 1992].

Due to the high losses in the C2 cycle photorespiration has always been a target in crop manipulation and facing the growing world population and global warming it might even gain in importance.

1.2.1.1 Hydroxypyruvate-reductases: many players for one aim

Photorespiration takes place in different cell compartments: the chloroplast, the mitochondrium and the peroxisome. Additionally it could be shown that also a cytosolic enzyme contributes to the C2 cycle [Timm et al., 2008].

The enzymes, which are part of photorespiration, were mostly found by mutant analysis. Plants defective in the pathway were not able to survive or showed at least severe growth reductions under normal air, but in high CO_2 they grew happily. One exception for this phenotype was the hydroxypyruvate-reductase 1 (HPR1) which converts hydroxypyruvate to glycerate in the peroxisomes. Glycerate gets afterwards allocated to the chloroplasts where it is phosphorylated to 3-PGA. *hpr1* plants survived also in normal air. It was hypothesized that a cytosolic hydroxypyruvate-reductase (HPR2) might exist [Kleczkowski and Randall, 1988]. For no plant species the HPR2 gene was known until the gene was finally identified in *Arabidopsis* [Timm et al., 2008]. The corresponding gene, At1g79870, turned out to have 51 % sequence similarity on protein level to HPR1 and the single *hpr2* loss-of-function mutants did, like *hpr1*, not show any remarkable phenotype. The *hpr1 hpr2* double mutant showed clear reduction in growth even though they did not die. Furthermore, an accumulation of hydroxypyruvate in *hpr1, hpr2* and its double mutant could be observed. *hpr1* accumulated 103 times more hydroxypyruvate, compared to wildtype, while *hpr2* accumulated only 3 times more, which also revealed that HPR1 contributes the major part to photorespiration. It was argued that the peroxisomal NADH level influences the grade to which extent the cytosolic bypass is active. Nevertheless, the survival of the double mutant indicates other components at this step of photorespiration which could be indeed identified. [Timm et al., 2008] The closest homolog of HPR2 in *Arabidopsis thaliana* is *At1g12550*, representing 45 % sequence identity. It could be shown that this protein is also able to convert hydroxypyruvate to glycerate and is therefore referred to as HPR3 [Timm et al., 2011]. HPR3 is also able to convert glyoxylate to glycine. The triple mutant *hpr1 hpr2 hpr3* showed stunted growth and reduced oxygen-dependent gas exchange compared to the *hpr1 hpr2* double mutant which could be rescued in high CO_2.

Checking the *hpr1 hpr3* and *hpr2 hpr3* double mutants, which did not reflect stronger growth retardation compared to *hpr1* and *hpr2* respectively, indicates that HPR1 and HPR2 are still the main contributors to this part of photorespiration. HPR3 seems to be located in the chloroplast, where it can bypass hydroxypyruvate and glyoxylate conversion [Timm et al., 2011].

1.3 WD40 and RIC1 domain containing proteins

Protein-protein interactions are the basis for all cellular signaling cascades. Different motifs and domains are known to be involved in these kind of processes, e.g. leucine-rich repeats (see section 1.1.2). *WINZLING (WIZ)*, a putative interaction partner of *SRF4*, is predicted to be part of the WD40 and RIC1 superfamily. WD40 repeats are abundant motifs, known to be involved in protein interactions. The conserved WD dipeptide and the length of one repeat, which is around 40 amino acids, gave the name to the motif [Fong et al., 1986]. As a basic principle, 4-8 WD40 repeats can form one domain [Paoli, 2001]. So far known proteins containing WD40 repeats, form a β-propeller (see figure 1.7), comprising of 7- to 8-blades [Xu and Min, 2011]. Geometrically, 7-blade propellors reflect the most stable structures of β-sheets and are therefore the most abundant proteins in the investigated WD40 structures [Murzin, 1992]. WD40 domains are among the 10 most abundant domains in eukaryotic genomes. In *S. cerevisae* they are in the fore of interacting proteins. They are not very prominent in prokaryotes, even though in bacteria some cases have been referred to [Stirnimann et al., 2010]. Many WD40 domain containing proteins developed additional functional domains [Stirnimann et al., 2010]. For *WIZ* this seems also to be the case as a RIC1 domain is predicted at its C-terminus. In plants so far nothing is known about proteins containing this signature.

1.3.1 WD40 domains provide scaffolds for different kind of interactions

WD40 domains are built up by 7-8 WD40 repeats from which it is known that one repeat gives rise to 4 β-sheets. A WD40 repeat comprises of a conserved GH dipeptide which is located 11-24 amino acids from the N-terminus. The conserved WD dipeptide is located at the C-terminus and is flanked by

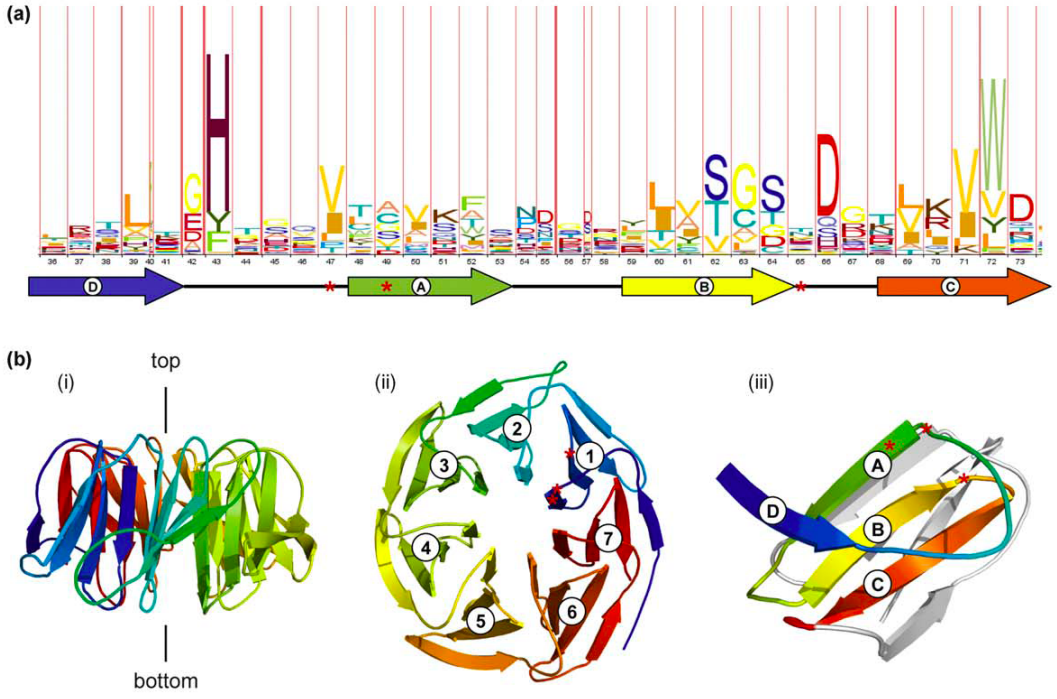

Figure 1.7: Overview of the WD40 motif sequence and structure. (a) The conservation of one WD40 motif is shown here. The secondary structure within one repeat is shown below the sequence logo. The residues 11-24 are not conserved very well, but several amino acids are critical: the glycine-histidine dipeptide (GH) behind the β-sheet D, three small amino acids at the end of strand B and a tryptophan-aspartate (WD) dipeptide at the end of strand C. (b) The tertiary structure of WD40 domains fold into 7 or 8 bladed β-propellors (ii). They build a funnel-like structure with the DA and BC loops defining the top (i). One WD40 repeat gives rise to strand D of one blade and to strand A, B, C of the next one and is therefore not equivalent to one propellor blade (iii). The red asteriks highlight the residues which are often involved in peptide interactions on the top of the propellor (ii). (Copyright © 2010, Elsevier, [Stirnimann et al., 2010])

several more or less conserved residues [Neer et al., 1994] [Smith et al., 1999] [Xu and Min, 2011]. Nevertheless, identification of WD40 repeats remains difficult as those domains are not very well conserved among each other. Often one or more repeats stay undetected by sequence analysis, whereas the structure reveals its presence [Stirnimann et al., 2010].

In general WD40 domains build a rigid framework for protein-protein interactions and moderate downstream incidents, such as ubiquitination [Xu and Min, 2011]. So far, no catalytic activity of WD40 domains themselves has been detected. But often they are fused to other functional active domains [Stirnimann et al., 2010]. Among the most common ones are domains known to be involved in ubiquitination, protein degradation, microtubule dynamics, phospholipid binding and vesicle coating. Therefore those proteins are able to

contribute in many different biological processes like apoptosis, cell cycle control, cytoskeletal adjustment and the regulation of vesicle trafficking, transcription or signal transduction [Xu and Min, 2011].

The structure of a WD40 propellor allows interactions at its top, the bottom or the side. Several peptide-protein and protein-protein interactions have been revealed, and most of the interactions take place at the top [Stirnimann et al., 2010]. The WD40 domain containing β-subunit of transducin, a protein consisting of three subunits which is involved in signal transmission, interacts with its α-subunit on the top and the side. The γ-subunit contacts the WD40 propeller from the bottom [Wall et al., 1995] [Lambright et al., 1996] [Sondek et al., 1996]. The residues mostly involved in interactions are marked in figure 1.7 with red asterisks. WD40 proteins are perfectly shaped to serve as hubs. For example CDH1, a WD40 protein, controls the ubiquitin ligase activity and the substrate specificity of the anaphase-promoting complex/cyclosome [Pfleger and Kirschner, 2000] [Stirnimann et al., 2010]. It communicates with many partners to execute its function. But not only proteins or peptides are interacting with WD40 domains. Also DNA can be a target for interaction. Some histone manipulating protein complexes are known to incorporate WD40 propellor proteins which can directly bind to nucleosomes [Suganuma et al., 2008] [Stirnimann et al., 2010]. It could also be shown that the WD40 propellor protein DDB2, which interacts with DDB1, a protein with three WD40 propellors, directly interacts with damaged DNA strands and participates therefore in the nucleotide excision repair machinery [Scrima et al., 2008]. DD1B and DD2B are highly conserved among eukaryotes, and in *Arabidopsis* they are known to be crucial for embryo development and needed throughout plant maturation [Bernhardt et al., 2010].

A control mechanism for WD40 proteins can be provided by exhibiting incomplete propellor structures which need to be completed by other proteins. For example SEH1 of the nuclear pore complex SEH1-NUP85 comprises a 6-blade propellor, whereas NUP85, with its three-stranded blade and a helical structure, completes the 7-blade propellor to build a stable and functional system [Hsia et al., 2007] [Brohawn et al., 2008].

Some proteins also exhibit a double-propellor structure. One example of such a protein is the yeast protein SRO7. It is crucial for the assembly of SNARE proteins, which are needed for fusion of secretory vesicles on the plasma membrane [Hattendorf et al., 2007]. The two propellors are rotated with respect

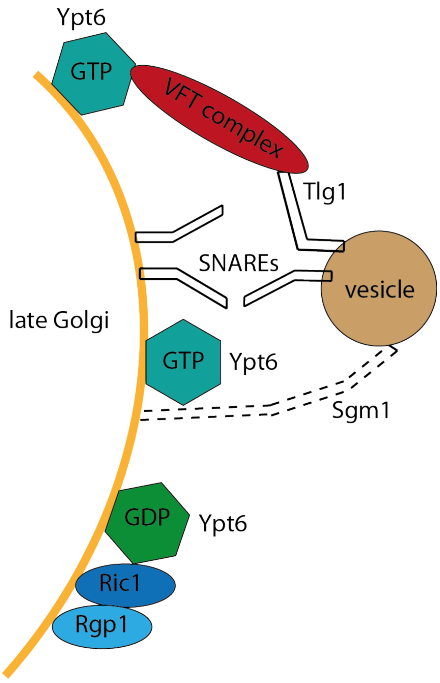

Figure 1.8: The role of RIC1 in the fusion of endosome-derived vesicles with the late Golgi. Ric1p and Rgp1p form a complex at the late Golgi which activates the GTPase Ypt6p by nucleotide exchange. The activated Ypt6p recruits the VFT complex which interacts with Tlg1p on vesicles. Subsequently, SNARE engagement and vesicle fusion follow. Another putative tethering factor is Sgm1p which can bind Ypt6p, but its role still has to be shown. (Adapted from [Siniossoglou and Pelham, 2001], Copyright © 2001, Rights Managed by Nature Publishing Group)

to each other and look like an open scallop.

1.3.2 RIC1 in yeast

Apart from the WD40 domain in *WIZ*, another superfamily, RIC1, could be detected. RIC1 is named after a protein identified in a mutant screen for proteins involved in **ri**bosomal **c**ontrol in *S. cerevisae* [Mizuta et al., 1997]. Defects in the *RIC1* gene interfere the transcription of ribosomal RNA as well as ribosomal protein genes [Mizuta et al., 1997]. It could be shown that a functional secretory pathway is important for ribosome synthesis [Mizuta and Warner, 1994]. Therefore, there was a strong indication that *RIC1* could be associated with membrane trafficking. In fact, later it could be shown that RIC1 builds a complex with RGP1 [Siniossoglou et al., 2000]. Together they are able to bind YPT6, a GTPase known to be involved in intracellular trafficking, which is required for the fusion of endosome-derived vesicles with the late Golgi [Siniossoglou and Pelham, 2001]. *In vitro* studies showed the ability of the

RIC1/RGP1 protein complex to provoke the guanine nucleotide exchange on YPT6. Therefore, it is likely that RIC1 is needed for the activation of YPT6 at the late Golgi membrane and is consequently a part of the fusion of vesicles to the Golgi. An overview of the fusion of a vesicle and the included players is shown in figure 1.8. Recently, a suppressor for YPT6 and RIC1, namely MYR, could be identified [Georgiev et al., 2008]. Furthermore, a homolog of *RIC1* in fission yeast was found to be involved in valproic acid (VPA) action, a drug used as anticonvulsant and mood stabiliser [Ma et al., 2010]. Unfortunately, so far nothing is known about proteins organized in the RIC1 superfamily in *Arabidopsis*.

1.4 Organ size control in *Arabidopsis thaliana*

Organ size is dependent on environmental conditions such as temperature or light, but also internal genetic characteristics are important. Given identical growth conditions, organ size within one plant species is nearby stable which indicates strong genetic control mechanisms. Some identified genetic regulators of organ size are involved in plant hormone signaling or they compile novel pathways. Others are transcription factors or control the cell cycle [Busov et al., 2008] [Krizek, 2009]. Organ size is controlled on cellular level, meaning organ proportions vary either due to cell proliferation or cell expansion. This includes cell widening and cell elongation. Control of organ size implies proportional expansion and proliferation. If this would be unbalanced also organ shape would be altered. The maintenance of leaf shape can be controlled by calculating the leaf index which is the ratio of length and width. Real regulators of organ size are therefore expected to show a nearby constant leaf index. Furthermore, the loss-of-function mutants should be smaller and gain-of-function mutants bigger [Anastasiou and Lenhard, 2007] [Krizek, 2009].

1.4.1 Transcription factors causing organs to grow

The *Auxin regulated gene controlling organ size (ARGOS)* and *AINTEGUMENTA (ANT)* are examples for transcription factors being positive regulators of organ size [Hu et al., 2003] [Krizek and Sulli, 2006] [Busov et al., 2008]. Respective loss-of-function mutants show smaller leaves, while overexpression leads to the opposite effect [Krizek, 2009]. *ANT* is known to promote organ size by extending the period of cell proliferation

[Mizukami and Fischer, 2000] [Anastasiou and Lenhard, 2007] [Krizek, 1999]. *ANT* and *ARGOS* are both involved in the auxin-regulated signaling cascade. The *ant* mutant can block *ARGOS* overexpression phenotype, which indicates *ARGOS* to be upstream of *ANT* [Busov et al., 2008]. An additional player in this pathway is the auxin-response factor *ARF2* which is thought to negatively regulate *ANT* expression [Schruff et al., 2006]. *ARF2* is known to be a transcription factor which represses auxin signaling [Okushima et al., 2005]. The *arf2* mutant shows larger leaves as well as bigger seeds, embryos, carpels and thicker stems [Schruff et al., 2006]. Its gain-of-function phenotype has not been described yet.

1.4.2 A receptor-like kinase in organ size control

The Ser/Thr kinase *TOR* (Target of Rapamycin) is an important player in organ growth in response to surrounding conditions, like stress or nutrient supply [Deprost et al., 2007]. *TOR* belongs to the phosphatidylinositol-3-kinase-related kinase (PIKK) family and could be found in two complexes *TORC1* and *TORC2* in yeast. In *Arabidopsis* only one ortholog of the *TOR* gene could be identified, *AtTOR*. *AtTOR* null mutants are embryo lethal [Menand et al., 2002], but RNAi lines, with a decreased expression level, show smaller leaves and roots whereas overexpression caused the opposite effect. By checking epidermal cells, an increased number could be detected [Deprost et al., 2007]. It could be shown that in *AtTOR* loss- and gain-of-function mutants *AtEBP1* expression is altered. *AtEBP1* is known to control cell growth and proliferation [Horvath et al., 2006]. An interesting fact is that its putative human ortholog is *ErbB-3*, an epidermal growth factor receptor binding protein. In humans *ErbB-3* is involved in many different regulatory processes like translational and transcriptional regulation and apoptosis [Zhang et al., 2005] [Ahn et al., 2006] [Squatrito et al., 2006]. *AtTOR* shows a decrease of polysome accumulation in the RNAi lines. It is furthermore shown to be involved in osmotic stress resistance. The RNAi lines are hypersensitive whereas the overexpression lines are resistant to high salt concentrations. Taken these results together, *AtTOR* seems to connect plant growth with external conditions, by regulation of translation [Deprost et al., 2007] [Krizek, 2009].

The TOR-kinase pathway is conserved throughout mammals, insects and yeast, were it is also known to control cell growth in constant touch

with environmental conditions [Arsham and Neufeld, 2006] [Krizek, 2009] [Soulard et al., 2009]. In yeast the *TOR* pathway is well understood which is the basis for the identification of conserved players in other organisms. In human, defects in the *mTOR* kinase lead to several severe deseases like cancer and diabetes. In Yeast two copies of the TOR kinase exist, present in two different complexes, TORC1 and TORC2. The proteins interacting in TORC1 and TORC2 are quite well known in mammals, whereas for *Arabidopsis* only Regulatory-Associated Protein of TOR 1A (RAPTOR1A) and RAPTOR1B as a homolog of the Yeast KOG1 and the mammalian RAPTOR gene were identified. It could be shown that *AtTOR* and *RAPTOR1* interact [Mahfouz et al., 2006] [Soulard et al., 2009]. *RAPTOR1* mutants, as well as *AtTOR*, are embryo lethal [Deprost et al., 2005] [Anderson and Hanson, 2005].

1.4.3 Of plants and animals

Also *KLUH (KLU)* promotes organ size by controlling cell division [Anastasiou et al., 2007]. *KLU* encodes the cytochrome P450 CYP78A5 whose catalytic activity has not been investigated any further but CYP78A1 in maize is known to be active in the omega-hydroxylation of fatty acids [Krizek, 2009] [Imaishi et al., 2000]. *KLU* expression is not completely correlated with mitotically active parts of the plant, and as KLU could not be shown to migrate it is hypothesized that KLU initiates a mobile signal which affects growth [Anastasiou et al., 2007]. *KLU* seems to be needed for sensing growth to control final size. If the *KLU* level is falling under a certain threshold, growth of the organ gets terminated. Actually this is similar to a growth model in *Drosophila melanogaster*. *Decapentaplegic (DPP)* expression forms a gradient in certain cells of the wing which promotes its growth [Affolter and Basler, 2007]. With *KLU* and *DPP* two possible mechanistic similarities between plants and animals in organ size control get enlightened. Furthermore *klu* mutant plants showed a faster initiation of new leaves [Wang et al., 2008]. This means, plants try to balance their biomass by producing more smaller leaves or less bigger leaves [Leishman, 2001] [Sargent et al., 2007].

1.4.4 The compensatory effect

Not all alterations on cell number or size result in drastically changed organ size. This is due to the so called compensation effect [Tsukaya, 2006]. For example the

cell number affecting genes *ANT* and *ANGUSTIFOLIA3 (AN3)*, for which the overall effect on leaf size is not that dramatic as the single cells grow bigger [Mizukami and Fischer, 2000] [Horiguchi et al., 2005] [Anastasiou and Lenhard, 2007]. This indicates a connection between cell number and postmitotic cell enlargement. Recent results showed that two pathways are responsible for the coordination of this connection [Kawade et al., 2010]. However, further investigation to identify the players is needed. Nevertheless, the effect of cell enlargement is not observed for all mutants with reduced cell number. *BIG BROTHER (BB)* plants for example, overexpressing this negative regulator of leaf size, show no compensation. BB is therefore thought to have some connection to the, so far missing, factor X which coordinates compensation [Disch et al., 2006] [Anastasiou and Lenhard, 2007].

1.4.5 Cell wall composition affects cell growth

Plant cells are embedded in a more or less rigid periphery, called the cell wall [Somerville et al., 2004]. Cell walls are needed to protect the protoplasts from mechanistic damage and allows them to build stable structures. Growth and morphology of the plant are tightly linked to its wall composition. Plants have a primary cell wall. Some cells (e.g. Xylem) also have a secondary one which is located inside of the primary wall to strengthen it. The most abundant biopolymer in cell walls is cellulose. Cellulose microfibrils are synthesized in the plasma membrane by the cellulose synthase complex and get embedded in a polysaccharide matrix afterwards. The matrix is composed of hemicelluloses and pectins. The main hemicelluloses are xyloglucan and arabinoxylan which form a tight and very strong network with cellulose by direct or indirect linking of the microfibrils [Fry, 1989] [Hayashi, 1989] [Talbott and Ray, 1992] [Carpita and Gibeaut, 1993]. The main pectins are rhamnogalacturonan I and II, homogalacturonan, xylogalacturonan and arabinan. The task of pectins is much more complex. They are known to form gel like structures to push microfibrils for growth reasons or to keep them in place when needed [Willats et al., 2001] [Vincken et al., 2003]. They are also the primary component of the middle lamella and they are the target of pathogens which try to invade the plant cell [Iwai et al., 2002]. Pectins and hemicelluloses are synthesized at the Golgi and are transported by vesicles to the extracellular matrix. As a dynamic adjustment of the cell wall during development is needed, it is no surprise that cell wall

composition is an important factor for cell shape and growth [Cosgrove, 2005].

1.4.5.1 Xyloglucan and cell growth

The hemicellulose xyloglucan is crosslinking cellulose microfibrils. Therefore, it is a major player in cell loosening by its degradation or it increases wall rigidity by crosslinking the microfibrils. Xyloglucan persists of a 1,4-β-glucan backbone with attached 1,6-α-xylosyl residues along the backbone [Cosgrove, 2005].

Xyloglucan heptasaccharide (XXXG) is able to loosen the plant cell wall as its presence is causing the xyloglucan endoglucanase (XET) to cleave the endogenous xyloglucan and form new crosslinks with XXXG [Hayashi and Kaida, 2011]. Cell wall loosening by XXXG could be shown to promote cell division and expansion in Tabacco cells [Kaida et al., 2010]. The overexpression of XET (*CaXTH3*) in *Arabidopsis thaliana* increased drought and salt tolerance, which might be due to closer linked xyloglucan fibers which increases cell wall strength [Cho et al., 2006]. Furthermore, the growth promoting hormone auxin was shown to increase the breakdown of xyloglucan [Labavitch and Ray, 1974] [Nishitani and Masuda, 1981]. Experiments on split *Pisum sativum* (pea) stems showed the influence of xyloglucans on cell elongation [Takeda et al., 2002].

Different phenotypes caused by a reduced amount of xyloglucans are known by now. Decreased levels of xyloglucans can be reached by overexpressing xyloglucanase or cellulase. Also the xyloglucan xylosyltransferase should cause complete absence of xyloglucan [Hayashi and Kaida, 2011]. The overexpression of poplar cellulase (*PaPopCel1*) in *Arabidopsis* as well as in *Paraserianthes falcataria* (sengon) caused enlarged leaves [Park et al., 2003] [Hartati et al., 2008]. In poplar it enhanced the growth of the complete plant [Shani et al., 2004]. The overexpression of *Asperigillus* xyloglucanse in poplar entailed faster growth due to further cell elongation [Park et al., 2004]. The knock-out of the xyloglucan xylosyltransferase (*AtXXXT*) in *Arabidopsis thaliana* involves different genes. *xxxt1* and *xxxt2* in *Arabidopsis* showed no obvious phenotypes as the amount of xyloglucan was not reduced too much, whereas the double mutant exhibits retarded growth and abnormal root hairs [Cavalier et al., 2008]. *xxxt5* showed shorter root hairs [Zabotina et al., 2008].

These results show that xyloglucans are a target for cell shaping and growth. The identification of potential control mechanisms will give new insights into size regulation *in planta*.

Chapter 2

Results

2.1 *SRF4* in organ size control

SRF4 (At3g13065) was demonstrated to be a positive regulator of leaf size [Eyuboglu et al., 2007]. In this thesis the aim was to concretize this result, to characterize *SRF4* molecularly and to identify potential downstream components of the *SRF4* signaling mechanism.

The *SRF* members are predicted to be receptor-like Ser/Thr kinases, which exhibit a various number of domains (see figure 2.2). *SRF4* is likely to be an atypical kinase which was tested with an *in vitro* kinase assay. The predicted transmembrane domain indicates the family members to be located in the plasma membrane. Moreover, a strong PEST signal suggests that the intracellular domain of *SRF4* can be cleaved and located elsewhere in the cell. To check whether this holds true, a reporter construct, where EGFP was translationally fused to the C-terminus of SRF4, was transformed to plants and analysed with confocal microscopy.

To get to know more about the biological role of *SRF4*, it was helpful to find out more about potential downstream targets. On that account, a Y2H-Screen was performed and among others *DLG* (At1g79870) and *WIZ* (At3g61480) were identified. *DLG* turned out to code for the cytosolic hydroxypyruvate-reductase. WIZ is a WD40 domain containing protein of unknown function.

To study *SRF4*, *DLG* and *WIZ* further, T-DNA or transposon lines as well as transgenic gain-of-function lines have been ordered or cloned (see section 4.1.3). For *SRF4* the lines *srf4-7* and *srf4-8* were used for closer studies. For *DLG* the lines *dlg-6* and *dlg-9* and for *WIZ* *wiz-1* and *wiz-2* have been subjects of

investigation. Their exact position in the genomic and protein sequence can be seen in table 2.1 and figure 2.1 and 2.2. For the close paralogue of WIZ, referred to as *WINZLING LIKE (WIZL)* T-DNA lines *wizl-1* and *wizl-2* were ordered and checked for phenotypes. Semi-quantitative RT-PCR revealed *srf4-8*, *dlg-6* and *wiz-1* to be no null alleles. They are likely to cause truncated proteins which are not functional. *wiz-2* could be shown to overexpress *WIZ* transcript (see transcript analysis in figure 2.3).

The results of the phenotypic characterization, the interaction studies and other biological and bioinformatical approaches can be seen in the following sections.

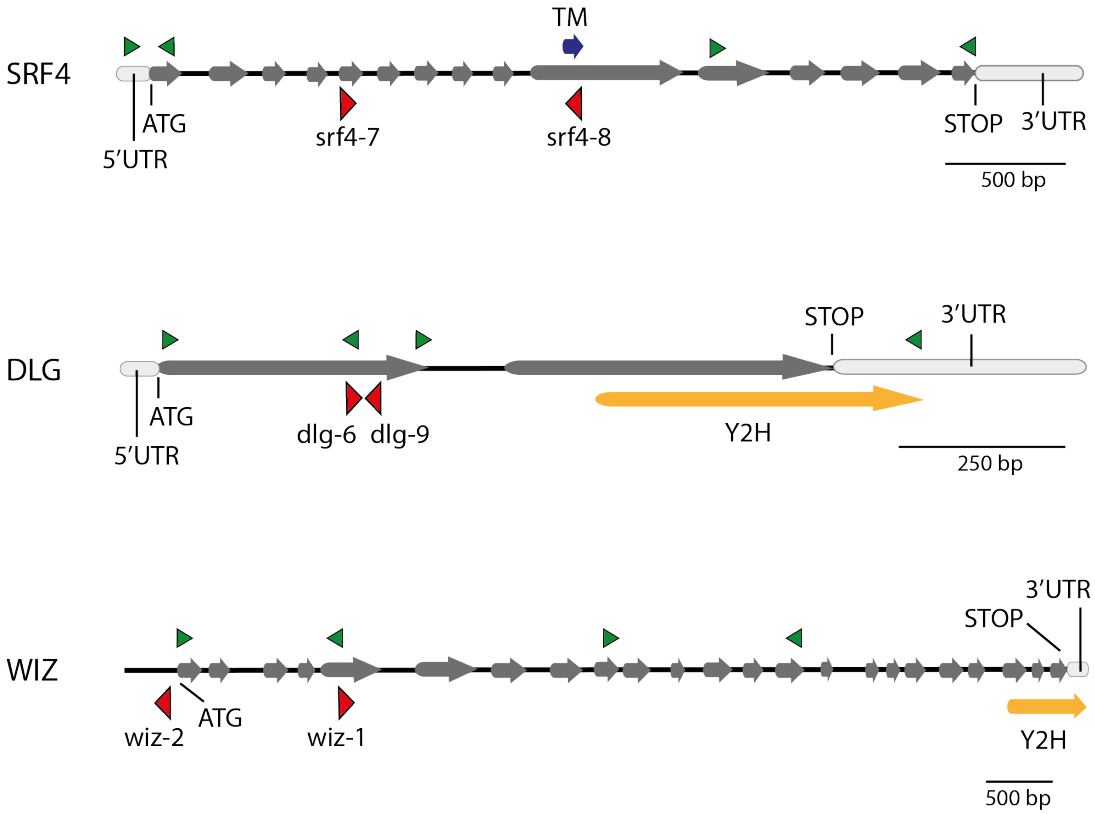

Figure 2.1: *SRF4*, *DLG* and *WIZ* gene structure. Dark grey arrows indicate exonic regions, light grey bars 5' and 3' UTR. Green arrows indicate primers used for transcript analysis, red arrows show T-DNA insertion sites. For DLG and WIZ the sequences used for the Y2H screen are labeled with yellow arrows.

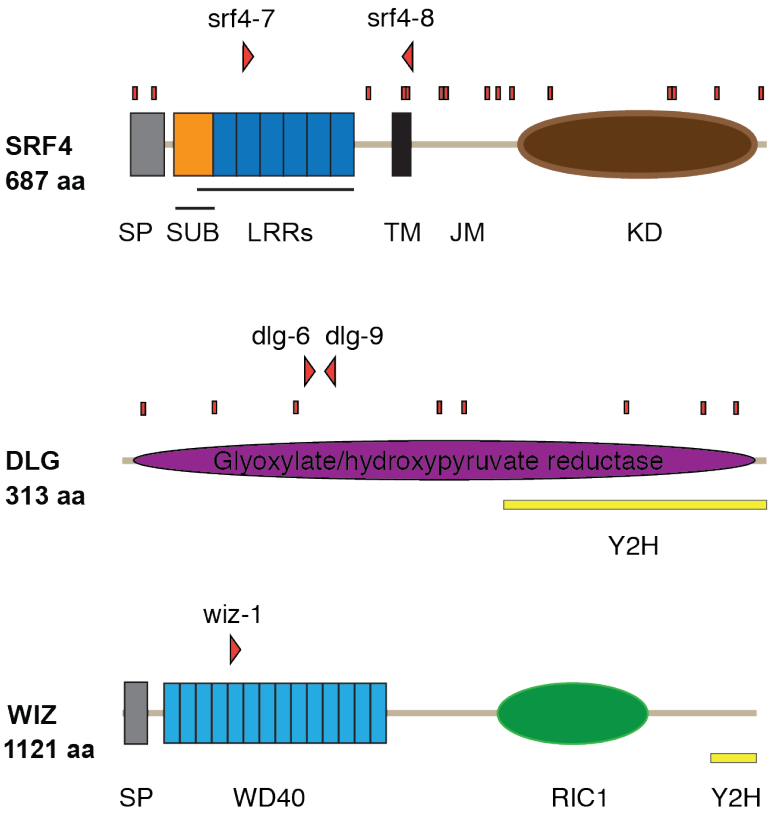

Figure 2.2: SRF4, DLG and WIZ protein structure. Red arrows: T-DNA insertion sites, yellow bars: part of the protein used for Y2H screen, SP: signal peptide, SUB: SUB-domain, LRR: leucine-rich repeat, TM: transmembrane domain, JM: juxtamembrane domain, KD: kinase domain, WD40: WD40 repeats, RIC1:RIC1-superfamily. The little red boxes above the domains of DLG and SRF4 indicate amino acid changes according to the 1001 genome project.

2.1.1 Phenotypic analysis of *SRF4*

The effect of *SRF4* on leave size was already shown by using two different T-DNA lines, *srf4-2* and *srf4-3*. Also a gain-of-function construct, where *SRF4* cDNA sequence was controlled by the *35S* promoter, was applied to check for influences on organ size. Unfortunately, *srf4-2* as well as *srf4-3* appeared to have problems with silencing of the phenotype. The *35S::SRF4* mutant lines also showed silencing effects in generation T4. Due to these problems, new T-DNA lines, *srf4-7* and *srf4-8* were ordered and analyzed. The *Arabidopsis* unrelated *35S* promoter was replaced by the *UBQ10* promoter and accordingly new gain-of-function mutant plants were generated.

Line name	Position	Additional bases	Stop codon	Protein Length
srf4-7	775 bp ds (Exon)	-	384 bp	128 aa
srf4-8	1733 bp ds(Exon)	-	-	∼300 aa
dlg-6	289 bp ds (Exon)	AGCTGCGGAC	396 bp	131 aa
dlg-9	298 bp ds (Exon)	-	-	∼100 aa
wiz-1	1196 bp ds (Exon)	T	573 bp	190 aa
wiz-2	118 bp us (Promoter)	-	-	1122 aa
wizl-1	613 bp ds (Intron)	-	-	1163 aa
wizl-2	176 bp us (Promoter)	TCTT	-	1163 aa

Table 2.1: Results of the T-DNA border investigation of the used plant lines in this thesis. ds = downstream of ATG of genomic sequence, us = upstream of ATG of genomic sequence, stop codon downstream of cDNA ATG, aa = amino acids, length of translated protein without stop codon.

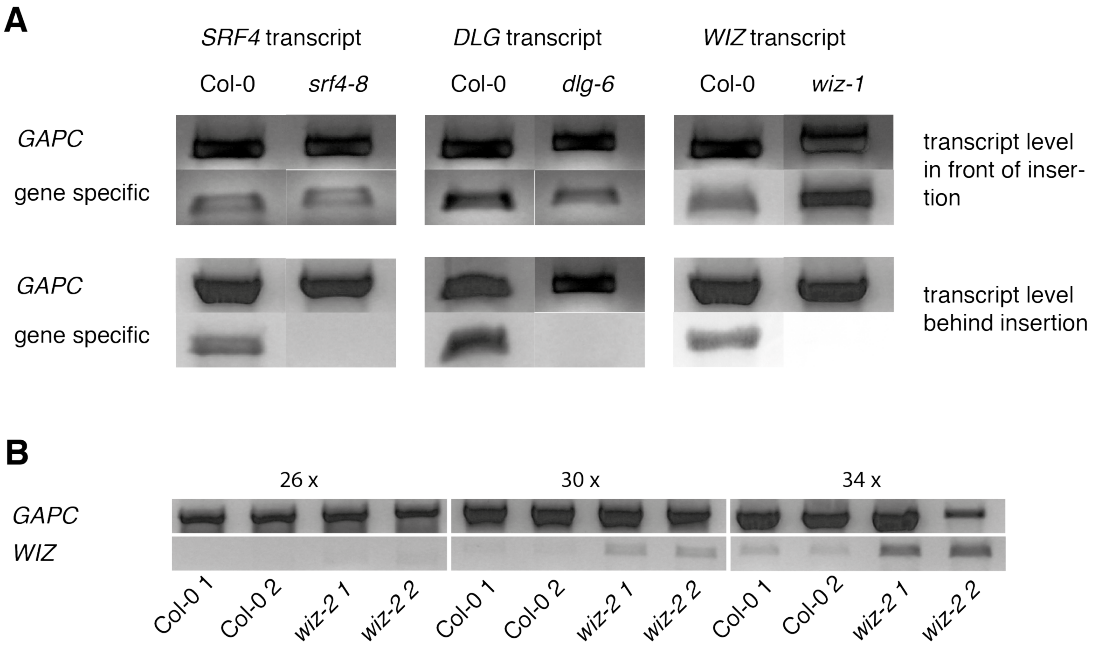

Figure 2.3: Transcript analysis of *srf4-8*, *dlg-6*, *wiz-1* and *wiz-2* in leaf tissue. A: For all three mutants transcript in front of the insertion can be detected, whereas behind the insertion none can be observed. B: Semi-quantitative PCR with two Col-0 and *wiz-2* samples after 26, 30 and 34 cycles.

srf4-8 could be shown to be no null allele, but to express a truncated version of the protein which is supposed to be inoperable. As it can be seen in figure 2.2, *srf4-8* abscises SRF4 directly behind the transmembrane domain which should make any kind of signaling impossible. The phenotype of *srf4-8* is quite variable. In cellar growth room, under 24 h light, a clear reduction of growth could be observed around 9 out of 10 times. In greenhouse, under long day conditions, it was mostly not visible. The unnatural growth conditions in the growth room

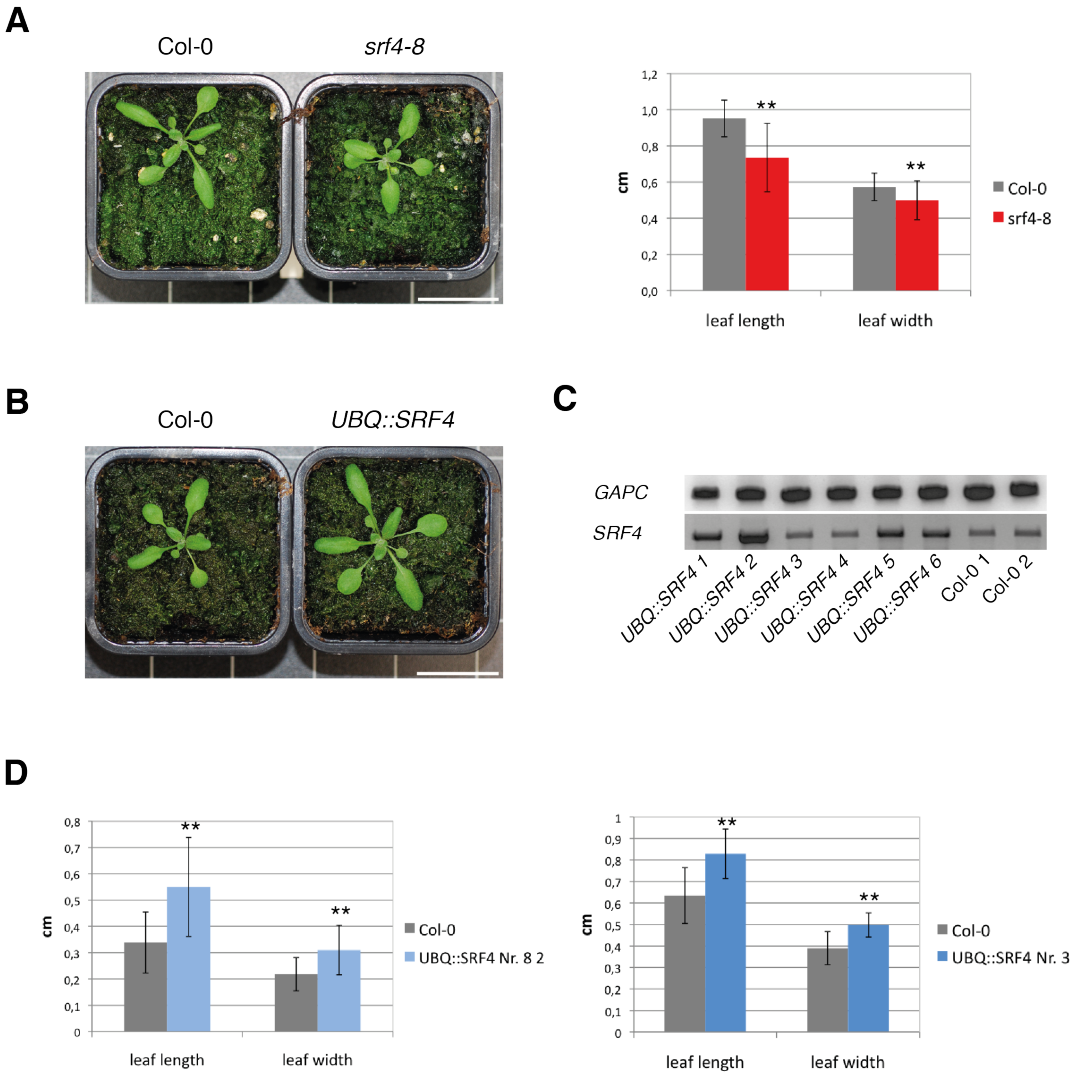

Figure 2.4: *SRF4* phenotype of the loss-of-function mutant and overexpression lines. A: Small leaf phenotype of *srf4-8* and the according measurements of the 5th rosette leaf of 20 plants grown in cellar growth room for 14 days. B: Gain-of-function mutant *UBQ::SRF4* exhibits bigger leaves. C: Semi quantitative RT-PCR of *UBQ::SRF4* sterile plant lines (1-3) and fertile lines (4-6). D: According measurements of 20 *UBQ::SRF4* plants of 2 different mutant lines, grown in greenhouse for 16 days. Asterisks indicate statistically significant differences, ** $p < 0.01$. Scale bar: 3 cm.

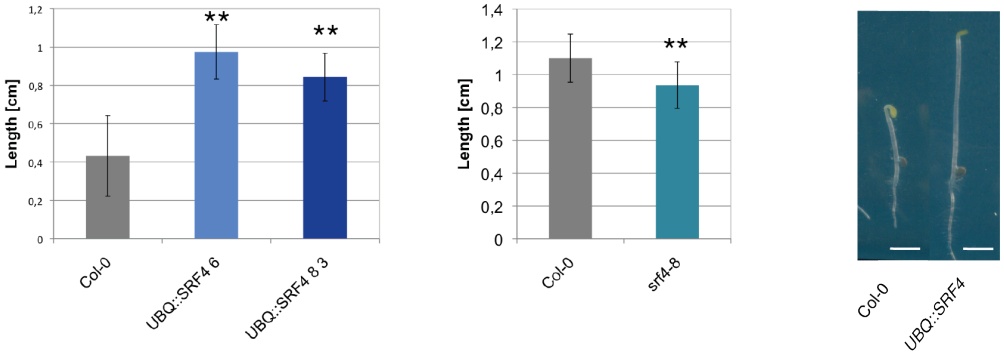

Figure 2.5: *SRF4* hypocotyl phenotype. Measurements of two independent gain-of-function mutants show clearly an increase in growth. *srf4-8* is slightly smaller compared to Col-0. Measured hypocotyls were grown 3 d in dark. Asterisks indicate statistically significant differences, ** $p < 0.01$. Scale bar: 0.26 cm.

might cause stress to the plant, a situation were the lack of *SRF4* might be of importance. The expression of *UBQ::SRF4 in planta* led to bigger rosette leaves. It can be excluded that the leaves are bigger due to early germination. Preliminary results indicate no changes in endoreduplication of *35S::SRF4* plants and therefore likely also not for *UBQ::SRF4* (data not shown). In general, the phenotypes of the new loss- and gain-of-function mutants confirmed the former results. The measurements and pictures of the phenotypes can be seen in figure 2.4.

As dark grown hypocotyls mostly elongate due to cell elongation as to cell proliferation [Gendreau et al., 1997] [Saibo et al., 2003], the mutant lines were analyzed for their phenotype on dark grown hypocotyls. Indeed, a clear effect could be observed for the gain-of-function lines. Plants carrying the *srf4-8* allele showed only a slight growth reduction. But also this decrease of hypocotyl length showed variability and was not as stable as the gain-of-function phenotype. Nevertheless, this result indicates an effect of *SRF4* on cell elongation.

Another interesting observation was the fact that around 20 % of *UBQ::SRF4* T1 plants showed sterility. That means siliques did not elongate properly. The immediate question to answer was whether a problem with the male or the female reproductive organs occurs. While having a closer look at the foral organs an obvious defect with anther dehiscence could be observed (see figure 2.7). As ovules, carpel and filaments looked normal this was assumed to be the source of sterility. The next question that arose was if closed anthers had pollen inside

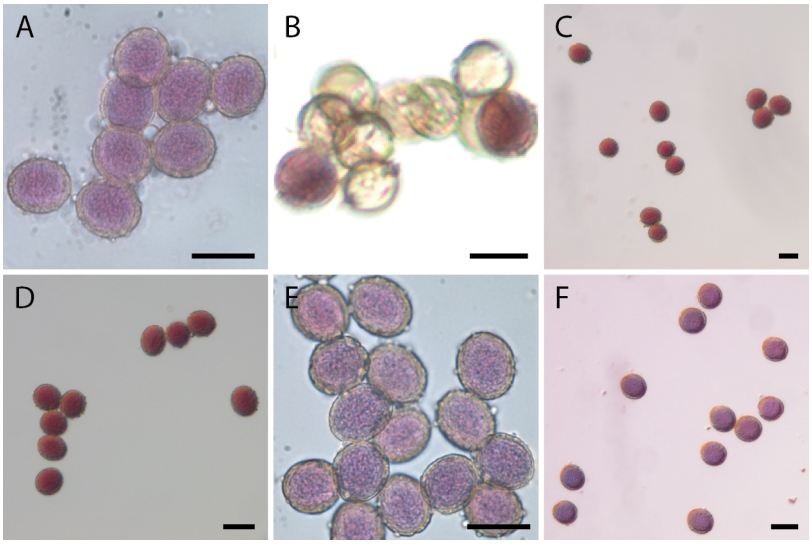

Figure 2.6: Pollen after staining with Alexander solution. All pollen grains, except the negative control, look like wildtype. A: positive control Col-0, B: negative control *wuschel-1 (wus-1)*, C: *UBQ::SRF4*, D: *35S::SRF4:EGFP*, E: *UBQ::DLG:EGFP*, F: *wiz-2*. Scale bar: 30 µm.

and, if yes, if the pollen was fertile. Accordingly, anthers were opened and the pollen was stained with Alexander solution which revealed viable pollen (see figure 2.6).

But why do 20 % of the plants show sterility? The assumption was that those transgenic plants exhibit an extraordinary high transcript level and cause therefore the phenotype. To confirm this hypothesis the RNA of three different sterile T1 lines compared to three different fertile plants was extracted and analyzed by semi- quantitative RT-PCR. All 6 lines showed a stronger expression of SRF4, but an extraordinary high level of SRF4 in the sterile lines could not be observed (see figure 2.4 C). Moreover, the expression of *SRF4* under its endogenous promoter also showed 20 % sterile T1 plants. Consequently, the distribution of sterile to non sterile plants is stable even when using another promoter. Again, transheterozygote plants between a sterile and a fertile T1 *UBQ::SRF4* plant did not support this assumption. Only ∼9 % showed sterility, whereas 50 % sterile plants should be observable if the transcript level theory holds true. The explanation why some plants are sterile and most are fertile remains therefore unclear and needs further investigation.

On each sterile plant 2-3 flowers were able to open their anthers and around 50-100 seeds could be collected. Investigation of the flowers of *UBQ::SRF4* revealed bigger sepals and petals which can be seen in figure 2.7. Another

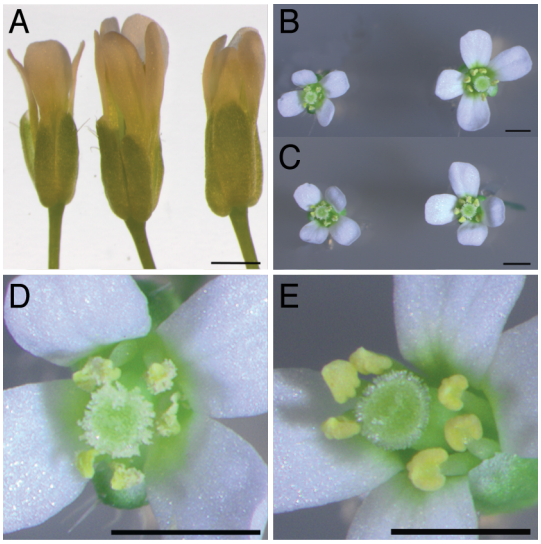

Figure 2.7: Flower phenotype of *UBQ::SRF4*. A: (from left to right) Col-0, *UBQ::SRF4* line Nr. 1 (sterile), *UBQ::SRF4* line Nr. 6 (fertile); B: left Col-0, right *UBQ::SRF4* line Nr. 1 (sterile); C: left Col-0, right *UBQ::SRF4* line Nr. 6 (fertile), D: close-up of Col-0 anthers; E: *UBQ::SRF4* line Nr. 1 with problem in anther dehiscence. Scale bar A-E: 1 mm

obvious observation was the fact that sterile plants seem to show a more severe size phenotype compared to fertile plants. This holds true for rosette leaves as well as for flowers.

2.1.2 SRF4: an atypical kinase?

As it was mentioned previously, proteins which exhibit a kinase domain are not necessarily able to phosphorylate other proteins or themselves. Alternative signal transduction mechanisms can take over and lead to a similar result (see section 1.1.4). SUB could be shown to be an atypical kinase. As *SRF4* bears substitutions at conserved amino acid residues important for kinase activity, it was interesting to test if *SRF4* is also an atypical kinase. The first attempt to answer this question was to perform an *in vitro* kinase assay. Second, a mutated kinase dead version of *SRF4*, was transformed to plants. The results are outlined in the following sections.

2.1.2.1 *In vitro* kinase assay of SRF4

To address the question whether *SRF4* is an active or an atypical kinase, like e.g. ErbB-3, an *in vitro* kinase assay was performed. As a transmembrane spanning RLK, *SRF4* bears an extra- and an intracellular part. The cDNA

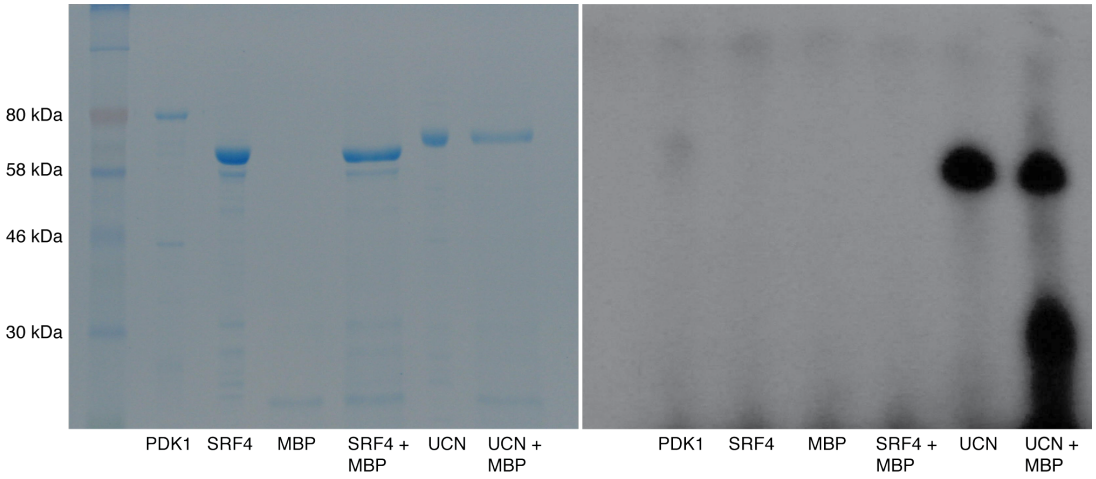

Figure 2.8: Kinase assay of *SRF4*. As positive controls PDK1 and UCN were used. SRF4 does not show any activity.

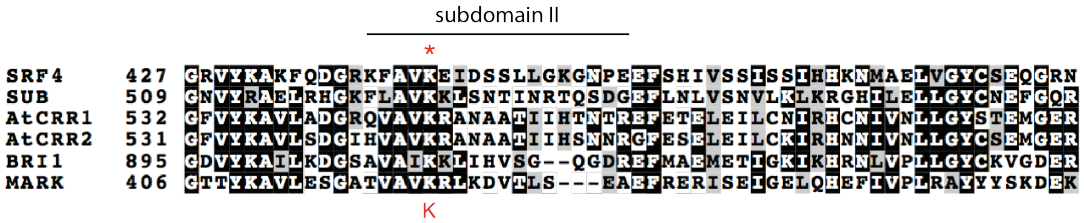

Figure 2.9: Multiple alignment of kinase subdomain II of different active and atypical kinases. The positively charged lysine (K) at position 443 of SRF4 is highly conserved.

sequence of the intracellular fragment, referred to as $SRF4_i$, was fused to GST and recombinantly expressed in *E. coli*. Subsequently, the fusion protein of around 69 kDa was purified via its GST tag and incubated with γ-^{32}p ATP. As positive controls PDK1 and UNICORN (UCN) were used [Deak et al., 1999]. GST:$SRF4_i$ was additionally incubated with the Myelin Basic Protein (MBP), a protein known to be useful as a general substrate in *in vitro* kinase studies. The assay was repeated 5 times and no signal for *SRF4* could be detected (see figure 2.8).

2.1.2.2 The kinase dead version of SRF4 yields no transformants

To confirm the result of the kinase assay, indicating SRF4 to be an atypical kinase, a kinase dead version of SRF4 ($UBQ::SRF4_{KD}$) was cloned and transformed to plants. For that purpose the conserved alkaline amino acid lysine (K), at position 443 in the kinase subdomain II of SRF4, was changed to the negatively charged glutamic acid (E) (see alignment in figure 2.9). Lysine in subdomain II is in active kinases known to coordinate the α and β phosphates

of ATP for catalysis [Huse and Kuriyan, 2002]. It could be shown that an exchange of this residue causes the loss of kinase activity [Hanks et al., 1988]. If SRF4 is an atypical kinase the expected result would be that this amino acid change would not have any influence on *UBQ::SRF4* phenotype in plants. Unfortunately, no transformants could be obtained even after 3 independent trials. In parallel, with another construct, transformed plants produced transgenic seed. This suggest that the kinase dead version of SRF4 has direct influence on the transformed cell and might be lethal. The reason for this remains unclear and can only be conjectured. This point is therefore left for discussions (see section 3.1).

2.1.3 SRF4 is located in the plasma membrane and in the nucleus

To check for the localization of proteins a well established method is to fuse them N- or C-terminally with the enhanced green fluorescent protein (EGFP). Those fusion proteins can be controlled by either their native promoter or, e.g. overexpression promoters like *35S* or *UBQ10*. To have a closer look throughout different tissues confocal laser scanning microscopy (CLSM) was used. With this technique different tissues could be examined and the localization of SRF4 protein was resolved.

SRF4 is predicted to be a RLK which exhibits a transmembrane domain and is therefore prognosticated to be located in the plasma membrane. To check this assumption a *SRF4::SRF4:EGFP* and *35S::SRF4:EGFP* construct were cloned and transformed into plants. As native promoter the 500 bp long intergenic region in front of the ATG was chosen. Interestingly no signal could be detected for the endogenous EGFP construct *SRF4::SRF4:EGFP*. Different tissues, including flowers, in T1 and T2 were investigated, but for none any signal could be observed. Plants transformed with *SRF4::SRF4:EGFP* showed around 20 % sterile plants in T1. As this is the exact phenocopy of the *35S::SRF4* overexpression construct, the expression of the transcript was likely. It seems that *SRF4* is naturally expressed only at a very low, not detectable level, and that changes cause immediate problems with sterility.

For the *35S::SRF4:EGFP* construct a signal in the plasma membrane could be observed. Plasmolysis was applied to make sure that the signal appears in the plasma membrane and not in the cell wall. Plasmolysis is happening by applying

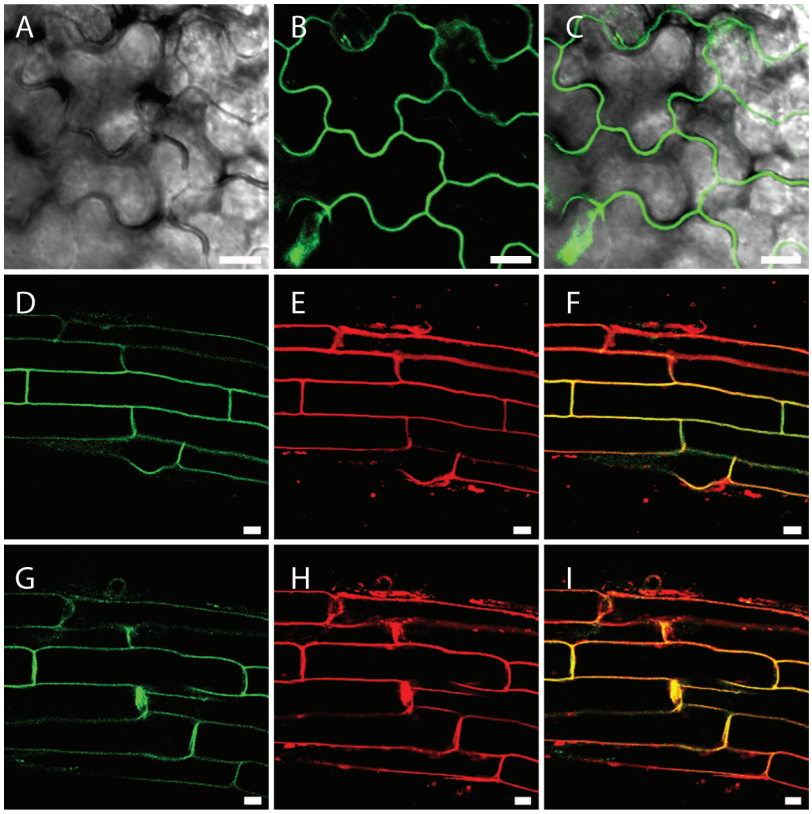

Figure 2.10: Signal of the *35S::SRF4:EGFP* construct. A-C: Localization in leaf epidermal cells. A: Bright Field. B: EGFP signal. C: Overlap of A and B. D-F: Root epidermal cells before plasmolysis. G-I: Root epidermal cells after plasmolysis. D, G: EGFP signal. E, H: FM4-64 signal; F, I: overlap of EGFP and FM4-64. Scale bar: 10 µm.

a hypertonic solution which causes a shrinkage of the plasma membrane due to osmosis whereas the cell wall stays stable. For SRF4 it could be clearly seen that it does not belong to the apoplast (see figure 2.10). As it is co-located with the plasma membrane marker FM4-64, it could be shown that it appears in the plasma membrane. Plants transformed with *35S::SRF4:EGFP* showed also problems with anther dehiscence in T1. The pollen could be shown to be viable (see figure 2.6 D).

An interesting observation was also that SRF4, even when controlled by the *35S* promoter, could be detected only in the epidermis of leaves and the root elongation/differentiation zone. This is a hint at a regulatory mechanism which controls protein localization of *SRF4*. This might be either a post transcriptional effect or some degradation mechanism on protein level. A control mechanism on protein level is possible as SRF4 has a strong intracellular PEST signal [Eyuboglu, 2008]. This signal is likely to be involved in degradation of proteins [Rogers et al., 1986]. If this assumption holds true, SRF4 might be detectable

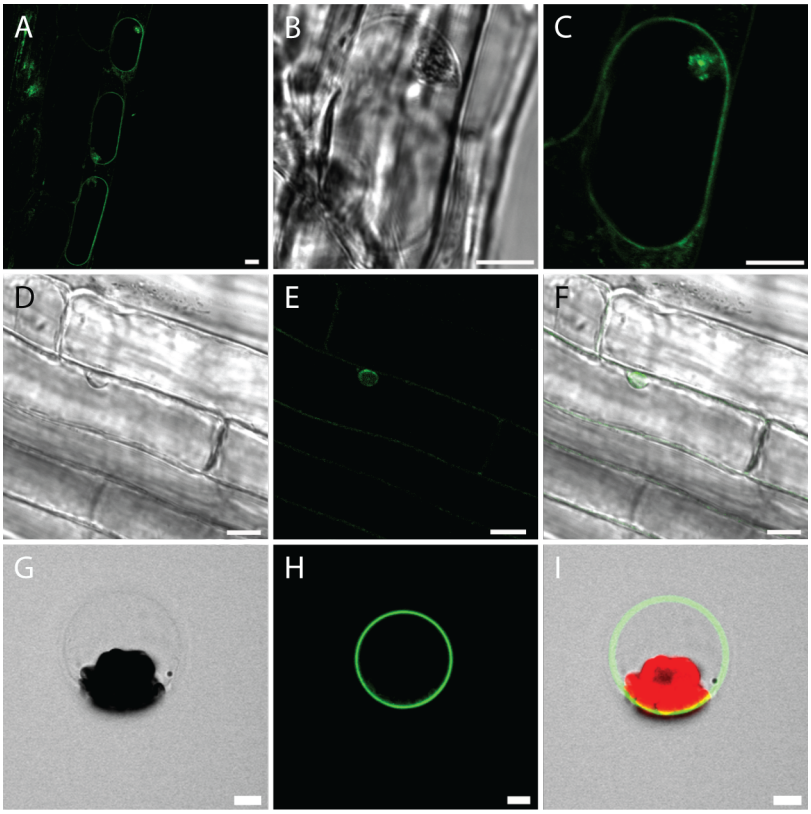

Figure 2.11: Signal of *35S::SRF4:EGFP* in the nucleus of root cells and in mesophyll protoplasts. A-C: EGFP signal of SRF4 after plasmolysis in the root. A: Three cells in a row show the signal in the compartment. B: Bright Field zoom of the upper of the three cells in A. C: EGFP signal of the cell in B. D-F: Root cell showing signal in the nucleus. D: Bright Field. E: EGFP signal: F: overlap of D and E. G-I: *35S::SRF4:EGFP* signal in protoplasts, G: bright field. H: EGFP. I: Overlap bright field, EGFP and auto fluorescent red chloroplasts. Scale bar: 10 µm.

not only in the plasma membrane but also in cell compartments involved in degradation processes. Indeed, a signal could be observed in independent transgenic lines in an organelle that might be the nucleus. Initially, this signal was observed after plasmolysis which might be very likely to happen due to stress. But after a closer inspection of normal root cells it was also detectable there. In figure 2.11 one can see the compartment in which SRF4 could be visualized.

2.1.4 *SRF4::GUS* staining pattern

To check where the promoter of *SRF4* is active, and therefore were the protein is likely to be expressed, the promoter GUS construct has been cloned and transformed to plants. The 500 bp long intergenic region in front of the ATG was taken as promoter region. For the analysis more than 20 transgenic lines

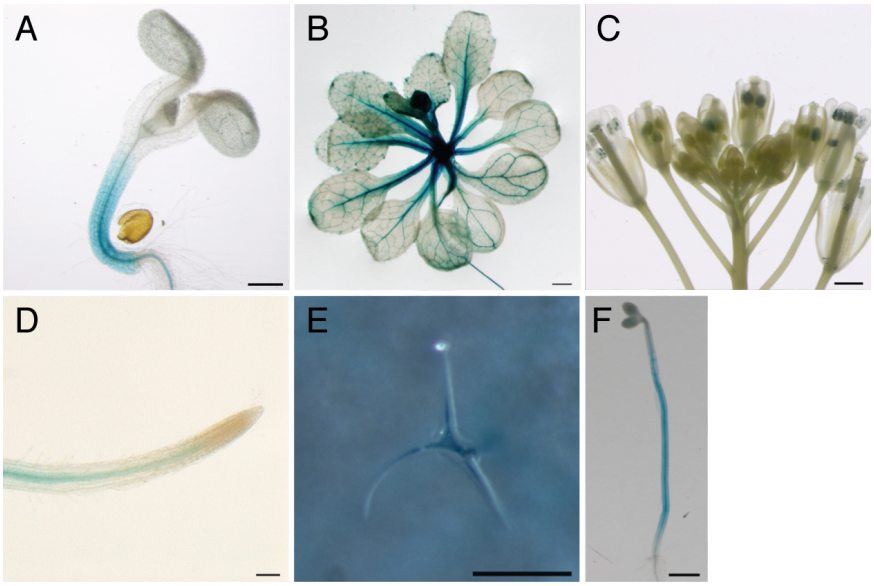

Figure 2.12: GUS pattern of *SRF4*. A: 10 d old seedling. Staining in the entire hypocotyl and in the cotyledon veins is visible. B: 20 d old seedlings. A strong staining in the leaf veins as well as in the marginal meristems can be observed. C: Staining of flowers. A strong staining in older anthers or rather pollen can be seen. In young pollen no staining is visible. D: *SRF4::GUS* shows staining of the vascular root tissue in the elongation and differentiation zone but no staining in the root tip and in the division zone. E: A strong trichome coloration throughout all leaf stages can be seen. F: 3 d dark grown hypocoytls show a staining according to RT-PCR results. Scale bar A, B, C, F: 1 mm. Scale bar D, E: 250 µm.

have been stained and scanned under the microscope. Figure 2.12 shows an overview of the *SRF4::GUS* staining pattern in different developmental stadiums and organs.

The *SRF4* promoter is active in different tissues. In younger seedlings a strong expression in the hypocotyl, as well as a weaker one in the vascular system of the cotyledons, could be observed. It can also be seen that in the youngest leaves of the seedling no expression is visible. In older seedlings a clear staining in the vascular bundles in addition to a weak staining throughout the whole leave tissue is detectable. Furthermore a clear staining in well defined spots at the leaf margin is obvious. Those spots are likely to be the marginal meristem. Marginal meristems are known to be regions of meristematic active tissue at the margins of leaf primordia. Those spots give rise to mesophyll and epidermis cells. No staining in the very early leaf developmental stages could be observed. Hence, *SRF4* is likely to be exclusively expressed during later leaf development when cell expansion contributes more to organ growth than cell division [Tsukaya, 2005].

In flowers, *SRF4* is expressed in mature pollen. In the very young flowers

and other floral organs rarely an expression could be detected. In roots, *SRF4* is clearly expressed only in the elongation/differentiation zone. There, the signal is limited to the vascular bundle. No signal in the root hair could be detected. In the lateral roots the same signal as in the main root was detectable.

Another interesting observation was made when looking at the trichomes. Those epidermal cells were strongly stained throughout all leaf developmental stages. Even in the very young leaves a staining of the very first trichomes could be seen. Trichomes did not show any obvious phenotype, neither for the loss- nor for the gain-of-function mutants.

As a strong phenotype in dark grown hypocotyls could be observed for *SRF4* transgenic plants, etiolated hypocotyls were also stained and an activity of the promoter could be shown there, too.

2.1.5 1001 genomes sequence analysis

The SRF4 amino acid sequence was checked for polymorphisms in other *Arabidopsis thaliana* accessions with benefit of the 1001 genomes project [Cao et al., 2011]. Due to sequence uncertainties, out of the 80 sequenced accessions, 67 could be used for this analysis. SRF4 revealed 15 polymorphisms. They are distributed throughout the protein, except for the region of the leucine-rich-repeats (see figure 2.2). This indicates that this region might be important for ligand binding and alterations might disturb this mechanism. Interestingly, the LRRs are not highly conserved within the *SRFs*. Detailed information about the polymorphisms can be found in table 2.2.

Position	Polymorphism	Accession
2	G→A	HKT2.4, ICE106, ICE111, ICE21, ICE216, ICE36, ICE63, ICE92, Pra-6, TueSB30-3, Bak-2, ICE138, ICE152, ICE163, ICE169, ICE213, ICE33, ICE75, ICE98, Istisu-1, Lag2.2, Mer-6, Nemrut-1, Nie1-2, Rue3-1-31, ICE91, ICE119, ICE72, Bak-7, Xan-1, Don-0, Ped-0, ICE60, ICE61, ICE7, ICE70, ICE71, ICE73, ICE102, ICE104, ICE107, ICE112, ICE127, ICE173, ICE181, ICE212, ICE29, ICE49, ICE50, ICE93, Qui-0, Vie-0, ICE1, Agu-1, Ey15-2, Star-8, ICE130, ICE134, Sha, Yeg-1
24	L→F	Ey15-2, Star-8, ICE130, ICE134, Sha, Yeg-1
258	R→H	ICE91
296	I→V	Star-8, Ey15-2
297	A→G	ICE60, ICE61, ICE7, ICE70, ICE71, ICE73
336	D→N	Bak-2, ICE138, ICE152, ICE163, ICE169, ICE213, ICE33, ICE75, ICE98, Istisu-1, Lag2.2, Mer-6, Nemrut-1, Nie1-2, Rue3-1-31, ICE91
338	M→T	ICE72
386	D→N	Bak-7, Xan-1
398	R→C	Don-0, Ped-0
412	A→T	ICE60, ICE61, ICE7, ICE70, ICE71, ICE73
455	P→L	Ey15-2, Star-8
586	D→Y	Del-10, HKT2.4, ICE106, ICE111, ICE21, ICE216, ICE36, ICE63, ICE92, Pra-6, TueSB30-3
587	P→L	Don-0
635	M→L	ICE119
684	K→M	Don-0, Ped-0

Table 2.2: SRF4 amino acid polymorphisms in different *Arabidopsis thaliana* accessions. 67 out of 80 sequences were used for the alignment, 15 polymorphisms could be found. Positional numbering is according to the N-terminal methionine of SRF4.

2.1.6 Evolution of *SRF4* and *SRF5* in *Viridiplantae*

SRF5 is the closest orthologue of *SRF4* within the *Strubbelig Receptor Family*. To get an idea how their evolution in plants proceeded, a sequence similarity based clustering approach (orthoMCL [Li et al., 2003]) was applied to generate gene families across the *Viridiplantae* kingdom. For the genes under investigation the gene clusters were extracted and organized in a phylogenetic tree (see methods 4.2.7 for details). An overview of the used plant genomes can be seen in table 2.3.

Genome
Arabidopsis thaliana (mouse-ear cress)
Brachypodium distachyon (purple false brome)
Brassica rapa (trunip rape)
Carica papaya (papaya)
Chlamydomonas reinhardtii (green algae)
Glycine max (soybean)
Medicago truncatula (barrel clover)
Oryza sativa (rice)
Physcomitrella patens (moss)
Selaginella moellendorffii (spikemoss)
Solanum lycopersicum (tomato)
Sorghum bicolor (sorghum)
Vitis vinifera (grapevine)
Zea mays (maize)

Table 2.3: *Viridiplantae* genomes used for calculation of phylogenetic trees.

Due to their sequence similarity *SRF4* and *SRF5* got organized in one cluster by orthoMCL. The following phylogenetic tree analysis revealed that no copy could be found in the basal plant genomes *Selaginella moellendorffii*, *Physcomitrella patens* and *Chlamydomonas reinhardtii*. This might be due to different reasons. Either an ortholog still exists, but could not be detected by orthoMCL as sequence similarities disappeared due to mutations over time. Or the gene is completely absent in algae, mosses and spike-mosses and originated in higher plants.

The subtree of *SRF5* nicely reproduces the currently accepted taxonomy. Monocotyledons, Fabaceae as well as Brassicales build a separate clade, with each one copy of *SRF5*. *SRF5* seems to be structurally and likely also functionally conserved throughout these genomes.

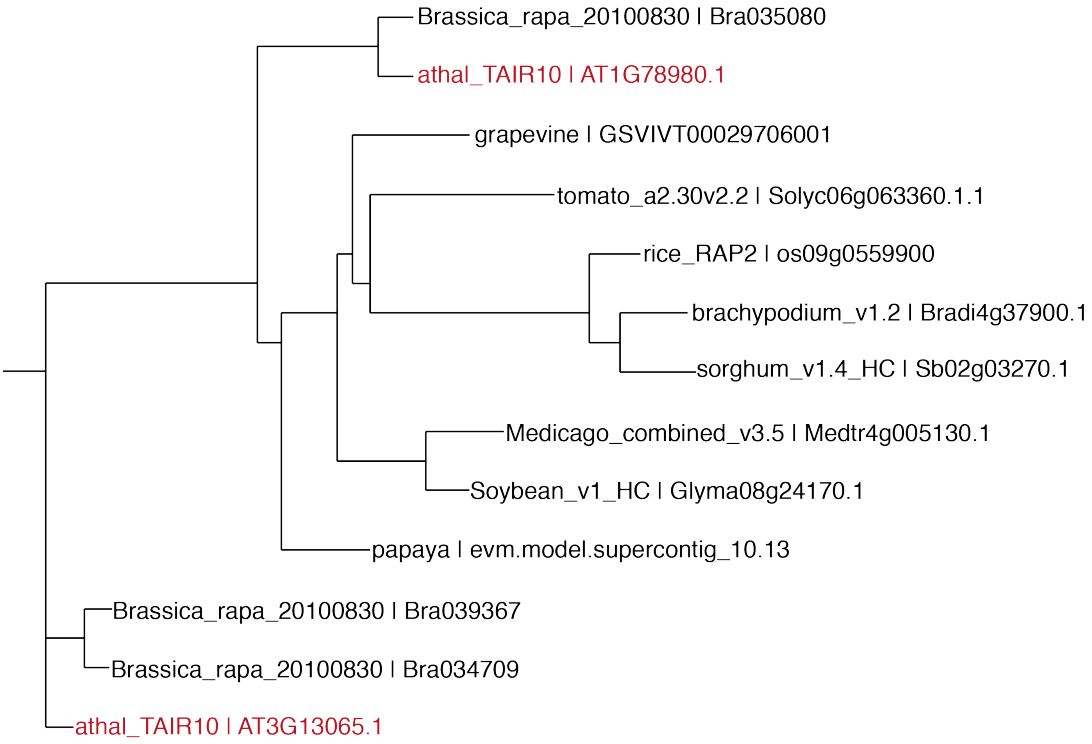

Figure 2.13: Phylogenetic tree of *SRF4* (At3g13065) and *SRF5* (At1g78980) in *Viridiplantae*. The red color indicates the position of both *Arabidopsis* genes in the tree.

Furthermore this tree suggests that *SRF4* might be only conserved in Brassicales. In *Brassica rapa SRF4* seemed to be duplicated. This finding corresponds with the postulated ancient genome triplication and ongoing gene loss [Wang et al., 2011].

2.2 The hydroxypyruvate-reductase *DLG*: a potential downstream partner of *SRF4*

To understand the function of *SRF4* in diverse developmental processes it is interesting to know with which proteins SRF4 might interact. For this purpose a Y2H screen with the intracellular part of SRF4 against a cDNA library was performed. The hydroxypyruvate-reductase *DLG* was identified as a potential interaction partner and was hence the aim of further investigations. An *in vitro* GST-pull down assay, different genetic approaches and reporter-gene experiments were performed to confirm the interaction and to find out more about the function of *DLG* in the *SRF4* signaling pathway.

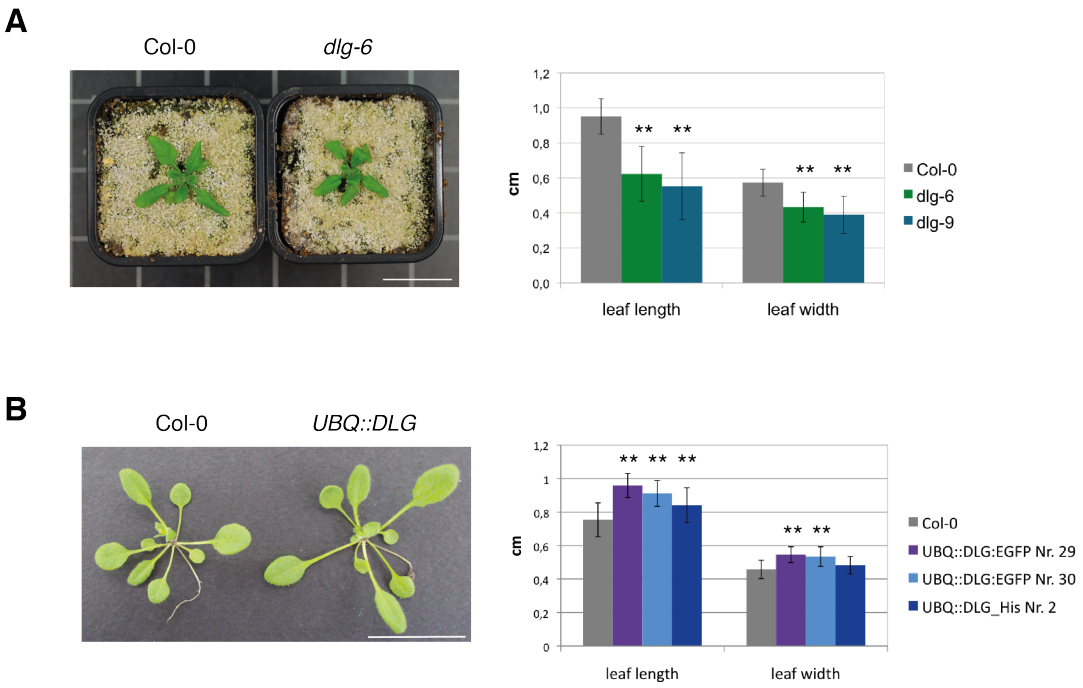

Figure 2.14: *DLG* phenotype of the loss-of-function and the overexpression mutants. A: Small leaf phenotype of *dlg-6* and the according measurements of the 5th rosette leaf of 20 plants grown in cellar growth room for 18 days. B: Gain-of-function mutant *UBQ::DLG* exhibits bigger leaves. According measurements of 20 plants of 3 different mutant lines, grown in greenhouse for 18 days, are shown. Asterisks indicate statistically significant differences, ** $p < 0.01$. Scale bar: 3 cm.

2.2.1 *DLG* phenocopies *SRF4*

The initial attempt was to order according T-DNA lines and to investigate the gain-of-function mutants of *UBQ::DLG*. The loss-of-function mutant lines *dlg-6* as well as *dlg-9* showed a reduction of leaf size. Plants, transformed with *UBQ::DLG*, showed an increase of leaf size. Pictures of the phenotype and the according measurements can be seen in figure 2.14. As *SRF4* showed a quite prominent phenotype on dark grown hypocotyls, *DLG* mutants were also checked for a phenotype in this organ. Two independent *UBQ::DLG* transgenic lines showed a clear increase in length. *dlg-6* caused a slight reduction in growth (see figure 2.15). But this reduction was not as stable as the gain-of-function phenotype and could not be observed always. Consequently, *DLG* phenocopies *SRF4* in leaves as well as dark grown hypocotyls, which indicates a possible connection between both genes. Neither the *DLG* nor the *SRF4* mutant lines showed any atypical answer to gibberelin or auxin on dark grown hypocotyls (data not shown).

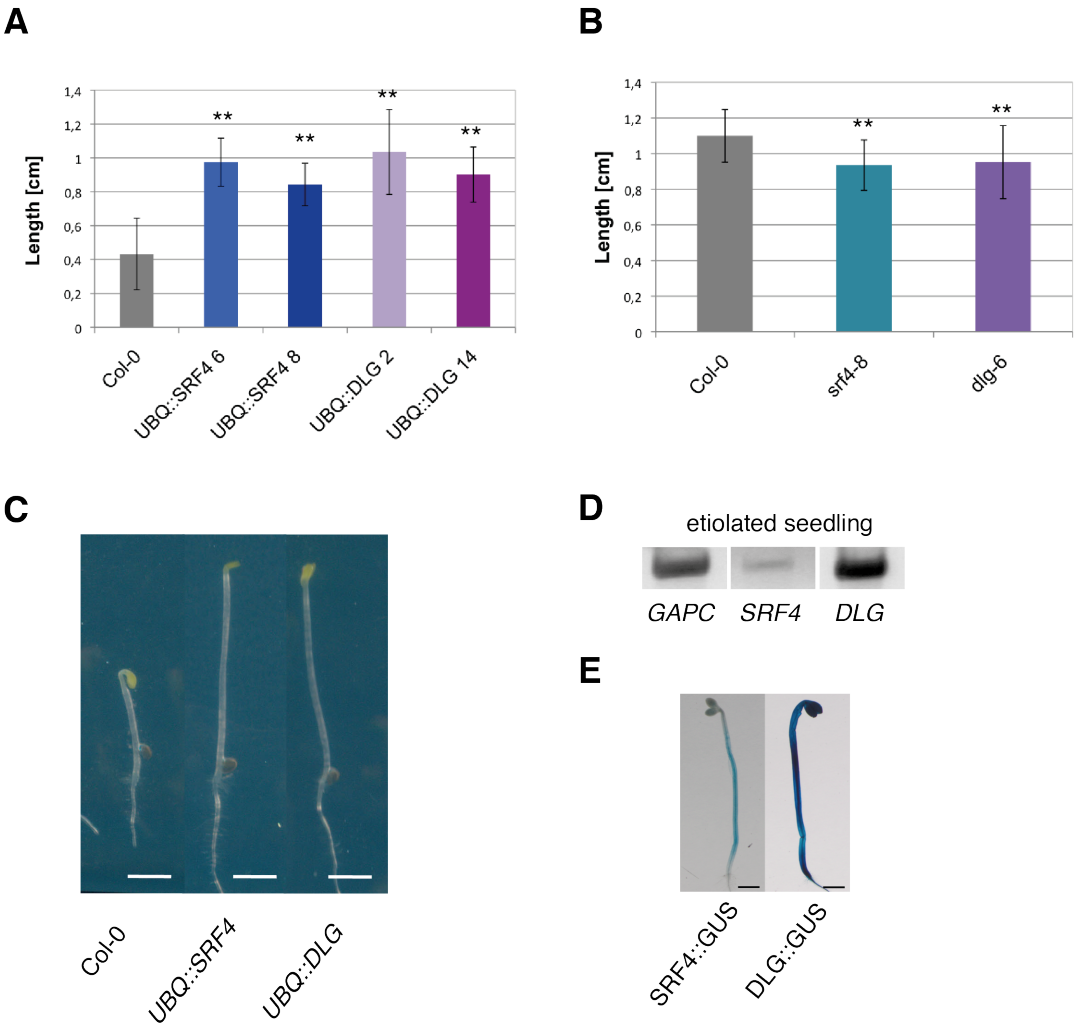

Figure 2.15: *SRF4* and *DLG* hypocotyl phenotype. A: Measurements of two independent gain-of-function mutants of SRF4 and DLG show clearly an increase in growth. B: *srf4-8* and *dlg-6* are slightly smaller compared to Col-0. C: Picture of *UBQ::SRF4* and *UBQ::DLG* hypocotyl compared to Col-0. D: Result of the semi-quantitative RT-PCR in dark grown Col-0 hypocotyls for *SRF4* and *DLG* transcript. E: GUS staining of 3 d old dark grown hypocotyls. Measured hypocotyls were grown 3 d in dark. Asterisks indicate statistically significant differences, ** $p < 0.01$. Scale bar C: 0.26 cm. Scale bar E: 1 mm.

2.2.2 Interaction studies between DLG and SRF4

Preceding Y2H screen was performed in Cologne in collaboration with Prof. Joachim Uhrig. The cloning of *SRF4 i* was done by Dr. Banu Eyueboglu. An overview of the isolated proteins and their predicted domains can be found in her PhD thesis [Eyuboglu, 2008]. As *DLG* seemed to phenocopy *SRF4*, it was focused on this gene. An overview of the DLG protein and the sequence part used for the Y2H screen can be seen in figure 2.2. To confirm the interaction between both proteins an *in vitro* GST pull-down assay was performed. The interaction in yeast was tried to reproduce. The connection *in planta* was also analysed by different genetic approaches.

2.2.2.1 DLG and SRF4$_i$ interact *in vitro*

The interaction between DLG and SRF4$_i$ was tested in an *in vitro* GST pull-down assay. DLG:His and GST:SRF4$_i$ were recombinantly expressed in *E. coli*. GST:SRF4$_i$ (∼69 kDa) was purified via sepharose beads and the cell lysate containing DLG:His (∼35 kDa) was applied on the beads. The flow-through was kept, the beads were washed and GST:SRF4$_i$ was eluted. All fractions, including the beads after the elution, were loaded on a SDS gel. A western blot was performed and DLG:His was detected via an Anti-HisG-HRP antibody. DLG could be detected in the flow through fraction, which indicates that not all protein could bind to GST:SRF4$_i$. In the wash and elution fraction DLG could not be detected. But in the beads fraction, where most GST:SRF4$_i$ was still bound, DLG could be detected. As control GST without SRF4$_i$ was used, and DLG could be only observed in the flow through fraction. Also empty beads did not interact with DLG. Consequently, it could be shown that DLG interacts with SRF4 *in vitro*. The whole setup was also applied on the partial DLG sequence used in the Y2H screen (ΔDLG) which showed also a clear interaction. In figure 2.16 the SDS gel and the according western blot can be seen. Figure A shows the results for ΔDLG and B for DLG full length. This experiment was performed by Eva Herold, a former Master student in the laboratory.

2.2.2.2 DLG and SRF4 in yeast

Yeast 2-hybrid The revealed interaction between DLG and SRF4$_i$ in a Y2H screen was tried to be reproduced. After several trials with full length DLG and ΔDLG in two different yeast strains which did not give the favored result,

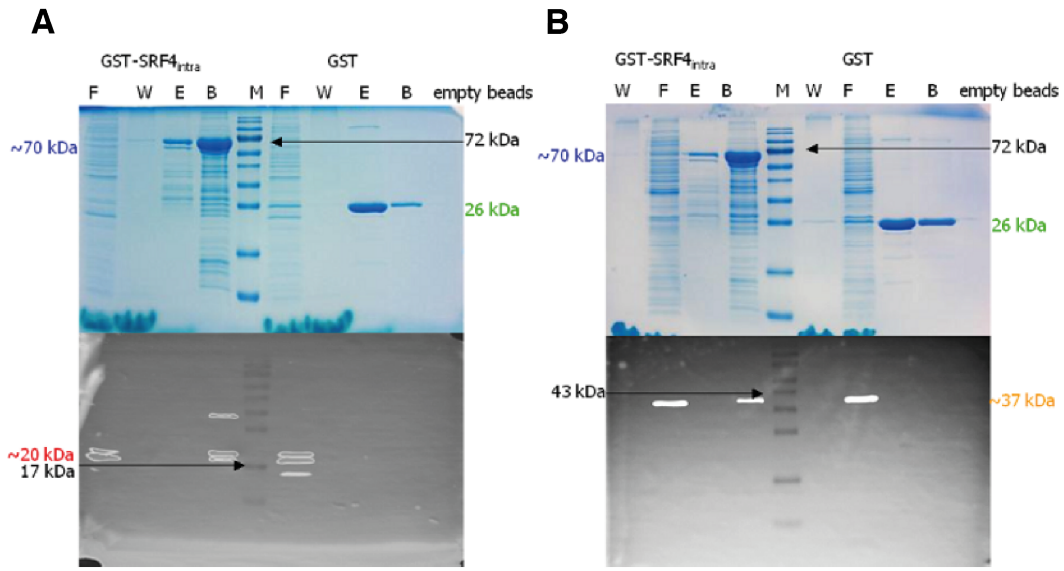

Figure 2.16: Results of the *in vitro* GST pull-down assay performed by Eva Herold. A: Pull-down assay with ΔDLG:His and GST:SRF4$_i$ and GST. The upper panel shows the SDS gel and the lower one the western blot. In the flow through and beads fraction of GST-SRF4$_i$ a ΔDLG:His signal can be detected at the expected size. For GST alone only a signal in the flow through could be observed. The GST control fractions and the empty beads did not show any interaction. B: Pull-down assay for DLG:His full length. The full length protein also interacts with GST:SRF4$_i$ but not with GST. F: flow through, W: final wash, E: elution, B: beads fraction. The picture was taken from [Herold, 2008].

the colonies, which were sent from Cologne and which include both constructs, were inspected. In this Y2H Screen DLG was identified in 5 different colonies. After a PCR was already once performed on those colonies, and the product of one was sent for sequencing, it was clear that the ΔDLG sequence was inside at least of one colony. To check whether some other mistake has happened the whole plasmid was prepared out of yeast and transformed in *E. coli*. After selection on ampicillin plates the plasmid of the colonies was extracted and sent for sequencing. Two independent results of two different yeast colonies showed that both contained the same plasmid with a frameshift between the GAL4 activation domain and the DLG insert. This results in a frameshift for ΔDLG and therefore a truncated protein with a wrong amino acid sequence.

If one takes the results of the other experiments into account, still strong parallels between both proteins are visible. Nevertheless, the consequence is that the interaction of DLG and SRF4 in yeast was not reproducible.

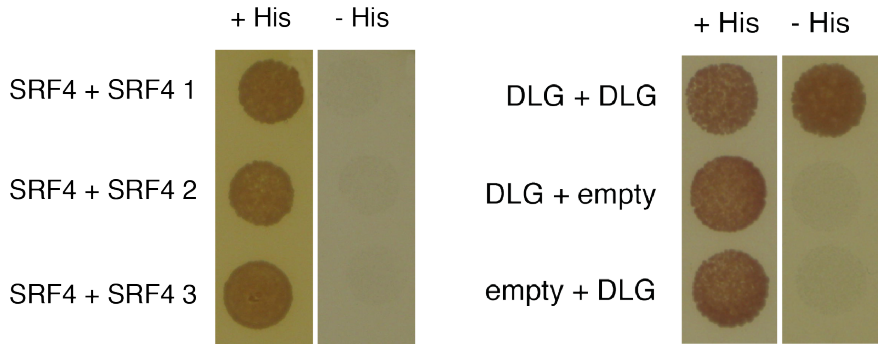

Figure 2.17: SRF4 does not make dimers, whereas DLG dimerizes in yeast. For SRF4 three different colonies, growing on +His media and not on -His media, are shown. For DLG one colony, able to grow on -His media, and the corresponding controls are shown.

Dimerization studies As some proteins are able to dimerize, it was tested if this holds also true for SRF4 and DLG. SRF4 was only tested with the intracellular domain as full length transmembrane domain containing proteins might cause trouble in recombinant systems. For DLG 3 independent colonies were tested with a histidine growth assay. All three colonies showed proper growth on -His plates. For DLG, dimerization could be a control mechanism which might be needed for the regulation of activity. Eventually DLG is only active when present as monomer, but not when it is trapped as dimer. This could also be one explanation for the lack of interaction in yeast. If DLG and SRF4 are expressed, DLG might make dimers and is therefore not able to interact with SRF4. Maybe under certain, so far unknown, conditions the dimerization is absent and SRF4 and DLG are able to interact. SRF4 did not show any sign of dimerization in yeast (see figure 2.17). But as only the intracellular domain of SRF4 was used, it cannot be excluded that SRF4 full length protein might build dimers *in planta*.

2.2.2.3 Genetic interaction studies between *SRF4* and *DLG*

***srf4-8 dlg-6* double mutant analysis** As it was mentioned before, *srf4-8* phenotype can vary. In cellar growth room a reduction in size is mostly visible. But sometimes no difference to wildtype at all can be observed which seems to depend on environmental conditions. Unfortunately, those conditions cannot be kept as stable as it would be needed for this phenotype. Nevertheless, in case of the *srf4-8 dlg-6* double mutant this effect was beneficial. For the double mutant no smaller plants compared to *srf4-8* or *dlg-6* could be observed which excludes synergistic effects. As *srf4-8* and *dlg-6* do both show a very similar way of

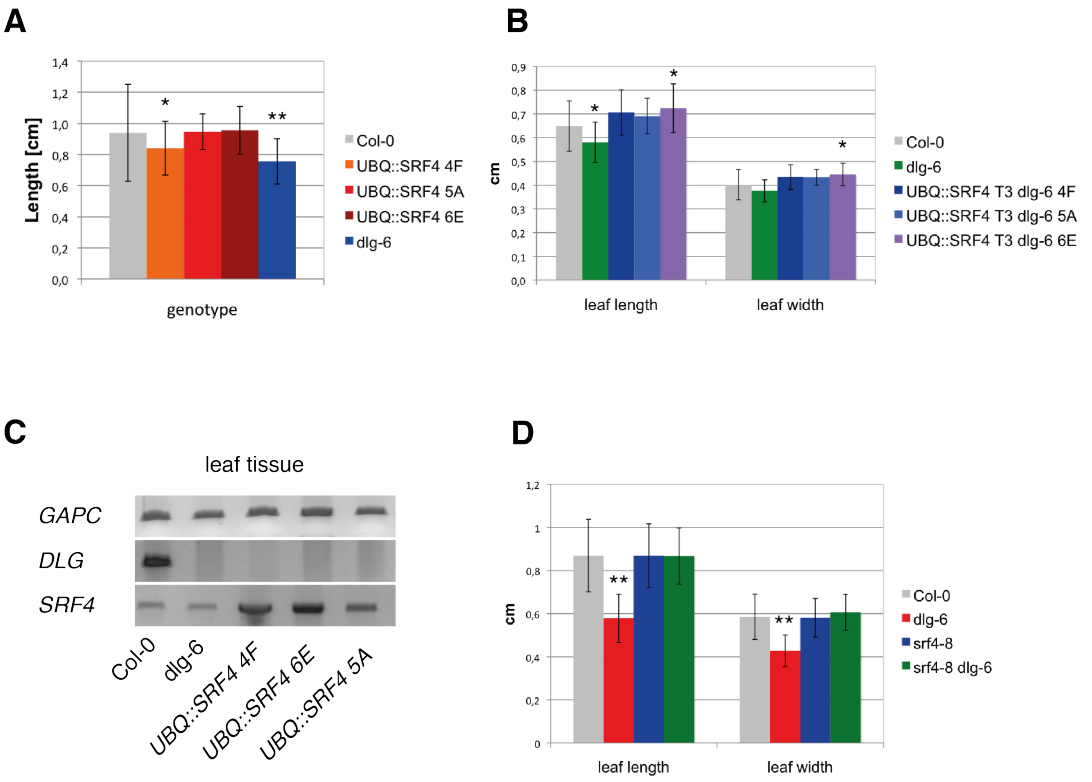

Figure 2.18: Results of the measurements for *UBQ::SRF4* in *dlg-6* background. A: Dark grown hypocotyls have been measured after 3 days of growth. B: The 5th rosette leaf has been measured after 16 d in greenhouse. C: *SRF4* and *DLG* transcript analysis in leaf tissue of 3 different UBQ::SRF4 lines in *dlg-6* background. D: Double mutant analysis of *srf4-8 dlg-6*. The 5th rosette leaf of 16 day old plants, grown in cellar growth room, were measured. Asterisks indicate statistically significant differences, * $p < 0.05$, ** $p < 0.01$.

growth reduction and the double mutant was also slightly smaller compared to wildtype, it was not possible to decide which gene is epistatic. But measurements were done when *srf4-8* was not showing its phenotype. Therefore it was possible to check epistasis. As it can be seen in figure 2.18 D, the double mutant shows that *SRF4* is likely to be epistatic to *DLG*.

***UBQ::SRF4* in *dlg-6* background** If *SRF4* and *DLG* are active on the same genetic pathway can be tested by ectopic expression of *SRF4* in *dlg-6* background. The question to answer was whether the *UBQ::SRF4* phenotype can be suppressed or not. For this *dlg-6* plants were transformed with *UBQ::SRF4*. Crossing was not possible as also the *UBQ::SRF4* phenotype disappeared in T4. In T1 none of the plants showed sterility, a phenotype that can be observed in 20 % of all *UBQ::SRF4* plants if transformed to wildtype. Three different homozygote T3 lines were selected for measurements. For all three the transcript level of *SRF4* was shown to be upregulated in leaf tissue (see figure 2.18

C). Leaves and dark grown hypocotyls were measured. For both organs a clear suppression of *UBQ::SRF4* phenotype could be seen (see figure 2.18 A and B). But it is also obvious that all three lines do not show *dlg-6* phenotype which would be expected if *SRF4* is acting only through *DLG* to regulate leaf size. One possible scenario is that another protein acts in parallel to *DLG*. Therefore the *UBQ::SRF4* phenotype is not fully suppressed. Taking the lack of sterile T1 plants into account this seems to be the most likely opportunity. Nevertheless, at that point it cannot be excluded that *SRF4* and *DLG* are acting on independent pathways and this phenotype is simply additive.

2.2.3 DLG is a cytosolic protein

To investigate the cellular localisation of *DLG*, two EGFP reporter constructs were cloned. One was the *UBQ::DLG:EGFP* construct to gain overexpression of the transgene. The other one was controlled by its endogenous promoter. *UBQ::DLG:EGFP* gave a very strong cytosolic signal throughout all root tissues which indicates that no additional regulatory step like for *SRF4* takes place. Pictures of the signal can be seen in figure 2.19. Like for *SRF4*, ∼20 % of T1 plants could be observed to be sterile. Anthers did not seem to open properly, but the pollen was viable (see figure 2.6 E). Due to that fact, this construct was assumed to produce functional protein. To check also for the natural occurrence of the DLG protein, transgenic *DLG::DLG:EGFP* plants were examined. As native promoter a ∼500 bp long intergenic sequence stretch in front of the ATG was chosen. Even after checking 25 T1 lines no relevant signal could be detected. Like for the ectopic EGFP construct, also for the endogenous promoter construct ∼20 % of T1 plants were sterile. Even after analyzing T2 plants, especially the sterile ones, no signal could be detected. This result indicates, that the native DLG protein might be expressed on a very low level. Possibilities of regulation are discussed in 3.3.1.

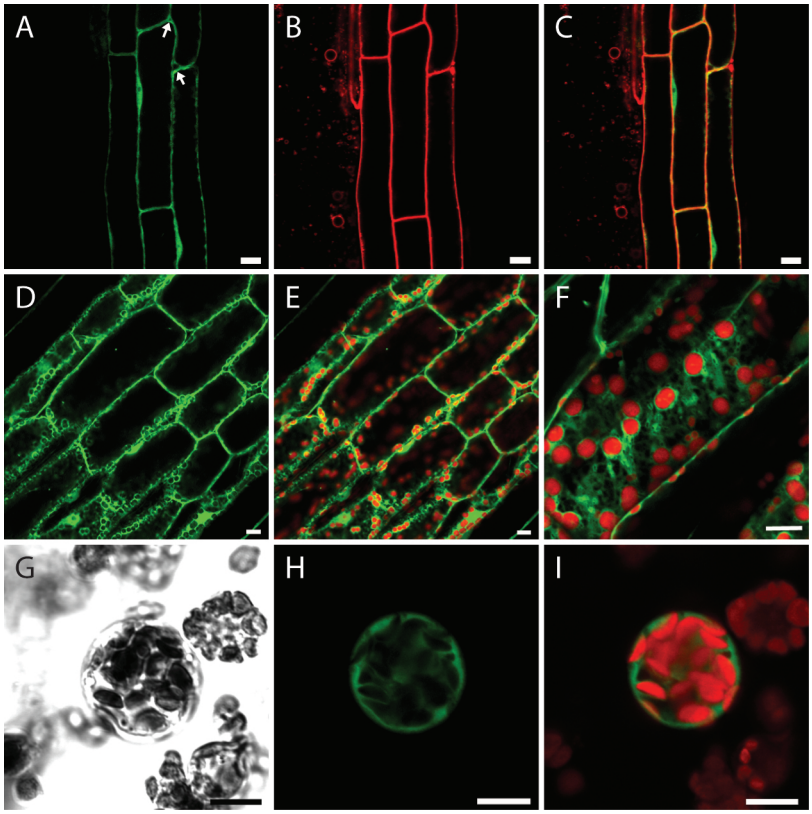

Figure 2.19: Signal of *UBQ::DLG:EGFP*. A-C: Signal in elongation/differentiation zone of root. A: EGFP. B: FM4-64. C: Overlap of A and B. D-F: Expression in the mid vein of the leaf tissue. D: EGFP. E: Chlorophyll autofluorescence. F: overlap of D and E. G-I: Expression in mesophyll protoplasts. G: Bright Field. H: EGFP. I: EGFP and chlorophyll autofluorescence. Scale bar: 10 µm.

2.2.4 DLG shows strong GUS expression pattern in different tissues

To check where the promoter of *DLG* is active, the *DLG::GUS* reporter gene construct was cloned and transformed to plants. The ∼500 bp long intergenic region in front of the ATG was taken as the native promoter. For the analysis more than 20 transgenic lines have been stained and analyzed. Figure 2.20 shows an overview of the promoter DLG staining pattern in different developmental stadiums and organs.

Whereas *SRF4* shows a specific staining in seedlings, *DLG* is expressed more or less everywhere. Also the vascular system is very strongly tinted. In seedlings a weaker staining can be seen in very young leaves, but also those leaves show a very strong staining of trichomes. Flowers do also show a strong staining in all developmental stages. In very young flowers mostly the carpel as well as the sepals are stained. Sepals seem to be mostly stained in the vascular bundle.

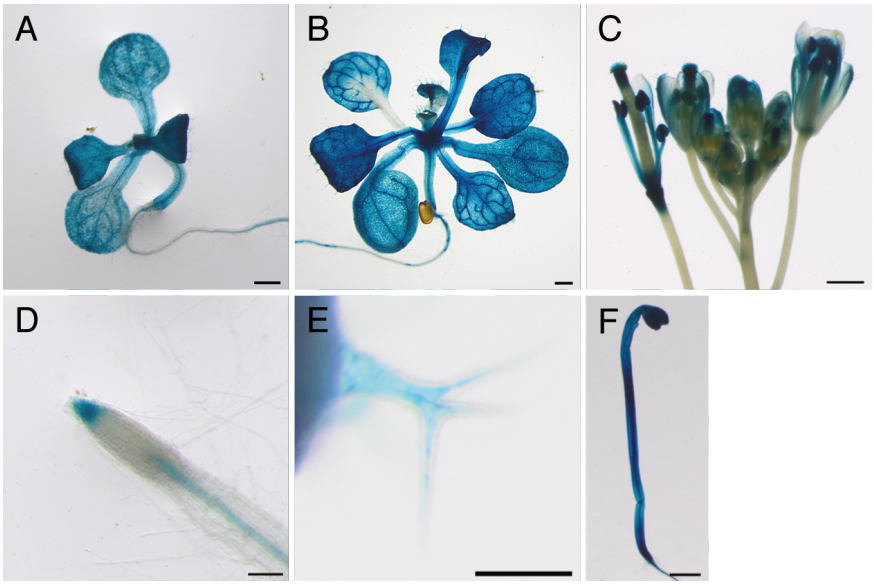

Figure 2.20: GUS pattern of *DLG*. A: Staining of 10 d old seedlings is visible throughout all tissues. B: Also after 16 d a very strong staining is still visible. The younger leafs are not that much stained except for the trichomes. C: Flowers are also stained very strong in carpel tips, older filaments and sepals. D: *DLG::GUS* shows expression in the vascular root tissue of the elongation/differentiation zone, no signal in the division zone but a signal in the root tip. E: A strong staining in the trichomes, throughout all leaf stages, could be observed. F: 3 d dark grown hypocoytls show a staining according to RT-PCR results. For *DLG* the staining is stronger compared to *SRF4*. Scale bar A, B, C, F: 1 mm. Scale bar D, E: 250 µm.

Older flowers show still a staining in the carpel tip, sepals and additionally a strong staining of stamen which cannot be observed in young flowers. From a developmental point of view it looks as if *DLG* is expressed in expanding organs. Like *SRF4*, *DLG* is expressed in roots in the expression/differentiation zone only in the vascular bundle. No staining could be observed in the division zone. But unlike *SRF4*, *DLG* is also expressed in the root cap. The same kind of staining could be observed in lateral roots. No expression in root hairs could be seen, but a strong trichome staining for young as well as old leaves could be observed. Also etiolated seedlings showed a strong expression. This supports the phenotype of *UBQ::DLG* in dark grown hypocotyls.

2.2.5 *DLG* in 1001 genomes

The DLG amino acid sequence was checked for polymorphisms in other *Arabidopsis thaliana* accessions with the help of the 1001 genomes project [Cao et al., 2011]. Due to sequence uncertainties, out of the 80 sequenced genomes, 78 could be used for the analysis of DLG. For DLG 8 polymorphisms could be

detected within the whole protein sequence (see figure 2.2). Six accessions show one single amino acid change and one accession two changes. Detailed information about the polymorphisms can be found in table 2.4.

Position	Polymorphism	Accession
8	M→I	ICE50
43	R→Q	Bak-7
84	G→R	ICE50
155	I→V	Dog-4
167	S→G	ICE29
247	E→D	Agu-1
285	V→L	Pra-6
301	A→R	ICE119

Table 2.4: DLG amino acid polymorphisms in different *Arabidopsis thaliana* accessions. 78 out of 80 sequences were used for the alignment, 8 polymorphisms could be found. Positional numbering is according to the N-terminal methionine of DLG.

2.2.6 Evolution of *DLG* in *Viridiplantae*

Sequence similarities in different *Viridiplantae* genomes were used to find orthologues and young paralogues of DLG. The phylogenetic tree of these genes revealed that at least one copy of the gene is structurally and potentially also functionally conserved throughout higher plants. Keeping *DLG*s function in primary metabolism into account this seems not to be surprising. Its two copies in *Physcomitrella patents* shows its existence already in basal plants. Monocotyledons, Fabaceae and Brassicales build single clades as well as *Physcomitrella patens* which is highly separated. The three consecutive copies of *DLG* in *Medicago truncatula* indicate two gene duplications of this gene. The same approach as for SRF4 was used to build the phylogenetic tree (see section 2.1.6).

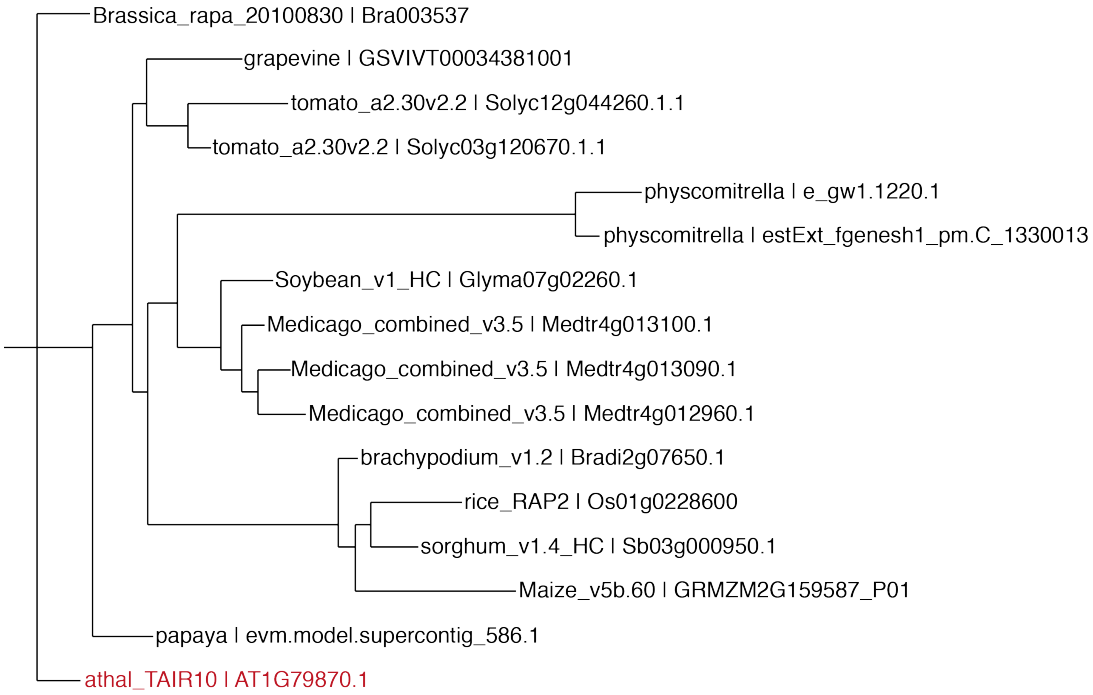

Figure 2.21: Phylogenetic tree of *DLG* (At1g79870) in *Viridiplantae*. The red color indicates the position of the *Arabidopsis* gene in the tree.

2.3 *WINZLING*: another potential downstream signaling partner of *SRF4*

A second promising interaction partner of *SRF4* was identified in the Y2H screen. *WIZ* obtained its name due to the small appearance of its T-DNA mutants, which seemed to fit the *SRF4* phenotype. *WIZ* is a gene of so far unknown function which bears a WD40 and a RIC1 domain. Its transcript could be detected in different plant organs (see figure 2.22 D). To get to know more about this protein and its connection to SRF4 and DLG was the intention of the following experiments. Phenotypic characterization, reporter GUS assays and various double mutant analysis were performed and revealed a clear connection between *SRF4*, *DLG* and *WIZ*. Nevertheless, their way of regulation stays fuzzy at this point.

2.3.1 The phenotype of *WIZ* gain- and loss-of-function mutants

The T-DNA insertion lines of *WIZ* showed either no phenotype (*wiz-3, wiz4, wiz-5*), small plants with bleached leaves (*wiz-1*) or small plants with dark green, roundish leaves (*wiz-2*). The phenotypes and the according leave size measurements can be seen in figure 2.22 A.

wiz-3, wiz-4 and *wiz-5* were predicted to be located at the very end of *WIZ* and to sit in intronic regions or the 3' UTR which would explain the absence of a phenotype. *wiz-1* is located at the beginning of the gene and is likely to disrupt the WD40 domain. It exhibits an obvious reduction in plant size and showed late flowering. Surprisingly this small phenotype is only visible in early developmental stages and is overcome in later phases of plant life. Figure 2.22 (B and C) illustrates that the influence of *wiz-1* on plant size is compensated in later plant development and gives rise to the assumption that another gene is taking over *WINZLINGS* role. A good candidate could be *WINZLING LIKE (WIZL)* which is a very close homologue to *WIZ*. A closer comparison of both genes can be found in section 2.3.2.

Another allele of *WIZ*, *wiz-2*, showed dark green leaves and also an obvious reduction in growth. Furthermore, some fertility problem and a roundish leaf shape could be observed. As leaf color is contrary to *wiz-1* and *wiz-2* is located in the promoter region of *WIZ*, it was assumed that *wiz-2* is an overexpressor of *WIZ*. Indeed it could be shown with semi quantitative RT-PCR that *wiz-2* expresses more transcript than wildtype (see figure 2.3 B). Furthermore wiz-1/wiz-2 transheterozygote plants showed wildtype phenotype which strengthens the assumption that *wiz-2* is an overexpressor (see figure 2.23).

To check for the cause of the fertility problem the flowers of *wiz-2* were subject of closer examination. It could be observed that a severe problem with seed production seemed to take place only in the early stages of flower development and are almost overcome in the later reproductive phase so that harvesting of an adequate amount of seed was possible. But still, even later, the elongation of siliques seemed to be reduced. The problem in the early phase seemed to be due to an excess growth of the carpel (see figure 2.24). As the other organs are only elongating to normal wildtype size, anthers cannot reach the stigma and the ovules can therefore not be pollinated. When performing crossings it was possible to reach seed with *wiz-2* ovules as well as with its pollen which shows

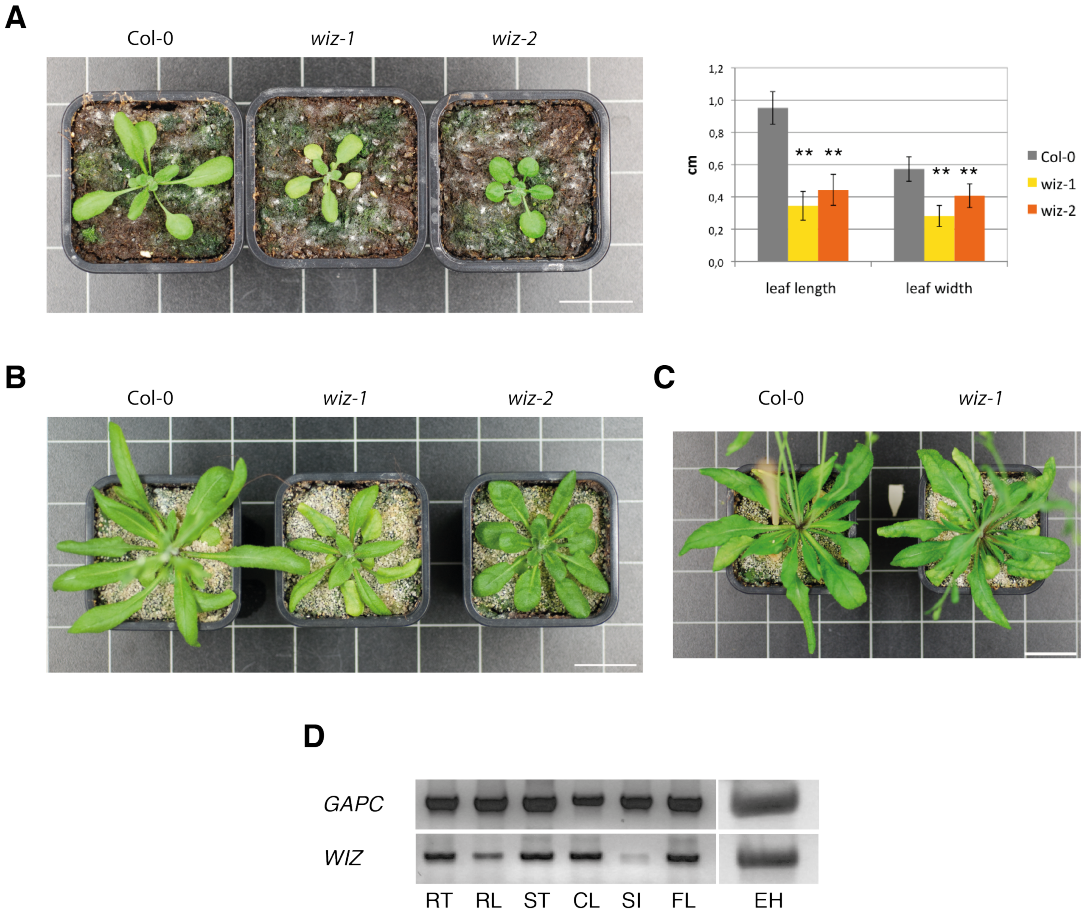

Figure 2.22: *WIZ* phenotype of the loss-of-function mutant and the overexpression construct. A: Small leaf phenotype of 16 day old *wiz-1* and *wiz-2* mutant plants. Measurements of 20 plants grown in cellar growth room for 14 d are shown on the right. B: Phenotype of 25 d old plants. C: Phenotype of *wiz-1* compared to Col-0 after 32 days. D: *WIZ* transcript in different tissues. It could be detected in all organs at a similar level, only in siliques it seems to be expressed poorly. RT: root, RL: rosette leaf, ST: stem, CL: cauline leaf, SI: silique, FL: flower, EH: etiolated hypocotyl. Asterisks indicate statistically significant differences, ** $p < 0.01$. Scale bar: 3 cm.

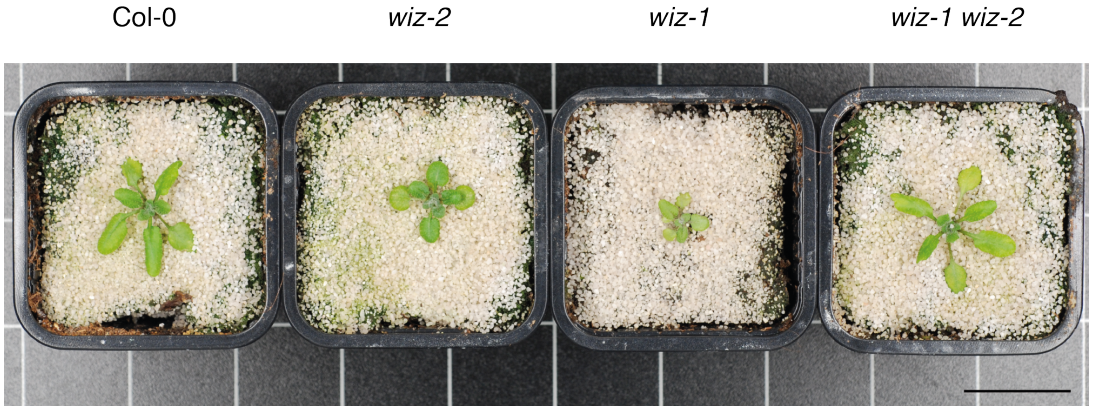

Figure 2.23: Transheterozygote F1 plants of *wiz-1/wiz-2* show wildtype phenotype. Scale bar: 3 cm.

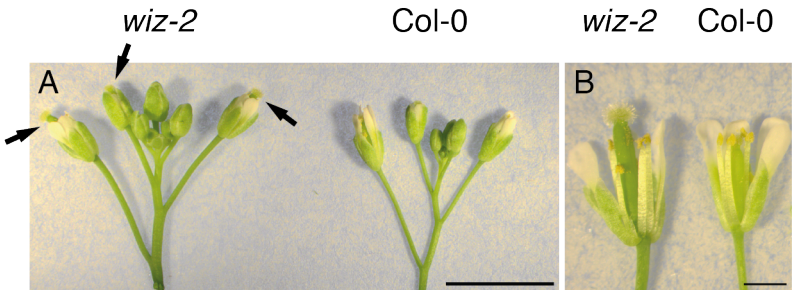

Figure 2.24: Flower phenotype of *wiz-2*. A: Inflorescence of *wiz-2* and Col-0. It can be clearly seen that the carpels elongate too much and anthers can therefore not reach the stigma. Arrows indicate over-elongated carpels. B: Flower close up. The carpel looks not only longer, but also broader and dark green. Scale bar A: 5 mm, B: 1 mm.

that no problems with these organs exist. To make sure that all pollen was viable an Alexander stain was performed. None of the stained pollen showed any obvious problem (see figure 2.6 F). The pollen of *wiz-2* plants looked like wildtype.

Chlorophyll content As *wiz-1* exhibits an obvious bleaching of the older leaves, the chlorophyll content of leaf 3 and 5 was measured. Two different environments were used, a cellar growth room and a phytochamber. In the growth room not more than 128 $\mu m^{-2}s^{-1}$ continous light was achieved. The phytochamber had 142 $\mu m^{-2}s^{-1}$. In the phytochamber long day conditions were applied. As expected, the results showed a clear reduction of chlorophyll for *wiz-1*. Interestingly a strong effect was visible in both environments for leaf 3. Leaf 5 showed stronger bleaching in the phytochamber whereas it had the same amount of chlorophyll like wildtype in cellar growth room.

The result in cellar growth room (see figure 2.25 A and B) shows that bleaching of leaves appears due to environmental stress. The older the leaves get the more they turn light green which can be also seen on the phenotype pictures. Results in phytochamber (see figure 2.25 C and D) show that a putative stress factor might be light as the light intensity is higher in this environment. Even the younger leaves experience already damages in the photosystem and are therefore bleached. The stress factor in phytochambers seems to be quite high, consequently. It is strongly believed that a clear reduction of light intensity might rescue the bleaching phenotype, but not the growth reduction.

Overall, *wiz-1* plants seem to show some kind of early senescence. If *WIZ* is a regulator of age control or if this effect is just a consequence of missing *WIZ*

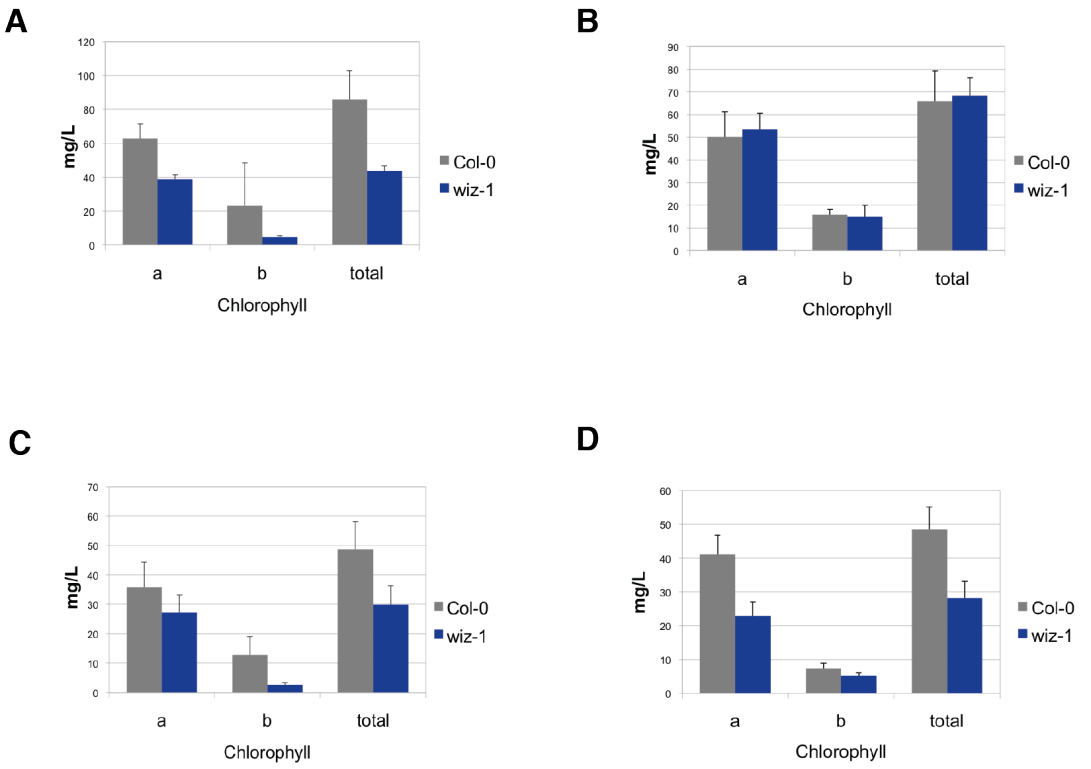

Figure 2.25: Chlorophyll content of *wiz-1* compared to Col-0 of the third and fifth rosette leaf in cellar growth room and in the phytochamber. A: Measurements in the growth room of the 3rd rosette leaf. B: Chlorophyll content in the growth room of the 5th rosette leaf. C: Chlorophyll measurements in phytochamber of the 3rd rosette leaf. D: Measurements of chlorophyll in the phytochamber of the 5th rosette leaf.

remains so far open and is an interesting field of investigation.

As *wiz-2* showed dark green leaf its chlorophyll level was also analysed. It could clearly be shown that *wiz-2* exhibits more chlorophyll (see figure 2.26).

Photosynthetic yield To see whether the photosynthetic efficiency was also influenced in *WIZ* mutants, which was very likely when looking at the phenotype, photosynthetic yield was measured. Even though *srf4* and *dlg* mutants did not show bleaching they were also tested. The result shows that *wiz-1* has a problem with light conversion whereas the other genotypes have similar rates to wildtype (see figure 2.27 A).

To show that the older leaves have more problems with photosynthesis than the younger ones, the yield was checked for 15 different *wiz-1* plants from leaf 1-8 (see figure 2.27 B). The result clearly shows that the problem in older leaves is more severe than in younger ones. Old leaves cannot reach the level of wild-type plants while a clear increase can be seen the younger the leaves are. The

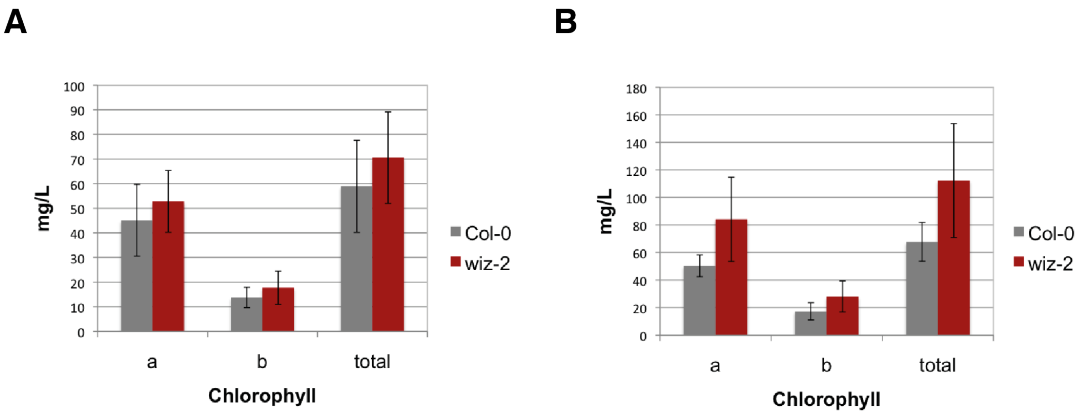

Figure 2.26: Chlorophyll content of *wiz-2* compared to Col-0 of third (A) and fifth (B) rosette leaf in cellar growth room.

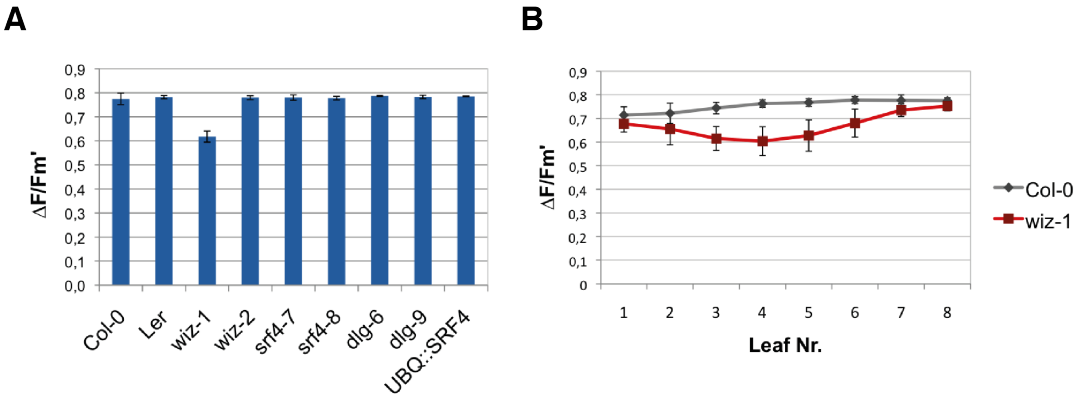

Figure 2.27: Photosynthetic Yield of all genotypes (A). The average of the 3rd rosette leaf of 2-4 individual plants was taken for measurements. Diagram B shows the photosynthetic yield of Leaf 1-8 of 15 individual *wiz-1* plants compared to Col-0.

similarity between wildtype and the oldest *wiz-1* leaves can be explained by the fact that also wildtype plants start aging after some time. Additionally are the smaller, older leaves of *wiz-1* shaded by the bigger, younger leaves and have, after a while, not that much light stress as the exposed ones.

2.3.2 *WINZLING LIKE* (*WIZL*) is a paralogue of *WIZ*

WIZ has a very close paralogue in the *Arabidopsis thaliana* genome. The striking identity between the two amino acid sequences is up to 98 %. Their genomic sequence (ATG-stop) shows 97 % sequence identity, only two specific sequence sections allowed for the discrimination of both for genotyping of the T-DNA lines. An interesting detail is the fact that they also share a high similarity in their promoter sequence as well as the 3' UTR and the following intergenic region. Both genes have an upstream intergenic region of ca. 3300 bp. Around 380

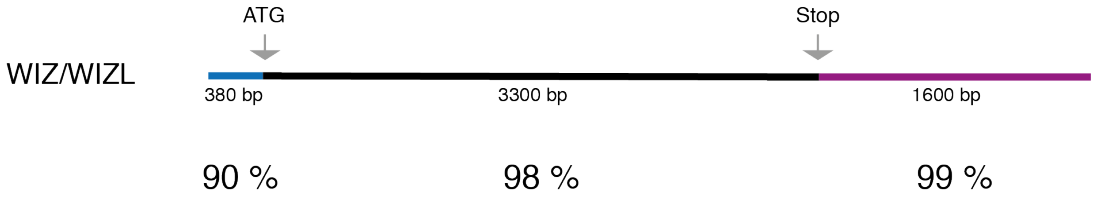

Figure 2.28: Overview of the similarity of WIZ and WIZL. Within their coding sequence from ATG-stop they show 98 % sequence identity, also on protein level. Also upstream and downstream regions seem to be partially conserved.

bp upstream of the ATG they are 90 % identical. Their intergenic downstream region seems to be completely conserved. Around 1600 basepairs are to 99 % identical, but the following downstream genes are different (see figure 2.28 for illustration).

For *WINZLING LIKE (WIZL)* (At5g28350) also T-DNA insertion lines were ordered, genotyped and checked for a phenotype. Plants carrying the homozygous insertions did not show any phenotype. This might be due to the fact that *wizl-1* is located in an intronic region whereas *wizl-2* sits in the putative promoter region (data not shown).

No homolog protein with known function could be detected in other *Viridiplantae* (MAtDB SIMAP implementation). The predicted WD40 domain of WIZ was used for homology modeling with Swiss Model [Arnold et al., 2006]. It gave rise to a double propeller structure which can function as stable scaffold to moderate protein-protein interactions (see structure prediction in figure 2.29). Many WD40 domain containing proteins also developed other functional domains. In case of WIZ and WIZL this seems quite likely as, behind the WD40 repeats, a hit with the RIC1 superfamily could be detected.

WIZL seems to be a functional protein with the conserved exon/intron structure of *WIZ* and an open reading frame of 3384 bp. Therefore it might be a putative candidate which neutralises the lack of *WIZ* and compensates the growth reduction in later developmental stages.

Evolution of *WIZ* and *WIZL* in *Viridiplantae* A phylogenetic tree (see figure 2.30) for the protein sequence of WIZ and WIZL was calculated with the same approach as for SRF4 (see section 2.1.6). At least one copy of WIZ/WIZL can be found throughout the *Viridiplantae* kingdom. The tree corresponds to the currently accepted plant taxonomy. Basal plants like the moss *Physcomitrella patens* and the spikemoss *Selaginella moellendorffii* have at least

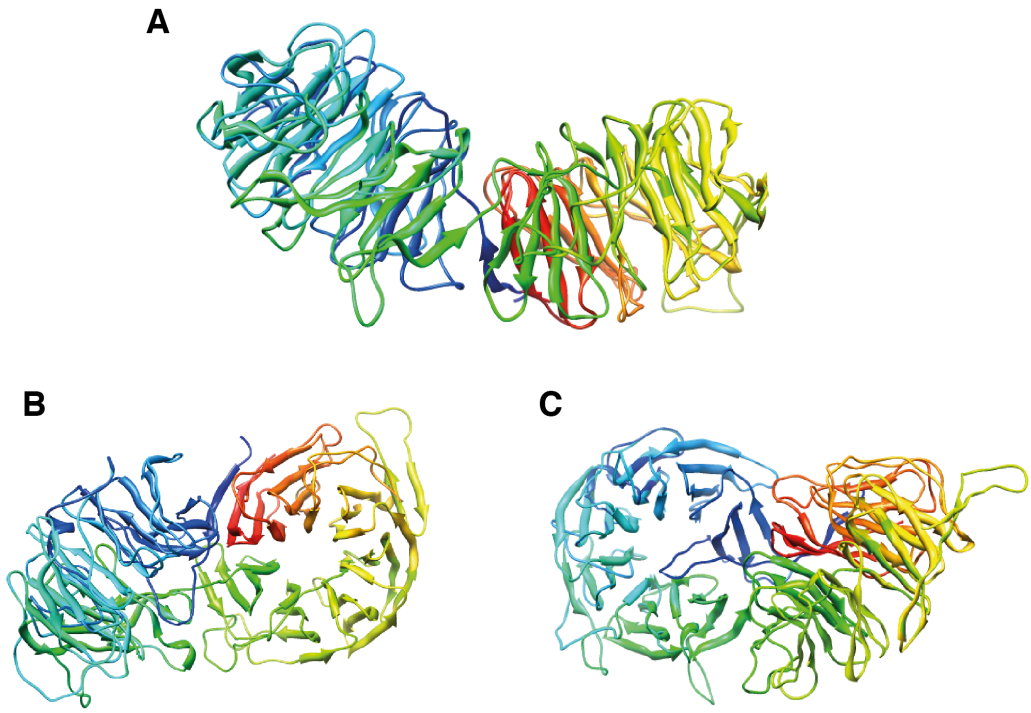

Figure 2.29: Homology modeling of the WINZLING WD40 domain. It can be clearly seen that WINZLING might comprise a double propeller. A: Side view. B: Topview of the right propellor. C: Topview of the left propellor. Both propellors seem to be rotated with respect to each other. The role model was 1nr0 from PDB.

one copy. Monocotyledons, Fabaceae and Brassicales are also covered in the tree. Interestingly only one copy could be identified in *Brassica rapa*.

Additional analysis of the *WIZ* sequence in *A.lyrata* draws a similar picture as *Brassica rapa* did in the phylogenetic tree. *A. lyrata* is the closest relative of *A. thaliana* and separated around 10 million years ago. One copy of *WIZ* in *A. lyrata* faces two copies in *Arabidopsis thaliana* [Hu et al., 2011]. Trying to map *WIZ* and *WIZL* to the lyrata genome results in only one hit on lyrata gene *fgenesh2_kg.5__2618__AT5G28350.1*. This gene is interestingly associated with *WIZL* (At5g28350), while *WIZ* reaches a higher score towards it (personal communication, Georg Haberer, MIPS). As the *WIZ/WIZL* sequences are still very well conserved, it is possible that a duplication event happend not to long ago, likely even after the divergence of *A. thaliana* and *A. lyrata*. This indicates a duplication event for *WIZ* out of which *WIZL* evolved. As the *A. lyrata* sequence is is likely not complete it might be possible that the second gene is missing so far. But as *Brassica rapa* seems to have also only one copy this seems quite unlikely. *WIZ* and *WIZL* might therefore be interesting targets for evolutionary studies of the two *Arabidopsis* lines.

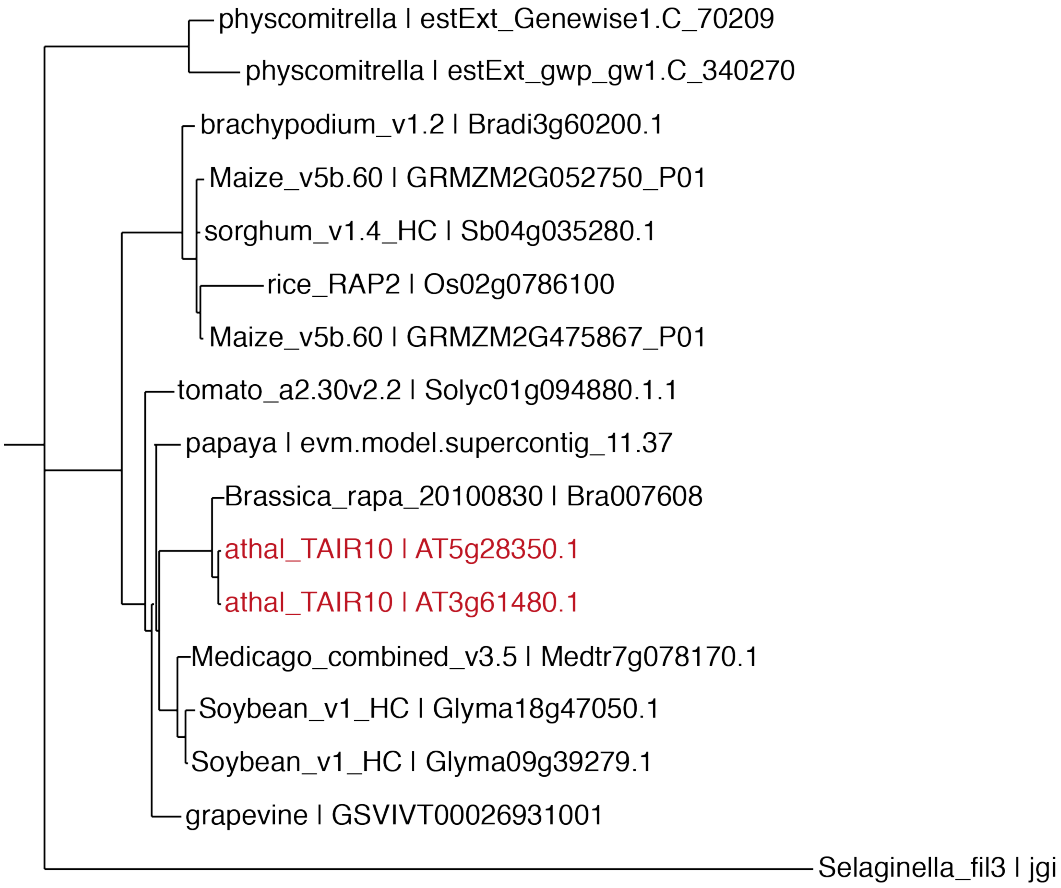

Figure 2.30: Phylogenetic tree of *WIZ* (At3g61480) and *WIZL* (At5g28350) in *Viridiplantae*. The red color indicates the positions of both *Arabidopsis* genes in the tree.

2.3.3 WIZ interacts with SRF4 in yeast

Also *WIZ* was identified in the Y2H screen and this interaction could be reproduced. An overview of the WIZ protein and the used sequence part for the Y2H screen can be seen in figure 2.2. For the interaction study full length WIZ was used, but it did not show the expected result. After cloning the short sequence part used in the initial Y2H screen, ΔWIZ, an interaction could be shown (see figure 2.31). Additionally, the interaction with DLG full length was tested, but no interaction between both proteins could be observed in yeast. A dimerization of full length WIZ in yeast could not be observed.

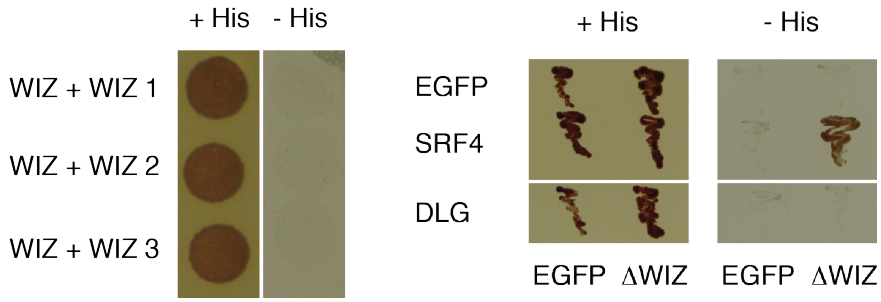

Figure 2.31: Left: Dimerization studies of WIZ. Three different colonies, growing on +His media and not on -His media, are shown. Right: Y2H results of ΔWIZ with SRF4 and DLG. ΔWIZ and SRF4 clearly interact.

2.3.4 Genetic interaction studies between *SRF4*, *DLG* and *WIZ*

If genes act in the same genetic pathway can be addressed by analysis of their double mutants. Therefore, different mutant alleles of *SRF4*, *DLG* and *WIZ* were crossed, and some overexpressor lines in mutant background were analyzed. *SRF4* and *DLG* seem to have an effect on *WIZ* function.

2.3.4.1 *srf4-8 wiz-1* double mutant rescues *wiz-1* phenotype

After a homozygote double mutant between *srf4-8* and *wiz-1* was found it was obvious that the mutant did not show the *wiz-1* phenotype. The bleaching of leaves was not visible any more, and growth reduction was not as severe as normal for *wiz-1* plants.

To make sure, whether the double mutant shows wildtype or *srf4-8* phenotype 20 plants were measured in the next generation. In figure 2.32 A and B it can be clearly seen that the double mutant shows *srf4-8* phenotype. Therefore, *SRF4* is epistatic to *WIZ*.

2.3.4.2 *srf4-8* is epistatic to *wiz-2*

As the *wiz-2* phenotype is very pronounced, it was easy to see that the double mutant did not appear to be *wiz-2* like. To check whether one gets a *srf4-8* phenotype or if the double mutant shows wildtype shape around 20 F3 plants were measured. The result showed that those plants have shorter leafs compared to wildtype and therefore exhibit the *srf4-8* phenotype. The width of the leaves does not account for such a clear result. The p-value there is 0.1 based on the

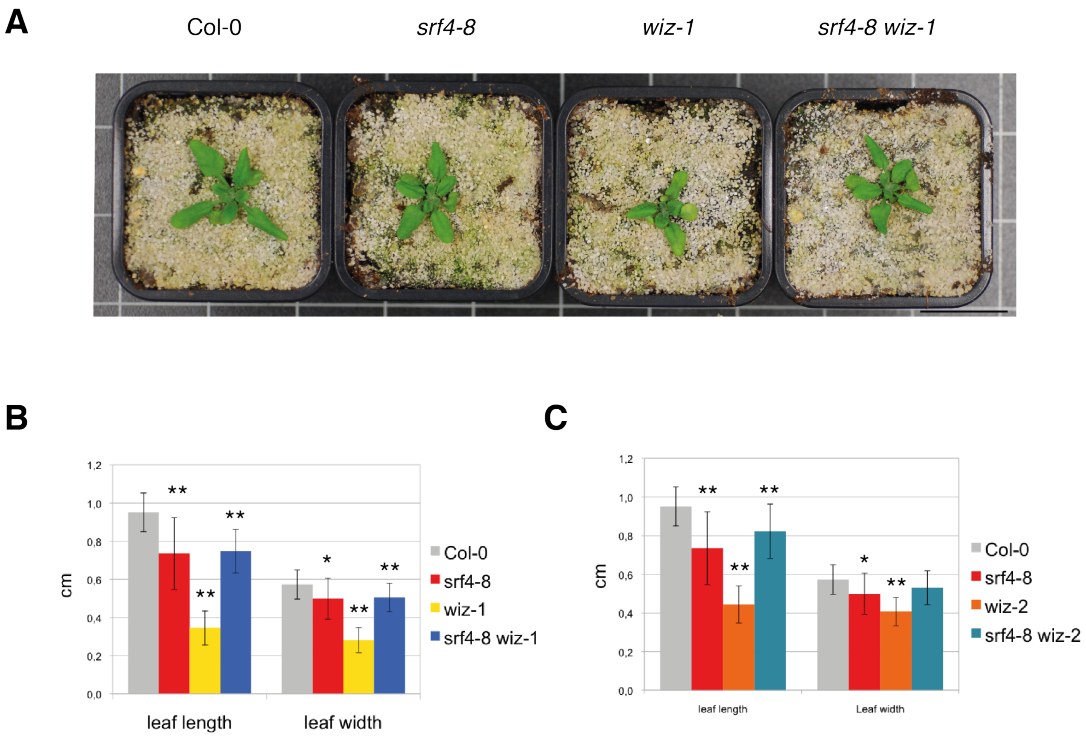

Figure 2.32: A: Phenotype of *srf4-8 wiz-1* double mutant after 18 d in cellar growth room. B: The results of the measurements of 20 plants grown in cellar growth room after 14 d. It is obvious that *SRF4* is epistatic to *WIZ*. C: The measurements of *srf4-8 wiz-2* leaf length show clearly that the double mutant shows *srf4-8* phenotype. p-value of *srf4-8 wiz-2* to *srf4-8* > 0.05 and to Col-0 it is < 0.05. For the leaf width the result is not so clear. Asterisks indicate statistically significant differences, * $p < 0.05$, ** $p < 0.01$. Scale bar: 3cm.

null hypothesis that the leaf width is that of Col-0. If the null hypothesis is that the double mutant leaf width is the one of *srf4-8*, around 30 % follow this hypothesis which makes it very likely that also the leaf width is the one of *srf4-8*. Hence, *srf4-8* is likely to be epistatic to *wiz-2*. The results of these measurements can be seen in figure 2.32 C.

2.3.4.3 *dlg-6 wiz-1* double mutant

As *srf4 wiz* double mutants showed a strong relation between both genes, and *DLG* is likely to interact with *SRF4*, it was tested whether *DLG* and *WIZ* are also in relation with each other. To check how this connection could look like the double mutants between *dlg-6* and *wiz-1*/*wiz-2* respectively were generated.

The *dlg-6 wiz-1* double mutant did not show *wiz-1* phenotype. It looked as if the double mutant exhibits a synergistic effect which is able to suppress *wiz-1* as well as the *dlg-6* phenotype. This could mean that both genes are on different pathways which might not be completely independent. Results of the

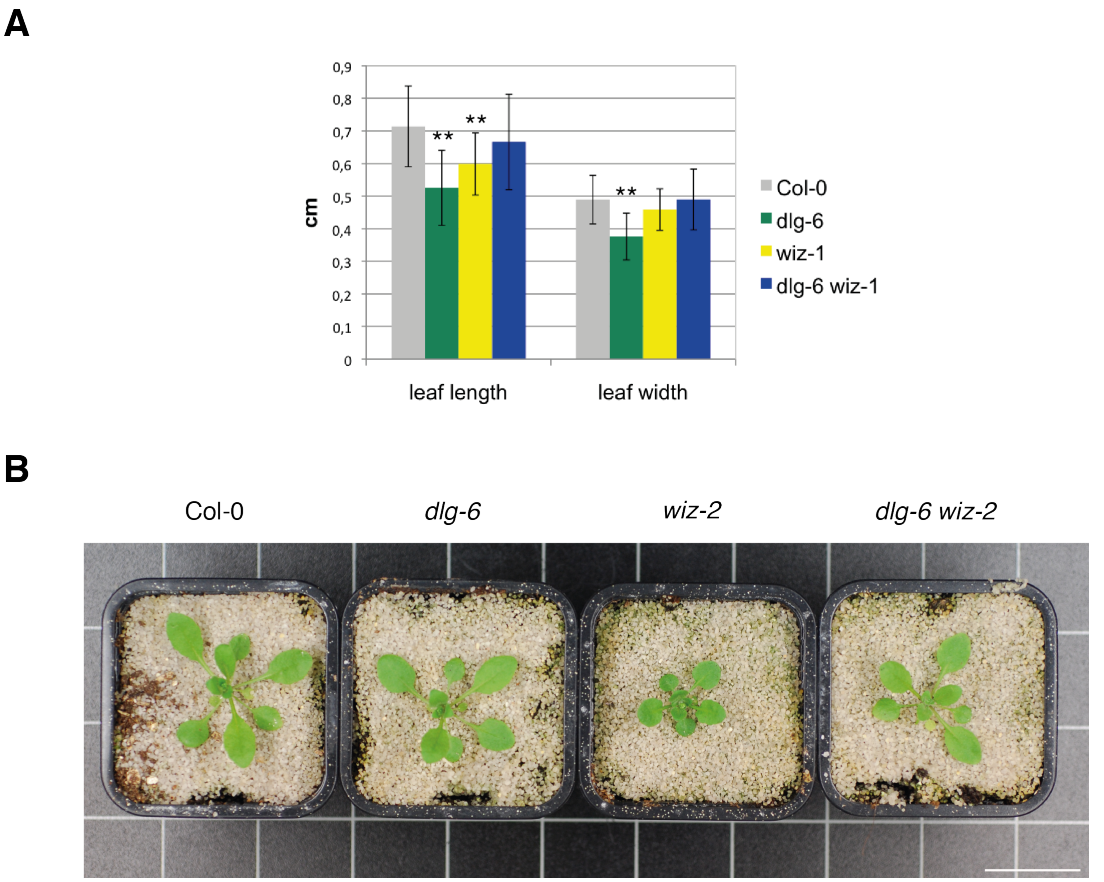

Figure 2.33: *dlg-6* double mutant phenotypes. A: Measurements of *dlg-6 wiz-1* double mutants. The phenotype seems to mimic neither *dlg-6* nor *wiz-1*. B: 18 d old plants showing *dlg-6 wiz-2* double mutant compared to wildtype and single mutant phenotypes. Asterisks indicate statistically significant differences, ** $p < 0.01$. Scale bar: 3cm.

measurements can be seen in figure 2.33 A.

2.3.4.4 *dlg-6 wiz-2* double mutant rescues wiz-2 phenotype

When crossing *dlg-6* with *wiz-2* a surprising effect could be observed. *dlg-6* rescues the *wiz-2* phenotype, like already *srf4-8* did. The phenotype of 18 d old plants can be seen in figure 2.33 B. This finding could support the assumption that *DLG* is epistatic to *WIZ*.

2.3.4.5 *SRF4* over-expression in *wiz-1* background shows additive phenotype

Interesting results for the crossings of *srf4* and *wiz* could be observed, which indicates *SRF4* to be epistatic to *WIZ*. It could be therefore helpful to express *SRF4* ectopically in *wiz-1* background, to solve the connection between both genes. In T1 male sterile plants could be already observed giving a hint that *wiz-1*

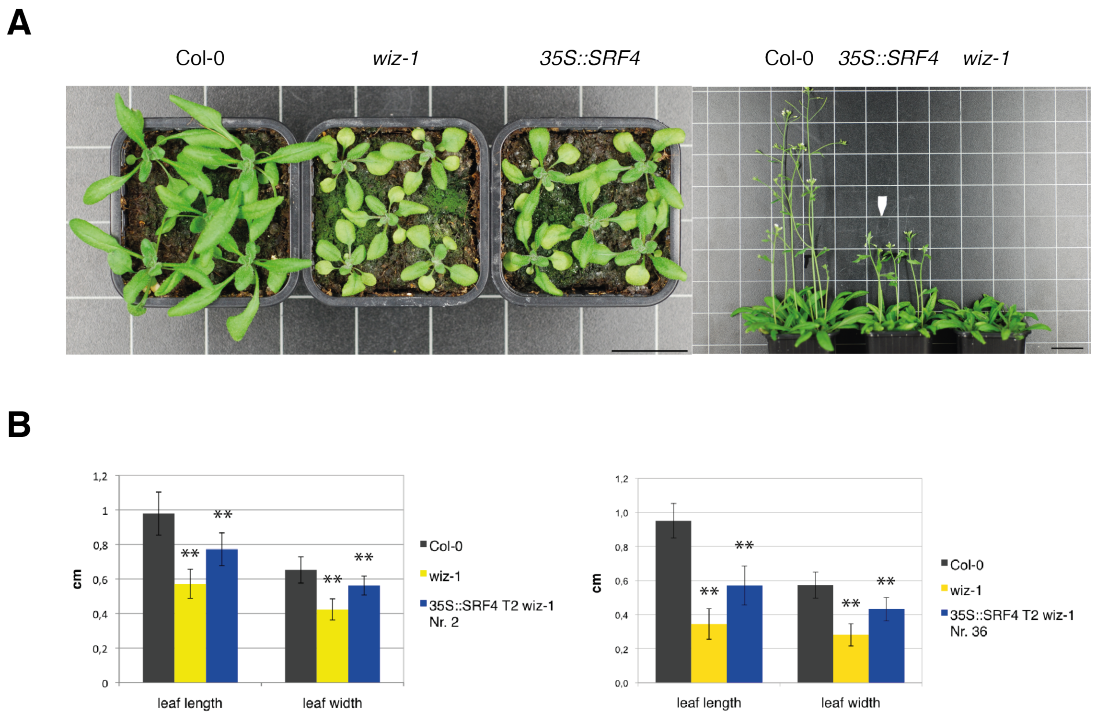

Figure 2.34: *35S::SRF4* in *wiz-1* background. A: On this picture line Nr. 36 is shown. On the left 16 d old seedlings can be seen. The picture on the right shows 25 d old flowering plants. Plants were grown in cellar growth room. B: Lines Nr. 2 (right) and Nr. 36 (left) have been measured after 16 d of growth in cellar. Both lines showed sterility in T1. Asterisks indicate statistically significant differences, ** $p < 0.01$. Scale bar: 3cm.

is not able to suppress the *UBQ::SRF4* phenotype. After harvesting T1 plants, two different male sterile lines were investigated in T2. The phenotype was quite additive as the transformants showed bleached, but bigger leaves compared to *wiz-1*. Additionally, sterility and flowering time supported the assumption. Pictures of the phenotype can be seen in 2.34 A, the results of the measurements are depicted in B. Preliminary results indicate also no rescue of *wiz-2* phenotype by *UBQ::SRF4*.

2.3.5 *WIZ::GUS* expression pattern

To see were the promoter of *WIZ* might be active the promoter GUS construct was cloned. For that purpose the intergenic sequence in front of the ATG was taken as promoter region. For *WIZ* this were ∼3000 bp.

The expression pattern of *WIZ* promoter in 10 d old seedling appeared to be very similar to *SRF4* (see figure 2.35). A strong staining in the hypocotyl as well as in the vascular system of the cotyledons is obvious. But additionally the shoot apical meristem seems to be tinted. In 16 d old seedlings the situation

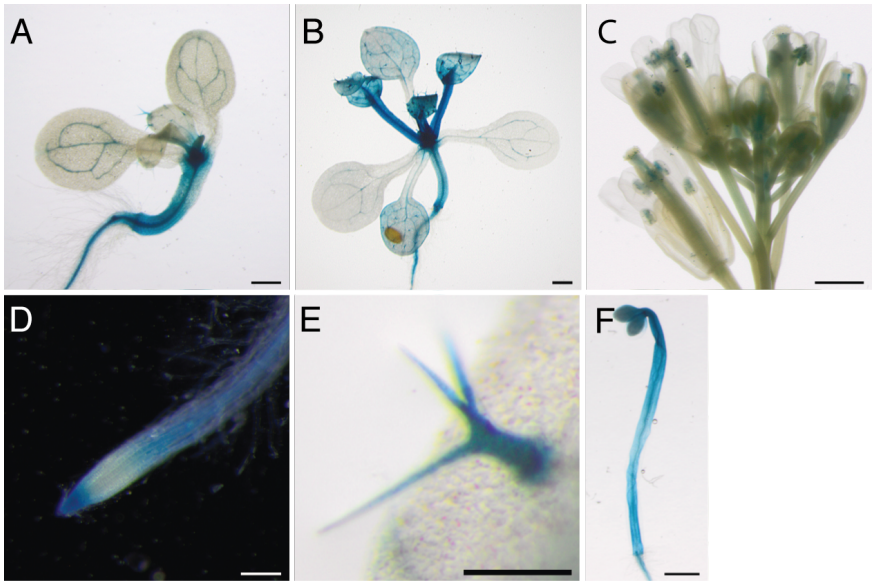

Figure 2.35: GUS pattern of *WIZ* promoter. A: 10d old seedling. *WIZ::GUS* shows a staining in the hypocotyl and in the cotyledon veins as well as a strong staining in the meristematic region. B: 16d old seedling. A strong staining of the younger leafs is visible. In older leafs the staining is weaker. The meristematic region seems also to be dyed strongly. C: *WIZ::GUS* staining in flowers. A staining in anthers and pollen as well as a strong staining in young carpels can be seen. The older the carpel gets the more the staining is located in the veins. It also looks as if there is a weak staining in the meristematic region. D: *WIZ::GUS* shows an overall staining of the root in the elongation/differentiation zone, no signal in the division zone and also a strong signal in the root cap. E: Trichomes showed also a very intense staining throughout all leaf stages. F: 3 d dark grown hypocoytls show staining according to RT-PCR results. The intensity of th GUS staining with *WIZ* is intermediate to *SRF4* and *DLG*. Scale bar A, B, C, F: 1 mm. Scale bar D, E: 250 µm.

looks different from *SRF4*. Whereas an overlap of expression can be seen in older leafs, a strong staining in young leaves can be seen. There, the overall leaf blade as well as the vascular bundles are strongly stained. In the floral organs a weak expression in young carpels can be seen, old flowers bear a strong staining in the pollen and a weaker one in the carpel veins. Unlike to *SRF4* and *DLG*, for *WIZ* an overall staining of the root in the elongation/differentiation zone can be observed. Not only the vascular bundle is affected. As well as for *DLG*, the root tip of *WIZ::GUS* plants show a strong staining. A strong staining of trichomes throughout all leaf developmental stages could be observed, exactly as for *DLG* and *SRF4*. An intermediate expression level between *SRF4* and *DLG* can be seen for *WIZ* when the expression in etiolated hypocotyls was checked. This result corresponds to the transcript analysis in etiolated seedlings.

Overall *SRF4*, *DLG* and *WIZ* are all active in the same tissues and overlap there in a significant way. In flowers *WIZ* expression looks like the intermediate

of *SRF4* and *DLG* expression. In roots *DLG* shows intermediate expression between *SRF4* and *WIZ*. All three do show a strong staining in trichomes and etiolated hypocotyls. Due to the expression patterns, not only the leaf phenotype, but also the trichome and root phenotype of *SRF4*, *DLG* and *WIZ* was examined in overexpression and mutant lines. For none of the genotypes an obvious phenotype, except for an influence on root growth, or problems during development could be observed.

2.4 Cell wall analysis

As reviewed in section 2.4, the cell wall can play an important role in cellular growth. To check whether the composition of the cell wall is altered in the single mutants carbohydrate composition was analyzed. The samples were prepared according to section 4.2.1.10 and analysed by the Cell Wall Group at the MPI Golm. The results of three different measurements for *DLG* and *SRF4* mutants can be seen in figure 2.36 and 2.37. The first measurements revealed a change in the xylose content. More xylose could be observed in the overexpressor lines, whereas the loss-of-function mutants showed less. Plants were grown for 21 d in greenhouse. To confirm this result a second measurement was done. Those plants grew in cellar growth room for 21 d. Unfortunately, the altered xylose content could not be reproduced. A third experiment, with 7 d old dark grown hypocotyls, revealed also no systematic change in the sugar components.

The experiment for *wiz-1* and *wiz-2* revealed alterations in different sugars. Arabinose and xylose are downregulated, whereas mannose galactose and glucose are upregulated ($p < 0.05$). *wiz-2* seems to be downregulated in its xylose content. The changes are not that prominent in dark grown hypocotyls which indicates different roles of *WIZ* in different tissues.

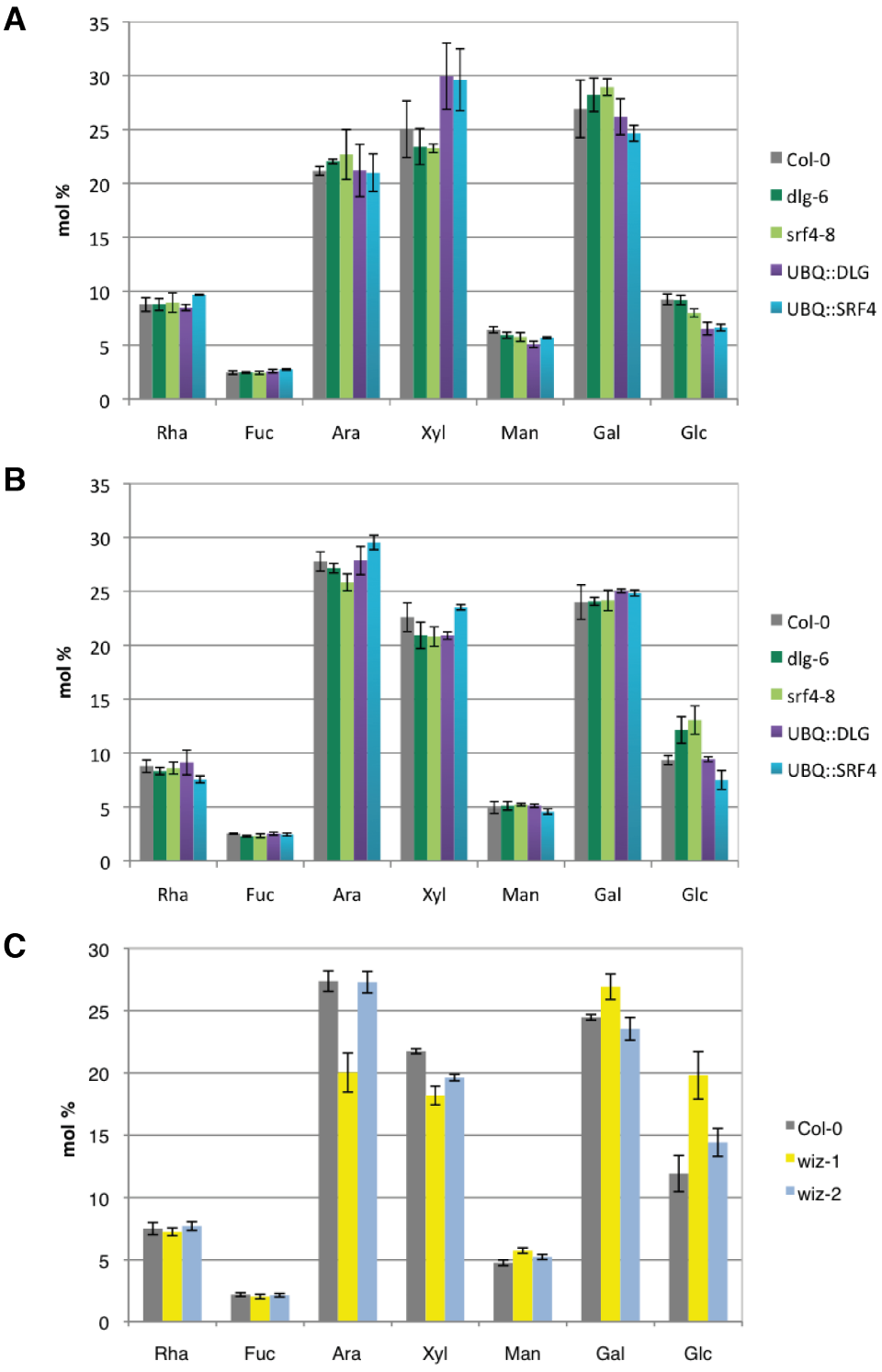

Figure 2.36: Results of the carbohydrate analysis of 21 d old plants. A: First measurement of plants grown in greenhouse. It revealed a change of xylose in the tested mutants. B: For the second measurement plants were grown in cellar growth room. The results of the first experiment could not be reproduced. C: *wiz* mutants were also analysed. They were also grown in cellar growth room for 21 d. (The results were produced via GC-MS approach by Colin Ruprecht of the MPI in Golm.)

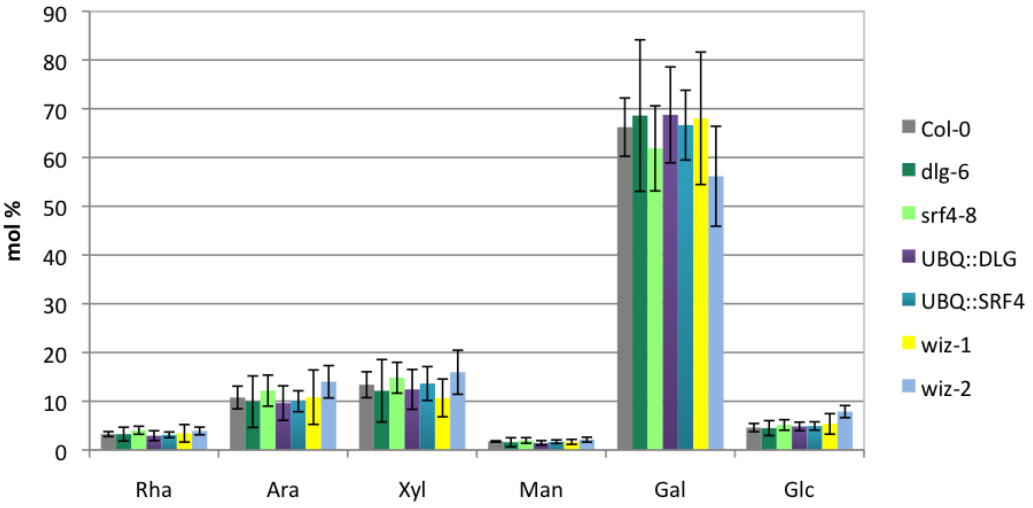

Figure 2.37: Results of the carbohydrate analysis of 7 d old etiolated hypocotyls. (The results were produced via GC-MS approach by Colin Ruprecht of the MPI in Golm.)

Chapter 3

Discussion and Outlook

The illustrated results for the potentially atypical kinase SRF4, the cytosolic hydroxypyruvate reductase DLG and the possibly double propellor comprising protein WIZ demonstrate an interesting but complex alliance of those three genes.

SRF4 and WIZ interact in yeast and the double mutant analysis revealed SRF4 to be epistatic to WIZ. Additionally, a catenation of WIZ and DLG is likely. Indeed, no direct interaction between both proteins could be shown, but the investigation of the double mutants suggests a connection.

The correlation between SRF4 and DLG was demonstrated by the ectopic expression of *SRF4* in the *DLG* loss-of-function mutant *dlg-6*. Hence, SRF4 signaling seems to happen partially via DLG. Furthermore, SRF4 and DLG could be shown to interact *in vitro*.

Results and continuative experiments, to enlighten open issues, are discussed in the following sections.

3.1 Is SRF4 an active kinase?

By sequence analysis it could be shown that *SRF4* is likely to code for an atypical kinase, like *SUB*. The results of the *in vitro* kinase assay showed that SRF4 might not be active. The *in vivo* experiment, the transformation of a kinase dead (KD) version of SRF4 *in planta*, did not yield a result. Three times in a row no transformants could be generated, while in parallel experiments it was possible.

In general two scenarios are can be imagined. In case one the kinase assay was incorrect and SRF4 is *in vivo* an active kinase. As SRF4 is predicted to be an unstable protein (SwissProt ProtParam) and as degradation products could be observed on the Western Blot, this might explain the inactivity of the protein *in vitro*. Another alternative would be that the used substrates (MBP and DLG) are not the ones getting phosphorylated by SRF4 and therefore no signal could be observed.

In the second case SRF4 would be an atypical kinase and the kinase assay was correct. If so the transformation of *UBQ::SRF4*$_{KD}$ to planta should mimic the phenotype of *UBQ::SRF4*. As this is actually not the case possibly other effects seem to happen *in planta*.

If the lack of transformed plants is real, and not only due to problems in the experimental setup, the question what mechanism might cause this effect remains. An overexpression of *UBQ::SRF4*$_{KD}$ K443E, functional or not, could lead to a neomorphic effect and cause lethality. A dominant negative effect of *UBQ::SRF4*$_{KD}$ should result in a *srf4-8* phenotype, which is not the case. But different control mechanisms might be able to explain this incident. If *SRF4* is transcribed partially or not at all, some other protein might be activated to take over its function. This might also explain the rather weak reduction of growth phenotype. If the SRF4 protein is already active in the system, but gets trapped by an invalid copy, this control mechanism might not be effective. The consequence would be lethality. *SRF4* is therefore indicated to be a negative regulator of transcription of a so far unknown gene. The potential localisation of *SRF4:EGFP* in the nucleus supports this hypothesis.

In each case this would indicate that this specific residue is important for SRF4 functionality. Within the 67 different *Arabidopsis thaliana* accessions analyzed no amino acid polymorphism at position 443 could be observed. Also another well conserved residue, an arginine (R) at position 517, did not show alterations. Even if those amino acids are not needed for phosphorylation of other proteins, they might be important for the correct folding of SRF4. Maybe the residues are also needed for the interaction with other proteins.

The question whether *DLG* or *WIZ* are putative phosphorylation partners to overcome the lack of activity of SRF4, like it is the case for ErbB-3 or MARK, can be addressed with the prediction of domains along the respective amino acid sequences. Neither for *DLG* nor *WIZ* a transmembrane helix could be detected as well as any active kinase domain. This makes both proteins very unlikely to

fulfill this function.

3.2 Does SRF4 interact with DLG and WIZ?

One still unresolved question is whether SRF4 really interacts with DLG and WIZ. The potential interaction partners were previously identified in a Y2H screen and consequently T-DNA lines were ordered and investigated.

SRF4 and DLG: the pros and cons The interaction between SRF4 and DLG is somewhat unclear. The Y2H interaction could not be reproduced. Also no *in vivo* interaction, via the BiFC method, could be shown. This could be due to problems in the experimental setup. Either the C-terminal YFP fusion to SRF4 and DLG could interfere with the interaction of the proteins or the signal caused by the interaction is too weak to be detected. N-terminal YFP fusion constructs could be tested for interaction to possibly overcome problems due to protein conformation. Furthermore, a co-immunoprecipitation could be helpful to confirm the *in vivo* interaction between SRF4 and DLG.

But there are many supportive facts for a connection of both genes. The GST pull-down assay showed a clear interaction *in vitro*. Moreover their phenotypes are very similar. *UBQ::SRF4* shows bigger, and to some extend sterile, plants and *srf4-8* smaller ones. One fact that holds also true for DLG. *UBQ::DLG* shows bigger leaves and the loss-of-function mutant smaller ones. *UBQ::DLG:EGFP* even exhibits 20 % sterile plants, which also fits the *SRF4* ratio. Furthermore *SRF4::SRF4:EGFP* and *DLG::DLG:EGFP* give no signal when controlled by their endogenous promoter. In addition, the cellular localization of *SRF4* in the plasma membrane and *DLG* in the cytosol would make an interaction possible. The *srf4-8 dlg-6* double mutant indicates *srf4-8* to be epistatic to *dlg-6*. Also their GUS patterns overlap. Both do show no staining in very young leaves, but in hypocotyls, trichomes and older leaves. These facts support an interaction between SRF4 and DLG.

Another genetic experiment, the transformation of *UBQ::SRF4* in *dlg-6* background, gave insight into the connection between the two genes. In T1 the typical sterility phenotype of *UBQ::SRF4* could not be observed. Leaf measurements in T3 clearly showed wildtype phenotype for 2 out of 3 lines, while one line was slightly increased in growth. Etiolated hypocotyls showed a similar effect. This indicates partial epistasis of *dlg-6* to *UBQ::SRF4*. Hence, *SRF4*

might act through *DLG* and another so far unknown protein to control growth regulation. This could be for example HPR3 which shares 45 % sequence identity with *DLG*.

SRF4 and WIZ The interaction between SRF4 and WIZ in yeast could be reproduced. Nevertheless, no *in vivo* interaction with BiFC could be shown.

The growth reduction of *wiz-1* is similar to *srf4-8*, which might be a hint that both proteins share a connection. Its bleaching phenotype also indicates an additional role in other pathways independent of *SRF4*. This is supported by the *wiz-2* gain-of-function phenotype which is also reduced in size.

Genetically, a clear connection between both proteins could be shown. *srf4-8* was able to rescue *wiz-1* and *wiz-2* phenotype, which indicates *SRF4* to be epistatic to *WIZ*. The overexpression of *SRF4* in *wiz-1* background gave an additive phenotype.

The expression pattern of *SRF4::GUS* and *WIZ::GUS* is similar to each other, while *WIZ* seems to be additionally expressed in the shoot apical meristem and in young leaves and carpels.

The transformation of *35S::SRF4:EGFP* in *wiz-1* background did not change the localisation of SRF4 to the plasma membrane (data not shown). *WIZ* seems therefore not to have any influence on the function of *SRF4* by dislocating it.

DLG and WIZ Interestingly, there seems to be also a connection between the two interaction partners of *SRF4*, *DLG* and *WIZ*. The double mutant analysis revealed *DLG* to be epistatic to *WIZ*. Preliminary results of the transformation of *UBQ::DLG* in *wiz-1* showed no rescue of the *wiz-1* phenotype. *DLG* therefore mimics the same effects on *WIZ* as *SRF4* does. No direct interaction between both proteins in yeast could be shown. It seems likely that the organ size phenotype of the *wiz-1* mutant is not due to a function in photorespiration as it could not be rescued by high CO_2 (data not shown).

These findings support the assumption that *SRF4* and *DLG* share a connection of so far unknown nature.

3.3 Regulation of DLG and SRF4

3.3.1 Potential control mechanisms of DLG

Taken the results of the EGFP and GUS lines together, one comes to the conclusion that they do not fit. Whereas *DLG::GUS* shows a very strong, almost overall expression, it was not possible to detect any signal for the *DLG::DLG:EGFP* construct. In contrast *UBQ::DLG:EGFP* showed a very bright signal. While any protein seems to be strongly expressed under the *DLG* promoter and the DLG protein is strongly expressed under the *UBQ* promoter, DLG protein regulated by the DLG promoter cannot be detected.

The very intense *DLG::GUS* staining in different organs correlates with the data provided by AtGenExpress [Schmid et al., 2005]. AtGenExpress signal intensity is quite strong and stable throughout all plant organs. On the other hand, *in situ* hybridization gave no signal for *DLG* transcript *in planta* (data not shown) and is therefore supporting the missing signal of the *DLG::DLG:EGFP* reporter gene construct. The colliding results do not allow any assessment of the mechanism of regulation of DLG.

However, an intrinsic regulation of the DLG protein itself seems to be likely. A hint was provided by the dimerization studies of DLG in yeast. In this system DLG protein is able to form dimers. It is suggested here that under wildtype conditions DLG dimerizes to provide a fast way of regulation and activity control. In EGFP lines autoregulation by dimerization might not be working as the EGFP tag is too big, but its biological function does not get disturbed. This could be the reason why sterility is only visible in transgenic *UBQ::DLG:EGFP* lines and not with the untagged *UBQ::DLG*.

3.3.2 SRF4 is regulated post-transcriptionally

SRF4 clearly undergoes some post-transcriptional regulation. *35S::SRF4:EGFP* only shows a detectable signal in the root and leaf epidermis while the *35S* promoter should be active throughout all root tissue. Possibly the transcript is controlled by mechanisms, such as blocking of the RNA by microRNA binding. For *SRF4* several putative binding sites have been predicted. The control may also happen on protein level. As it has been mentioned already, *SRF4* bears a strong PEST signal (+16.87) which is known to be involved in protein degradation by the 26S proteasome or the calpain protease [Rechsteiner and Rogers, 1996]

[Wang et al., 2003]. This site might be important for the protein half life and might be responsible for the changed expression pattern of the *35S* promoter. Still *SRF4* was not detectable in *in situ* hybridizations (data not shown), which indicates a regulatory mechanism already on transcript level. Nevertheless, *35S::SRF4:EGFP* was also transiently expressed in mesophyll protoplasts. The cell type seems therefore not to be important, but the organization of the cells in the tissue might be the clue to the control of *SRF4*.

The degradation of SRF4 via its PEST signal might be the reason for its localization in the nucleus. As the PEST motif is located after the TM membrane in the intracellular part of *SRF4*, the cleaved part might have an additional function there. But nevertheless so far it cannot be excluded that it is simply degraded protein without any specific function. As SRF4 was shown to be quite unstable in *E. coli* (data not shown) it is also likely that the signal might be unbound EGFP which localises in the nucleus and the cytoplasm. As never a signal for SRF4 in the cytosol was observed *in planta*, it is possible that some kind of guided mechanism is tracking SRF4 to its subcellular incidence. To lighten up this issue it is needed to perform a Western Blot to check for the degradation of SRF4:EGFP *in planta*.

As the additive phenotype of *35S::SRF4* in *wiz-1* background already indicated, *WIZ* seemed to have no influence on *SRF4* transcript level. The fact was proven by checking the *35S::SRF4:EGFP* signal in *wiz-1* lines. *SRF4* was still detectable in the plasma membrane (data no shown).

The reporter gene constructs of *SRF4*, *SRF4::GUS* and *35S::SRF4:EGFP*, showed a clear signal. The *SRF4::GUS* data is supported by AtGenExpress (data not shown). An increase of transcript could be detected in flower tissue. In mature pollen and stamen of stage ≥ 12 a strong increase of expression could be observed. This correlates to the GUS pattern of SRF4 in flowers. Furthermore, does rosette leaf two show low expression after 7 d but a much stronger one after 17 days of growth. A weaker signal in other investigated organs could be also observed. However, for the *SRF4::SRF4::EGFP* construct no signal was detectable. *In situ* hybridizations showed also no staining. Thereby, conclusions can be hardly drawn. Surprisingly, the results of the reporter gene analysis of *SRF4* mirror the results for *DLG*. This indicates a hidden mechanism that might have a regulative function on *DLG* and *SRF4*.

3.4 Possible functions of *SRF4*, *DLG* and *WIZ*

As an Receptor-Like Kinase *SRF4* is very likely to bind a ligand and transport a signal to the cytoplasm by spanning the plasma membrane. The ligand has not been identified so far. The phenotype of *SRF4* indicates it to be a positive regulator of leaf size. The intracellular signaling cascade was tried to enlighten with the Y2H screen and the nature of *DLG* and *WIZ* might give insight into the function of the *SRF4* pathway.

3.4.1 Putative functions of WIZ in growth and age control

The function of *WIZ* is so far unknown. Its loss of function phenotype indicates some role in growth and senescence regulation. Due to the bleaching of the leaves the photosynthetic yield is reduced and photosynthesis cannot produce as much energy as in healthy leaves. This might therefore result in smaller leaves. While growth reduction is overcome in later developmental stages, the bleached leaves are still present. This fact in mind indicates that some other protein might overtake *WIZ* function in growth regulation. As the leaves are already damaged suggests that the bleaching is not responsible for the growth reduction. *WIZ* seems to have therefore at least two functions: growth and age control. Its role in growth regulation can be explained with the connection to *SRF4* and *DLG* which both also show slight reduction of organ size under certain conditions. However, the question whether *wiz-1* shows a photorespiratory phenotype can be answered with no. For *wiz-1* no rescue of the phenotype could be achieved under high CO_2. A phenotype due to photorespiration should be overcome by avoiding the binding of O_2 by RuBisCO. Maybe *SRF4* and *DLG* are not only part of photorespiration but have also other functions in cellular signaling. The senescence phenotype was not observed for any of the *SRF4* and *DLG* mutants.

It can be assumed that *WIZ* is involved also in other pathways that might be responsible for age control. As chlorophyll is a very powerful molecule and it is an potential phototoxin which can damage the cell, it is crucial to understand chlorophyll metabolism in detail. Proteins involved in chlorophyll breakdown either stay green for longer time or show bleached leaves as a form of cell death [Hortensteiner and Krautler, 2011] [Hortensteiner, 2004]. *wiz-1* shows bleached leaves, while the overexpressor *wiz-2* has more chlorophyll in its leaves. This opposite phenotype indicates a role in chlorophyll metabolism.

Also cytokinins are known to be a negative regulator of senescence [Nooden et al., 1979] [Gan and Amasino, 1995]. When checking the Genevestigator and ArrayExpress Data it can be seen that *WIZ* expression level, under the context of the cytokinin signaling pathway, is changed. *AHK2*, *AHK3* and *AHK4* are cytokinin receptors. The *ahk3 ahk4* double mutant showed a clear reduction of *WIZ* transcript. Also in the *arr10 arr12* double mutant, two transcription factors downstream of the *AHKs*, a reduction of *WIZ* transcript could be observed when the cytokinin t-zeatin was applied [Yokoyama et al., 2007] [Muller and Sheen, 2007]. Furthermore a connection between the cytokinin and the ABA signaling pathway could be shown [Nishiyama et al., 2011]. Interestingly, *WIZ* transcript level is downregulated in *gia3*, an ABA insensitive mutant [Kinoshita et al., 2010]. Taken the expression results and the *wiz-1 phenotype* together, a connection between *WIZ* and the cytokinin pathway seems very likely. As all cytokinin deficient mutants seem to be quite tolerant to drought and salt stress, it might be helpful to test the *wiz* mutants for their stress resistance [Nishiyama et al., 2011].

An overflow of *WIZ* can end in a changed leaf shape which might be due to problems in the control of polar cell expansion or proliferation. As almost no phenotype in dark grown hypocotyls could be observed (data not shown) and the *WIZ::GUS* staining revealed a strong signal in young leaves it might be likely that rather than cell expansion, cell proliferation might be affected. For *wiz-2* dark grown hypocotyls looked also slightly broader compared to wildtype which might indicate also an additional function in polar cell expansion. *wiz-2* expresses a similar phenotype to *rotundifolia3* and *rotundifolia4-1D* for which the polar cell elongation and proliferation is disturbed, respectively [Kim et al., 1998a] [Narita et al., 2004][Tsukaya, 2006]. The leaf index of *wiz-1* seems to be stable, which indicates that the loss-of-function causes more an effect in non-polar cell expansion or proliferation.

On a biochemical level *WIZ* belongs to the WD40 repeat containing protein with an unknown RIC1 domain *in planta*. It could be shown that WD40 domain proteins are involved in protein-protein interactions and that they build a strong scaffold [Xu and Min, 2011]. It can also serve as some kind of hub to which many different proteins can bind to, and different interactions can be facilitated. It is therefore likely that this protein might be involved in different pathways. The RIC1 domain is involved in vesicle fusion to the Golgi apparatus in yeast. This might provide a hint to a potential function in guiding vesicles to their

destination in the cell. The localization of *WIZ* in the cell will help interpreting its function.

3.4.2 *SRF4* and *DLG* in photorespiration

As *DLG* codes for HPR-2, this might be the pointer to the phenotype of both genes. If *SRF4* is able to regulate HPR2, there would be a direct link to primary metabolism. If this mechanism gets disturbed by knocking out one or the other gene less carbon is recycled and toxic intermediates might accumulate. This is likely to have a direct influence on plant growth. Another fact is that the phenotype of *UBQ::SRF4* as well as *35S::SRF4* plants gets silenced in T4 generation. Also the phenotype of *srf4-2* and *srf4-3* disappeared due to so far unknown reasons. Interestingly, tobacco plants which were selected for low rates of photorespiration, could as well not be maintained across several generations [Zelitch, 1992]. This indicates a strong maintenance of photorespiratory pathways and its importance for plants. Maybe this mechanism is also active on *SRF4*.

The conversion of hydroxypyruvate to glycerate by *HPR1* is taking place in the expected compartment: the peroxisome. The discovery of the cytosolic *HPR2* was in one way surprising. It was shown that hydroxypyruvate was not able to pass peroxisomal membranes [Heupel et al., 1991] [Reumann et al., 1994]. But an indirect link between the peroxisomal and the cytosolic *HPR* was shown, as a double mutant exhibited severe growth problems while the single loss-of-function lines were only slightly reduced [Timm et al., 2008]. The cytosolic *HPR2* seemed to be therefore able to bypass the lack of the peroxisomal *HPR1*. It is hypothesized that the availability of NADH might regulate the hydroxypyruvate flux from peroxisomes to the cytosol. If no NADH is present in peroxisomes, *HPR1* is not able to convert its substrate. The source of peroxisomal NADH comes from the chloroplasts and mitochondria by malate oxidation [Scheibe et al., 2005] [Reumann and Weber, 2006]. The regulation of those fluxes might be the critical step and under different environmental conditions regulated sensitively. Therefore, the cytosolic bypass might be important only under special conditions which are not identified yet. Maybe, this is be the reason for the sensitiveness of the *srf4-8* phenotype to environmental changes. The 24 h light in cellar growth room and the therefore stable high temperatures might change the redox homeostasis of the peroxisomes and cause a shift to the

cytosolic bypass in which *SRF4* might be involved. The interaction between *SRF4* and *DLG* might be consequently hard to demonstrate under temperate, long day conditions. To find out whether SRF4 is a part of photorespiration it is suggested to check for changed metabolites which are involved in this pathway, like it was done for DLG [Timm et al., 2008].

The results presented in this thesis indicate SRF4 and DLG to be positive regulators of leaf size. Interaction studies of both genes suggest that SRF4 might control this process partially through the cytosolic hydroxypyruvate reductase DLG.

Chapter 4

Materials and Methods

4.1 Materials

In this chapter comprehensive information about the used Materials can be found.

Company name	City	Country
Amersham Biosciences	see GE Healthcare	
Applichem	Darmstadt	Germany
Fermentas	St. Leon-Rot	Germany
Finnzymes	Espoo	Finland
Fluka	see Sigma	
GE Healthcare	Waukesha (WI)	USA
Genomed	Löhne	Germany
Kodak	Stuttgart	Germany
Macherey-Nagel	Düren	Germany
Merck	Darmstadt	Germany
Millipore	see Merck	
New England Biolabs	Ipswich (MA)	USA
Pierce	Rockford (IL)	USA
Patzer	Sinntal-Jossa	Germany
Roche	Basel	Schweiz
Roth	Karlsruhe	Germany
Sigma	Munich	Germany
Stratagene	La Jolla (CA)	USA
Takara	Otsu	Japan
X-Gluc Direct	West Yorkshire	United Kingdom
Whatman International	Maidstone	England

Table 4.1: Detailed company information.

4.1.1 Chemicals, enzymes, hard- and software

4.1.1.1 Chemicals and solutions

All chemicals used in this study were purchased from either one of the companys mentioned in table 4.1. The main suppliers of chemicals were Sigma, Fluka, Roth and Applichem. Solutions were prepared according to [Sambrook and Russel, 2001] unless it is mentioned different in this thesis.

4.1.1.2 Enzymes

Restriction endonucleases have been used from New England Biolabs (NEB). For cloning either *Pfu* ultra high fidelity polymerase (Stratagene), *Phusion* High-Fidelity DNA polymerase (Finnzymes) or *Primestar* HS DNA Polymerase (Takara Bio Inc.) were applied to amplify templates.
cDNA synthesis was done with M-MuLV Reverse Transcriptase (Fermentas) unless it was done with the Revert Aid First Strand cDNA Synthesis kit (Fermentas).
For standard PCR reactions (e.g. genotyping, RT-PCR) *Taq* DNA polymerase (NEB) was used. Ligation reaction was performed with T4 DNA Ligase (NEB).

4.1.1.3 Primers

Primers were either ordered from Operon or Sigma. The list of primers used for genotyping of the main T-DNA lines used in this thesis can be found in table 4.2. Specific Left-Border (LB) and Right-Border (RB) primers used for the SALK, SAIL and Gabi-Kat T-DNA insertion lines as well as the LB for the Gene Trap line are also given. The primers used for cDNA amplification and cloning can be seen in table 4.3 and 4.4, respectively.

4.1.1.4 Antibodies

For the detection of GST-tagged proteins a monoclonal mouse IgG GST-HRP antibody (Millipore) coupled to horseradish peroxidase was applied whereas for His-tagged proteins an Anti-HisG-HRP-antibody was used. Both can be detected with the Super Signal West Femto Maximum Sensitivity Substrate (Pierce).

Primer Name	Genotyping of	Sequence 5' → 3'
srf4-6/7_F	*srf4-7*	aatggtttgatactcttcaccgattc
srf4-6/7_R	*srf4-7*	acatatactcaatgaagtt
srf4-5F	*srf4-8*	ggctctataaatgctctcagggacctcc
srf4-5R	*srf4-8*	ccggattgccttttcctaacagagaaga
N605874_F2	*dlg-6*	gggcccaaaaataggcccatctttatcg
N605874_R2	*dlg-6*	acgggcatgcgacgacgaggat
GK471A09_R	*dlg-9*	accaccgtcggataatacttgtag
WiZ_Specific_F	*wiz-1*	gcattgtttgttcttggggttttt
N835013_R	*wiz-1*	gttcatcacaaaattccaccatccct
N541026_F	*wiz-2*	cataaaccggtcgggcaattcc
WIZ_specific_R	*wiz-2*	ctcagctggataaagattgat
N801017_F	*wizl-1*	cggcgtgtactgggcgcgagacgtctct
N801017_R	*wizl-1*	tctcagctggagaaagtgac
N810180_F	*wizl-2*	tctacctggatcgtgtccgtcttcg
N810180_R	*wizl-2*	gcacaaagaattcaatgcagatg
LBb1.3_SALK	SALK LB	attttgccgatttcggaac
R175_SALK_LB	SALK LB	aatcagctgttgcccgtctcactggtgaa
R409_SALK_RB	SALK RB	attaaactccagaaacccgcggctgag
pDAP101_LB1	SAIL LB	gccttttcagaaatggataaatagccttgcttcc
pDAP101_RB1	SAIL RB	attaggcaccccaggctttacactttatg
GeneTrap_LB	GeneTrap LB	ccgttttgtatatcccgtttccgt
GK_LB1	Gabi-Kat LB	ataataacgctgcggacatctacatttt

Table 4.2: Primers used for genotyping of *srf4*, *dlg*, *wiz* and *wizl* insertion lines.

Primer Name	cDNA level of	Sequence 5' → 3'
srf4-cDNA_f	*srf4-8* before	tcgtgtgtttccttcatccc
srf4-cDNA_r	*srf4-8* before	gtttttgcaagaacaacgga
SRF4_cDNA_Fnew	*srf4-8* after	ggaagagttttcacacatagtgtcgagtat
SRF4_cDNA_Rnew	*srf4-8* after	ctacactagcctcttcaatgcctccaccac
OR_seq_F	*dlg-6* before	atggaatcaatcggagtccttatgatgtgc
dlg-6_RTPCR_rev	*dlg-6* before	gtgttggtgacgcggatc
DLGcDNA_specific_f	*dlg-6* after	ctcactaccaagtttagtgga
OR_pGBKT7_PstI_R	*dlg-6* after	aaaactgcagaaatccgttccttatatacgaca
At3g61480_cDNA_F	*wiz-1* before	atggcttacgggtggccgcaggtga
At3g61480_cDNAlevel_R	*wiz-1* before	gcccattaccaagagtgtaggac
wiz-1_cDNAlevel_specific_F	*wiz-1* after	gaagataatttgtcttctgatttgtcagaa
WIZ_cDNA_Rnew	*wiz-1* after	gttgttgatatcccagcagc
GapCscDNA	*GAPC* (control)	cacttgaagggtggtgccaag
GapCas	*GAPC* (control)	cctgttgtcgccaacgaagtc

Table 4.3: Primers used for transcript amplification before and after the T-DNA insertion site are shown here with their name and the sequence.

Primer Name	**Sequence 5'→ 3'**	**amplification of**
UBQ10(KpnI)_F	taggtaccgtctagctcaacagagcttttaac	UBQ10 promoter
UBQ10(AscI)_R	aaggcgcgcccttgatcacggtagagagaatt	
UBQ::DLG_HindIII_for	cccaagcttggggtctagctcaacagagcttttaac	
uni51-Fwd	ctgttggtgtgtctattaaatcg	insert of pUNI 51 cloning vector
uni51-Rvs	tggctggcaactagaaggcac	
SRF4_f_PacI	ccttaattaaggatgggaccaaatctgca	SRF4
SRF4_r_FLAG_SpeI	gactagtctttatcatcatcatctttataatccactagcctcttcaatgcc	
SRF4_Phusion_AscI_F	ctgtcggatcggcgcgccatgggaccaaatctgcagcaatcgta	
SRF4intra_pGEX_4T_SalI	acgcgtcgaccgaagaaagaactctaatgattc	*SRF4*$_{intra}$
SRF4intra_pGEX_4T_NotI	ataagaatgcggccgccactagactacactagcctctt	
SRF4intra_PGBKT7_SalI_f	acgcgtcgacgaagaaagaactctaatgattc	
SRF4intra_NdeI_f	atatcatatgcgaagaaagaactctaatga	
SRF4intra_XmaI_r	atatcccgggctacactagcctcttcaatg	
pSRF4_KpnI_f	ggggtaccccgtcatgcatagatttggttttgatgaagcatg	*SRF4* promoter
pSRF4_AscI_r	ggcgcgccgatccgacagttttaagctcaaaaatcaaaatc	
DLG_SpeI_HIS_r	atatactagtgacgaccggagtcagaagtg	*DLG*
ORfull_AscI_f	ggcgcgccatggaatcaatcggagtccttatgatgt	
DLG_AatII_r	cgcagcggcagcggcagcagccctgacgtcgacgaccggagtcagaagtg	
DLG_AscI_f	ggcgcgccatggaatcaatcggagtccttatgatgt	
DLG_SpeI_r	atatactagtgacgaccggagtcagaagtg	
Orfull_pGBKT7_NdeI_f	ggaattccatatgatggaatcaatcggagtccttatgatgtgc	
Orfull_pGBKT7_XmaI_r	tccccccgggtcagacgaccggagtcagaagtgatttccc	
DLGprom_KpnI_f	atatggtaccgagaatcaaaagggaaggagaagct	*DLG* promoter
DLGprom_NcoI_r	atatccatggatctccttttctctgttttttttttttatttttc	
DLGprom_AscI_r	ggcgcgccatctccttttctctgttttttttttttatttttc	
WIZ_SalI_f	atatgtcgactggcttacgggtggccgcag	*WIZ and WIZL*
WIZ_NotI_r	atatgcggccgctcaagagatggaacctct	
WIZ_XmaI_f	atatcccgggggcttacgggtggccgcagg	
WIZ_XhoI_r	atatctcgagtcaagagatggaacctctat	
At3g61480_cDNA_F	atggcttacgggtggccgcaggtga	
At3g61480_cDNA_R	tcaagagatggaacctctattgctt	
WIZprom_pC1305.1_KpnI_f	atataggtaccatctctctcttacctttctctctttccgaa	*WIZ* promoter
WIZprom_pC1305.1_PstI_r	atgcgcctgcagatacatctttggctacctcg	
SRF4EGFP_PmeI_r	gggtttaaacccgcatgcctgcaggtcctg	*EGFP*
EGFP_AatII_r	gacgtcagggctgctgccgctgccgctgcg	
OCS3_HindIII_r	atataagcttgcatgcctgcaggtcctgctgagcc	OCS3 terminator

Table 4.4: Primers used for cloning of constructs used in this thesis.

Name of the Kit	Wherefore	Company	Catalog Nr.
NucleoSpin Extract II	Gel extraction	Macherey-Nagel	740609.250
JetStar 2.0	Midi Prep	Genomed	210025
NucleoBond PC 100	Midi Prep	Macherey-Nagel	740573.100
NucleoSpin Plasmid	Mini Prep	Macherey-Nagel	740588.250
NucleoSpin RNA II	RNA preparation	Macherey-Nagel	740955.20
Revert Aid First Strand cDNA Synthesis kit	cDNA synthesis	Fermentas	#K1622
Protino Ni-TED 2000 packed columns	His-tagged protein purification	Macherey-Nagel	745120.25
Phire Plant Direct PCR Kit	Genotyping of plant tissue	Finnzymes	F-130
CloneJET PCR Cloning Kit	Cloning of PCR products	Fermentas	K1231

Table 4.5: Table of Kits used for different requirements. For detailed company information see table 4.1.

4.1.1.5 Transfer membrane

The nitrocellulose polyvinyle-difluorid (PVDF) membrane Immobilon^{TM}-P Transfer Membrane for the Western Blot was ordered from Millipore. The used pore size was 0.45 µm.

4.1.1.6 Kits

For convenience and efficiency reasons different kits for variable intentions have been used. In table 4.5 the used kits and their purpose are listed.

4.1.1.7 Devices

The devices used for Protein and Nucleic Acid work are listed in table 4.6.

4.1.1.8 Growth media

Bacterial growth media Lysogeny-Broth (LB) or LB Agar (1.5 %) were used to culture *E.coli* [Bertani, 1951] [Bertani, 2004]. Alternatively after trans-

Device	Name	Company
Centrifuges	5810 R	Eppendorf
	5417 R	Eppendorf
	5415 D	Eppendorf
	Avanti J-26 XP	Beckmann Coulter
PCR machine	Tpersonal	Biometra
Blotter	Trans-Blot SD	BIORAD
Photometer	Biophotometer	Eppendorf
Shaker	Incucell	MMM Medcenter
Thermoshaker	Thermomixer compact	Eppendorf
	Thermomixer 5436	Eppendorf
Protein electrophoresis	Mini Protean Tetra Cell	BIORAD
GelDoc	EpiChemie^{3}Darkroom	UVP Bioimaging Systems
Spectrophotometer	Uvikon 820	Kontron
	Ultrospec 2000	Pharmacia Biotech
Vacuum Dryer	SpeedVac Concentrator	Savant Instruments
Electroporator	2510	Eppendorf
Luminescence Analyzer	LAS-4000 mini	Fujifilm
Special accuracy weighing machine	LP620P Präzisionswaage	Satorius
Microscopes	SZX12	Olympus
	BX61	Olympus
	IX81 Fluoview FV1000	Olympus

Table 4.6: Devices used for this thesis. Standard equipment like Stirrer, Power Supplies and so forth are not listed.

formation or for Protein induction also Super Optimal Broth (SOB) with 10 mM $MgCl_2$ can be used.

Yeast growth media Yeast were grown in YPD or YPD Agar (1.5-2.0 %) full medium. Transformed Yeast were grown in corresponding Synthetic Drop-Out (SD) or SD agar medium. For media preparation the recipes in [Gilmartin and Bowler, 2002], chapter 9 was followed. The used drop-out mix was not self made but ordered from Sigma (Y2001, Yeast Synthetic Drop-out Medium Supplements without histidine, leucine, tryptophan and uracil).

Plant growth media *Arabidopsis* seeds were germinated on Murashige and Skoog (MS) medium with additional 1 % sucrose and 0.9 % agar

[Murashige and Skoog, 1962]. If plants were directly grown on soil Einheitserde, Typ T (Patzer) was used.

4.1.2 Microorganisms and the corresponding vectors

For cloning, transformation and interaction studies different kind of microorganisms are needed as host, carrier or model organism. In the following paragraphs the strains and the used vectors are described.

***Escherichia coli* strains and vectors** For standard DNA manipulations like the propagation of vectors and cloning the *E. coli* strains DH5α or DH10B have been used [Grant et al., 1990]. The *E. coli* strain BL21 (DE3) pLysS was used for protein expression [Studier and Moffatt, 1986] [Davanloo et al., 1984]. The genotypes of the used strains can be found in table 4.7. For detailed vector information check table 4.9.

***E. coli* strain**	**Genotype**
DH5α	F⁻ *endA1 hsdR17* (r_k^-, m_k^+) *supE44 thi-1* λ^- *recA1 gyrA96 relA1 deoR* Δ*(lacZYA-argF)*-U169 Φ80d*lacZ*ΔM15
DH10B	F⁻ *araD139* Δ*(ara, leu)7697* Δ*lacX74 galU galK rpsL deoR* Φ80d*lacZ*Δ*M15 endA1 nupG recA1 mcrA* Δ*(mrr hsdRMS mcrBC)*
BL21 (DE3) pLysS	F⁻ *ompT gal dcm lon* $hsdS_B(r_B^- m_B^-)$ *λ(DE3) pLysS*(cm^R)

Table 4.7: Used *E. coli* strains and their genotypes.

***Agrobacterium* strains and vectors** *Agrobacterium tumefaciens* strain GV3101 (pMP90), a rifampicin and gentamycin resistant bacteria, was used for plant transformations. The used binary vectors for these experiments can be found in table 4.9 [Koncz and Schell, 1986].

***Saccharomyces cerevisiae* strains and vectors** For the yeast two-hybrid screen PJ69-4A was used as host [James et al., 1996]. For the individual yeast two-hybrid interaction studies AH109 was utilized [Gilmartin and Bowler, 2002]. The genotypes of the strains can be found in table 4.8 and the corresponding vector information in table 4.9.

***S. cerevisiae* strain**	**Genotype**
PJ69-4A	*MAT***a** *trp1-901 leu2-3,112 ura3-52 his3-200 gal4*Δ *gal80*Δ *LYS::GAL1-HIS3 GAL2-ADE2 met2::GAL7-lacZ*
AH109	*MATa, ura3-52, his3-200, lys2-801, ade2-101, trp1-901, leu2-3,112, gal4*Δ *gal80*Δ*, LYS::GAL1$_{UAS}$-GAL1$_{TATA}$-HIS3, GAL2$_{UAS}$-GAL2$_{TATA}$-ADE2, URA3::MEL1$_{UAS}$-MEL1$_{TATA}$-LACZ*

Table 4.8: Used *S. cerevisiae* strains and their genotypes.

4.1.3 Plant lines and the corresponding vectors

For all experiments *Arabidopsis thaliana* (L.) Heyn var. Columbia (Col-0) and var. Landsberg (*erecta* mutant) (L*er*) were used as wild-type strains. T-DNA or Gene-Trap lines were recieved from the **N**ottingham **A**rabidopsis **S**tock **C**entre (NASC) [Scholl et al., 2000]. An overview of the investigated plant lines is listed in table 4.10. *srf4-8* as well as *dlg-6* are meant to exhibit kanamycin resistance but both seem to have problems with growth on kanamycin plates. This indicates that the resistance gene might be silenced. The other lines should be able to grow on corresponding selective media.
In this thesis transgenic lines have been created and used for further investigations. An overview of those lines can be found in table 4.11. The vectors which have been used for plant transformation can be found in table 4.9.

4.1.4 Software and databases

For this thesis different helpful programs in order of data handling and retrieving have been used. For sequence analysis and ordering of T-DNA lines, BACs or cDNA clones different databases have been accessed. The used software is listed in table 4.12 and the databases in table 4.13. Standard text editing and presentation software is not mentioned here. This thesis has been written in LaTeX using the MacTeX-2010 software package with the Aquamacs Emacs editor.

Vector Name	Purpose	Company	Organism	Resistance
pJet1.2/blunt	PCR product direct cloning	Fermentas	*E. coli*	ampicillin
pGEM-T Easy	Cloning	Promega	*E. coli*	ampicillin
pCAMBIA1305.1	Binary vector for plant transformation with GUS reporter gene	CAMBIA	*E. coli*	kanamycin
			Agrobacterium	kanamycin
			Plant	hygromycin
pCAMBIA1390	Binary vector for plant transformation	CAMBIA	*E. coli*	kanamycin
			Agrobacterium	kanamycin
			Plant	hygromycin
pCAMBIA1390*	Binary vector for plant transformation	CAMBIA	*E. coli*	kanamycin
			Agrobacterium	kanamycin
			Plant	kanamycin
pCAMBIA2300	Binary vector for plant transformation	CAMBIA	*E. coli*	kanamycin
			Agrobacterium	kanamycin
			Plant	kanamycin
pGADT7	Y2H: protein fusion to GAL4 Activation Domain	Clontech	Yeast	encodes Leucine
			E.coli	ampicillin
pGBKT7	Y2H: protein fusion to GAL4 Binding Domain	Clontech	Yeast	encodes Tryptophan
			E.coli	kanamycin
pGEX-4T-3	Inducible expression of GST fusion proteins in *E. coli*	Amersham Biosciences	*E. coli*	ampicillin
pSPYCE [1]	Transient expression of C-terminal YFP fusion protein for in vivo interaction studies		*E. coli*	ampicillin
pSPYNE [1]	Transient expression of N-terminal YFP fusion protein for in vivo interaction studies		*E. coli*	ampicillin

[1] [Walter et al., 2004]

Table 4.9: Information about the vectors used in this thesis. pCAMBIA* labels a modified version of the orignal pCAMBIA1390 vector which exhibits hygromycin resistance in plants. The modified version has kanamycin resitancy.

4.2 Methods

4.2.1 Plant work

4.2.1.1 Plant growth conditions

Plants were grown either in a greenhouse under Philips SON-T Plus 400 Watt fluorescent bulbs on a long day cycle (16 hrs light) or in a growth room under Osram L 36W/840 Lumilux Cold White bulbs on 24 hrs light in cellar. Dry seeds were sown on soil (see 4.1.1.8) situated above a layer of perlite, stratified for 2-4 days at 4 °C and then placed in the greenhouse or growth room. Plants on MS-agar plates were grown in a cell-culture room at 22 °C next to vertically

Name	Identifier	Gene of interest	Background	Resistance
srf4-7	CS26952	At3g13065	L*er*	kanamycin
srf4-8	SALK_05554	At3g13065	Col-0	kanamycin
dlg-1	SAIL_1289_A11	At1g79870	Col-0	glufosinat
dlg-2	SALK_105874	At1g79870	Col-0	kanamycin
dlg-3	SALK_105883	At1g79870	Col-0	kanamycin
dlg-4	SALK_123913	At1g79870	Col-0	kanamycin
dlg-5	SALK_105875	At1g79870	Col-0	kanamycin
dlg-6	SALK_105876	At1g79870	Col-0	kanamycin
dlg-7	SALK_105876	At1g79870	Col-0	kanamycin
dlg-8	SALK_105884	At1g79870	Col-0	kanamycin
dlg-9	GABI-Kat 471A09	At1g79870	Col-0	sulfadiazine
wiz-1	SAIL_783_C08	At3g61480	Col-0	glufosinat
wiz-2	SALK_041026	At3g61480	Col-0	kanamycin
wiz-3	SALK_017426C	At3g61480	Col-0	kanamycin
wiz-4	SAIL_291_F03	At3g61480	Col-3 (*quartet*)	glufosinat
wiz-5	GABI-Kat 337B09	At3g61480 or At5g28350	Col-0	sulfadiazine
wizl-1	SAIL_20_D04	At5g28350	Col-0 (*quartet*)	glufosinat
wizl-2	SAIL_220_A03	At5g28350	Col-0 (*quartet*)	glufosinat

Table 4.10: Ordered and/or investigated plant lines in this thesis.

arranged the same fluorescent bulbs used in cellar growth room.

4.2.1.2 Plant transformation

Reagents

- LB-medium
- Sucrose
- Silwet L-77
- according antibiotics

After transformation of the construct of interest to *Agrobacterium tumefaciens* (see section 4.1.2 and 4.2.3.2) a single colony was inoculated in 5 ml LB with adequate antibiotics (see table 4.14). After allowing the preculture to grow for 24 hrs at 30 °C while rotation, 2 ml were transferred to a 1 l flask containing 250 ml selective media (LB). This liquid culture was grown at 30 °C under agitation until an OD_{600} = 2.8-3.0 was reached. This will take around 18 hrs. After

Line Name	Used Vector	Purpose	Background
UBQ::SRF4	pCAMBIA1390, pCAMBIA1390*	Overexpression of *SRF4*	*Col-0* *dlg-6* *srf4-8*
UBQ::SRF4 K→E	pCAMBIA1390	Overexpression of SRF4 kinase dead version	*Col-0*
35S::SRF4	pCAMBIA2300	Overexpression of *SRF4*	*Col-0* *wiz-1* *wiz-2*
35S::SRF4:EGFP	pCAMBIA2300	Cellular localization of *SRF4*	*Col-0*
SRF4::SRF4:EGFP	pCAMBIA2300	Cellular localization of *SRF4* with endogenous promoter	*Col-0*
UBQ::DLG	pCAMBIA1390	Overexpression of *DLG*	*Col-0* *wiz-1*
UBQ::DLG:EGFP	pCAMBIA2300	Cellular localization of *DLG*	*Col-0*
DLG::DLG:EGFP	pCAMBIA2300	Cellular localization of DLG with endogenous promoter	*Col-0*
SRF4::GUS	pCAMBIA1305.1	Putative transcript localization of *SRF4*	*Col-0*
DLG::GUS	pCAMBIA1305.1	Putative transcript localization of *DLG*	*Col-0*
WIZ::GUS	pCAMBIA1305.1	Putative transcript localization of *WIZ*	*Col-0*

Table 4.11: Overview of plant lines created and/or used in this thesis.

Software	**Purpose**
Geneious [1]	design of clones and sequence analysis
ImageJ [2]	plant organ measurements
Olympus FluoView1000	confocal microscopy
cellP and cellF	binocular and fluorescence microscope
DA-2000	photosynthetic yield
VectorNTI	design of clones
Adobe Illustrator	picture assembly
Adobe Photoshop	picture editing
MacTEX-2010	LaTeX package for Mac
Aquamacs	editor
CAP3 [3]	assembly of WIZ cDNA sequence
Blast [4]	local sequence alignment
ClustalW2 [5]	multiple sequence alignment
MAFFT [6]	multiple sequence alignment
Swiss Model [7]	homology modeling
Chimera [8]	protein structure viewer
TMHMM v. 2.0 [9]	prediction of transmembrane domains
MicroInspector [10]	prediction of micro RNA binding sites
ClustalW2-Phylogeny	phylogentetic tree calculation
RAxML [11]	phylogentetic tree calculation
OrthoMCL [12]	clustering of orthologs based on sequence similarities

[1] [Drummond et al., 2010]
[2] [ImageJ, 2010]
[3] [Huang and Madan, 1999]
[4] [Altschul et al., 1990]
[5] [Thompson et al., 1994]
[6] [Katoh et al., 2009]
[7] [Arnold et al., 2006] [Schwede et al., 2003]
[8] [Pettersen et al., 2004]
[9] [Krogh et al., 2001]
[10] [Rusinov et al., 2005]
[11] [Stamatakis, 2006]
[12] [Li et al., 2003]

Table 4.12: Software used in this thesis.

Database	Purpose
TAIR [1]	ordering BACs, T-DNA lines, cDNA clones, sequence analysis
NASC [2]	ordering of T-DNA lines
MAtDB [3]	gene analysis
NCBI [4]	sequence analysis and Pubmed search
SwissProt [5]	Protein sequence analysis
RIKEN [6]	ordering cDNA clones
SIMAP [7]	protein similarity search in different organisms
PDB [8]	protein structures
ArrayExpress [9]	gene expression data at the EBI
Genevestigator [10]	gene expression data
1001 Genomes [11]	*A. thaliana* genetic varitations
Conserved Domain Database (CDD) [12]	prediction of conserved domains
Interpro [13]	sequence analysis and classification
AtGenExpress [14]	microarray data

[1] [Huala et al., 2001]
[2] [NASC, 2011]
[3] [Schoof et al., 2002]
[4] [NCBI, 2011]
[5] [Gasteiger et al., 2003]
[6] [RIKEN, 2011]
[7] [Rattei et al., 2010]
[8] [Berman et al., 2002]
[9] [Rocca-Serra et al., 2003]
[10] [Hruz et al., 2008]
[11] [Cao et al., 2011]
[12] [Marchler-Bauer et al., 2009]
[13] [Hunter et al., 2009]
[14] [Schmid et al., 2005]

Table 4.13: Databases used for sequence analysis.

obtaining the favoured OD_{600} the cells were centrifuged down (15 min, 14 °C, 4000 g). The cell pellet was resuspended in 700 ml fresh 5 % sucrose solution. To make the *Agrobacteria* suspension stick well to the plant an amount of 0.034 % Silwet was added.

To transform the flowering plants around 300 ml of the *Agrobacteria* solution was poured in a beaker. The plants should be healthy, not stressed or treated with any kind of chemical. The selected plants were dipped into the beaker and kept there for 1-2 min. Following the moistened plants were moved to a new tray and after transforming 4-8 pots of one genotype the tray was covered with a plastic lid and moved away from any too close light source. After no longer than 24 hrs the plants were brought back to light and the lid was taken off. The

protocol was adapted from [Clough and Bent, 1998].

4.2.1.3 Seed sterilization

Reagents

- 13 % NaClO
- 3 % NaClO
- 37 % HCl
- 70 % Ethanol
- 0.1 % Agar

After harvesting the seeds were dried at room temperature in a desiccator with silica gel for 1 week. Before long term storage the seeds were sterilized. For that reason 100 ml of 13 % NaClO were poured into a beaker. After placing the seeds and the beaker in a desiccator, 3 ml of concentrated HCl was added. The desiccator was closed immediately as the following reaction is producing chloric gas.

$$NaClO + 2HCl \rightarrow Cl_2 + H_2O + NaCl$$

For security reasons the desiccator was kept under the hood.

To keep seeds under sterile conditions, like it is necessary for selection of plants on plates, an additional surface sterilization was required. This ensured less contamination with funghi etc. First the seeds were washed 5 min. in ethanol. After removing the ethanol the seeds were incubated in 3 % NaClO for 10 min. Afterwards the NaClO was removed and the seeds were washed 4 times with dH_2O. The washed seeds were kept in agar which helped to place the seed in an adequate manner on plate.

4.2.1.4 Plant selection

Plant selection was carried out on plates with MS-Media containing the adequate antibiotics. For that purpose the hot MS-Media was cooled down to ∼50 °C and the antibiotic was added in the correct concentration. An overview of different antibiotics used in this thesis and their concentration for plant selection can be

found in table 4.14. To screen for transformants around 120 mg seed for one big plate (⌀ 145 mm) was used.

Name	Selection concentration	Stock concentration
Ampicillin	100 µg/ml	1000x in H_2O
Gentamycin	25 µg/ml	1000x in H_2O
Glufosinate (Basta)	10 µg/ml	1000x in H_2O
Hygromycin	20 µg/ml	2500x in H_2O
Kanamycin	50 µg/ml	1000x in H_2O
Rifampicin	10 µg/ml (GV3101)	2500x in DMSO
Sulfadiazine	5 µg/ml	1000x in H_2O

Table 4.14: Used antibiotics and their concentration for plant selection.

4.2.1.5 Crossings

To perform crossings it was necessary to have a closer look at the stem and the inflorescence. If the plants looked healthy any siliques, open flowers and open buds were removed with clean forceps. Those organs were already self fertilized and useless. It was attended not to damage the plant to much while removing those parts. Accordingly carefully sepals, petals and anthers of a closed bud were removed. The anthers were checked for immaturity, so that the pollen has not yet been released. While doing this the carpel was protected from any damage. On the other hand a suitable mature flower with opened anthers was used to rub it on the Stigma of the emasculated plant. For each cross 2-3 buds on each inflorescence were prepared. The meristem in the center and all smaller buds were removed to prevent further development as this would led to confusion with the crossed flowers. The inflorescence was marked precisely to avoid later confusion. The crossings were checked after 1-2 days if an obvious elongation of the carpel was visible. The developed seed were harvested before the silique shattered [NASC, 2010].

4.2.1.6 Phenotypic analysis

For phenotypic analysis plants were sown at a maximum density of 5 plants per pot (7 cm x 7 cm). Leaf blade measurements were done using images of dissected fifth rosette leaves that had been scanned into the computer. Length, width and

area have been examined with the help of ImageJ software [ImageJ, 2010]. The amount of measured plants used for statistics was n≥20.

4.2.1.7 Hypocotyl measurements

For size measurements of dark grown hypocotyls dry seeds of the corresponding phenotypes were surface-sterilized, plated on MS-medium, stratified for 2-4 days at 4 °C in the dark and then moved to a cell-culture room at 22 °C and 24 hrs light. Plates were exposed 8 hrs vertically next to vertically arranged fluorescent bulbs and then kept for 3 days under aluminium foil in the dark. For the measurements of line *UBQ::SRF4 8 3* the amount of measured hypocotyls was n=8. For all other lines n≥17.

4.2.1.8 Chlorophyll content

To measure the chlorophyll content 50 mg of leaf tissue was harvested in 1 ml Dimethylformamid (DMF). The solution was incubated for 12-15 hrs in the dark at 4 °C as the chlorophyll can degrade. The mixture was diluted 1:10 (with DMF) prior measurement. To determine the absorbance 1 cm glas cuvettes were used. DMF would destroy plastic cuvettes. Chlorophyll *a* has its maximum of absorbance at 664.5 nm and Chlorophyll *b* at 647 nm. The absorbance was measured with a spectrophotometer and the amount of chlorophyll a and b as well as the total amount of chlorophyll in mg/L was determined with the following equations [Inskeep and Bloom, 1985]. Do not forget to take the dilution into account.

$$Chl\ a = 12.7\ A_{664.5} - 2.79\ A_{647}$$

$$Chl\ b = 20.7\ A_{647} - 4.62\ A_{664.5}$$

$$Chl\ total = 17.9\ A_{647} + 8.08\ A_{664.5}$$

4.2.1.9 Photosynthetic yield measurements

Photosynthetic yield was measured with the Portable Chlorophyll Fluorometer PAM-2000. By sending a strong light impulse it is possible to measure the

chlorophyll fluorescence which gives a direct clue to changes in photochemical processes. In general parlance: the more efficient the photosystem transforms light energy to chemical energy the less de-excitation in terms of fluorescence and heat occurs and the higher is the photosynthetic yield.
More detailed information can be found in the PAM-2000 user manual [WALZ, 2011].

4.2.1.10 Carbohydrate analysis

Reagents

- 70 % ethanol
- methanol/chloroform (v:v, 1:1)
- 100 % acetone

To perform a carbohydrate analysis via gas chromatographie-mass spectrometry (GC-MS) a special preparation of the plant tissue was needed. Prior harvesting the plants were removed from any light source for 12 hrs to insure starch reduction. Then the tissue was harvested and frozen immediately in liquid nitrogen. The tissue was ground with mortar and pestle until a fine powder was achieved. Keep the sample as cool as possible during that procedure. The powder was put in a 50 ml falcon tube containing 20 ml of 70 % ethanol and kept there for at least 10 min. Subsequently the mixture was centrifuged (10 min, 4000 rpm, RT) and the supernatant was discarded. Then the pellet was washed with 20 ml methanol/chloroform and centrifuged down with the same conditions previously mentioned. This step was repeated once. Afterwards the pellet was washed with 100 % acetone to remove remaining chlorophyll. After one last centrifugation step, most of the acetone was removed and the pellet was dissolved in the remaining liquid. The suspension was moved to a 2 ml tube and centrifuged for 2 min (11000 rcf, room temperature). Excess acetone was removed and the samples were kept under the hood for drying overnight.
The corresponding prepared samples were sent for GC-MS analysis to the Plant Cell Wall Group at the Max-Plank-Institute in Golm, which supported the protocol by personal communication.

4.2.1.11 GUS staining

Reagents

- GUS staining solution (10 mM EDTA pH 8, 0.1 % Triton X-100, 2 mM $K_4Fe(CN)_6(3H_2O)$, 2 mM $K_3Fe(CN)_6$, 100 µl/ml chloramphenicol, 50 mM Natrium Phosphate Buffer pH 7) **Keep at 4 °C, light sensitive**
- 50 mM Natrium Phosphate Buffer (29 mM Na_2HPO_4, 21 mM $NaH_2PO_4(H_2O)$)
- X-Gluc stock solution (50 mg/ml 5-bromo-4-chloro-3-indolyl-beta-D-glucuronic acid in Dimethylformamid) **Keep in -20 °C**
- 70 % acetone

To remove the outer wax layer of the *Arabidopsis* leaves, harvest them in 70 % acetone and keep the tissue for 10 min. in the solution. Replace the acetone with 5 ml staining solution and add 100 µl X-Gluc stock solution (X-Gluc Direct). Then apply vacuum for 20 min. Afterwards change the solution and incubate at 37 °C until the staining is fine. To get rid of the chlorophyll wash the samples overnight in 70 % Ethanol. Change the Ethanol the next day and keep the tissue at 4 °C [Jefferson et al., 1987].

4.2.1.12 Protoplast transformation

Reagents

- Enzyme solution (20 mM MES pH 5.7, 1.5 % (wt/vol) cellulase R10, 0.4 % (wt/vol) macerozyme R10, 0.4 M mannitol, 20 mM KCl, 10 mM $CaCl_2$, 0.1 % BSA) **Prepare fresh! Filter through a 0.45 µm syringe filter**
- WI solution (4 mM MES pH 5.7, 0.5 M mannitol, 20 mM KCl)
- W5 solution (2 mM MES pH 5.7, 154 mM NaCl, 125 mM $CaCl_2$, 5 mM KCl)
- MMG solution (4 mM MES pH 5.7, 0.4 M mannitol, 15 mM $MgCl_2$)
- PEG-calcium transfection solution (20-40 % (wt/vol) PEG4000, 0.2 M mannitol, 100 mM $CaCl_2$) **Prepare at least 1 h before transfection!**

Solutions were prepared according to [Yoo et al., 2007].
Up to 20 well expanded healthy leaves were cut with a sharp razor blade into

thin stripes and subsequently incubated in the enzyme solution for 3-4 h at room temperature in the dark. The leaf strips were vacuum infiltrated for 30 min. just ahead incubation. The leaves were treated very carefully. Do not let them dry out and handle them with care! Following the incubation and after swirling the protoplast mixture, the solution was diluted with an equal volume of W5 buffer. Subsequently the solution was filtered with a 75 µm nylon mesh, wetted with W5 buffer. The flow-through was pelleted (100g, 1-2 min, RT) in a round 15 ml falcon tube, as much liquor as possible was removed and the protoplasts were re-suspended in 5 ml W5 solution. The protoplasts were kept on ice for 30 min. Afterwards as much as possible W5 buffer was removed and they were re-suspend in 2-5 ml MMG solution (depends on how many protoplasts you have). The amount of protoplasts was counted under the microscope and the solution was diluted to the needed concentration of 2 x 10^5 ml^{-1} and kept at room temperature. The so prepared protoplasts were ready for the DNA-PEG-calcium transfection. 10 µl DNA (1-2 µg/µl) were prepared in a 2 ml tube. 100 µl of protoplasts plus 110 µl of PEG solution was added and mixed gently by tapping the tube. The mixture was incubated for 5 min at room temperature. Then 400 µl W5 buffer were added subsequently and centrifuged down (100g, 2 min, RT). The supernatant was removed and the protoplasts were re-suspended with 1 ml WI. After an incubation period of 20-24 h in the dark the protoplasts were checked for a signal under the microscope.

For protoplast transfection the protocol provided by [Yoo et al., 2007] was followed.

4.2.2 Yeast two-hybrid

4.2.2.1 Yeast plasmid isolation

Reagents

- Lysisbuffer (10 mM Tris-HCl pH 8, 1 mM EDTA, 100 mM NaCl, 1 % SDS, 2 % Triton X-100)
- Phenol/Chloroform/Isoamylalcohol (25:24:1)

Centrifuge 10 ml of a yeast culture (grown ∼24 hrs at 30 °C) stepwise in a 2 ml Eppendorf tube (13000 rpm, 30 sec, RT). Re-suspend in 200 µl lysisbuffer. Add first 0.3 g glasperls (0,25-0,5 mm ∅) and then 200 µl Phenol/Chloroform/Isoamylalcohol. Vortex the mixture for one minute. Shock frost

for one minute in liquid nitrogen and defrost at room temperature. Repeat the freezing step. Centrifuge (13000 rpm, 5 min) and take the upper liquid phase to a new 1,5 ml tube. Precipitate the DNA with 200 µl 100 % icecold Ethanol at -20 °C for 30 min to 1 hr. Centrifuge for 15 min (13000 rpm, 4 °C). Wash the pellet with 200 µl 70 % icecold Ethanol. Let the pellet air dry and take it up in 20 µl dH_2O. 0.5 µl is more than enough for a PCR.

4.2.2.2 Small scale yeast transformation

Reagents

- 10x LiAc (1 M lithium acetate, pH 7.5)
- 10x TE (100 mM Tris-HCl pH 8, 10 mM EDTA)
- 50 % PEG (wt/vol, polyethylene glycol, MW = 3350) **Prepare fresh**
- 2 mg/ml carrier DNA (sheared salmon sperm DNA)
- 100 % DMSO

Inoculate one yeast colony in 25 ml YPD or SD medium and let it grow to an OD_{600} = 1.5-2.0. Dilute them 1:4 and let them grow again 2-3 hrs. Then centrifuge them down (1000 g, 5 min) and wash the pellet with 25 ml 1x TE. Repeat the centrifugation step and take the pellet up in 500 µl 1x TE/1x LiAc and keep at room temperature until DNA is prepared.
Pipette the right amount of DNA (500 ng-1 µg) in a reaction tube. Preheat the carrier DNA (-20 °C) to 70 °C, let it cool down and add 25 µl of a 2 mg/ml stock in the tube with the DNA. Combine the mixture with 50 µl of yeast Cells and add afterwards 300 µl of 40 % PEG/1x LiAc/1x TE and mix by pipetting. Let the cells incubate for 1 hr at 30 °C at ∼200rpm. Accordingly subjoin 35 µl of DMSO and heat shock for 15 min at 42 °C. Snap cool the cells 1 min on ice before you pellet them down (1000 g, 1 min). Discard the supernatant and re-suspend them in 1 ml 1x TE. Pellet them again and remove 900 µl of the supernatant. Take them up in the remaining 100 µl and put them on the appropriate SD plates. Colonies will be visible after 2-3 days [Schiestl and Gietz, 1989] [Gietz et al., 1992].

4.2.2.3 Screening for interaction

As a preliminary test for interaction 10-20 colonies of each genotype were streaked out on SD -Leu-Trp-His plates to verify the His3-reporter gene expression. Also the controls were streaked out on the selective media to rule out auto-activation. Let the colonies grow 3-5 days at 30 °C. Be careful: some interactions only take place at 25 °C. If the colonies of interest grow while the control does not one can go on with a more sensitive screen for interaction like the following.

Histidine growth assay One to three $His3^+$ colonies and one of each control were inoculated in 3-5 ml SD -Leu-Trp liquid media and grown for around 24 hrs. After measuring the OD_{600} each culture was diluted to an $OD_{600} = 1$. To reach a dilution series with the biggest dilution of 1:100000 the culture was 5 times sequentially diluted 1:10. 15 µl of each dilution was brought on plate and grown on SD -Leu-Trp-His media for 3-5 days at 25-30 °C.

Quantitative β-galactosidase assay

Reagents:

- Z-buffer (60 mM $Na_2HPO_4(7H_2O)$, 40 mM $NaH_2PO_4(H_2O)$, 10 mM KCl, 1mM $MgSO_4(7H_2O)$, pH 7)
- ONPG (4 mg/ml O-nitrophenyl β-D-galactopyranoside in Z-Buffer)
- Z-buffer + β-mercaptoethanol (Z-buffer + 0.27 % β-mercaptoethanol)
- 1 M Na_2CO_3

1 ml of overnight culture grown in SD -Leu-Trp was transferred to 4 ml of YPD and incubated at 30 °C at 200 rpm until the cells reached an $OD_{600} = 0.5$-0.8. Write down OD_{600} before centrifuging 1 ml of this culture (13000 rpm, 30 sec). The pellet was washed in 1 ml Z-buffer and resuspended in 100 µl Z-buffer. Subsequently the solution was frozen in liquid nitrogen and thawed at 37 °C. The freeze/thaw step was repeated twice. 700 µl Z-buffer + β-mercaptoethanol and 160 µl ONPG was added to the reaction. The tubes were incubated at 30 °C. After the yellow color developed, the reaction was stopped by adding 0.4 ml Na_2CO_3 and the elapsed time in minutes was recorded. The reaction solution was cleared by centrifugation (13000 rpm, 10 min). After transferring the supernatant to cuvettes OD_{420} was determined relative to the blank (Z-buffer

+ β-mercaptoethanol and ONPG). Now the activity of β-galactosidase can be assumed by calculating the Miller Units. Experience shows if

$$1000 \cdot \frac{OD_{420}}{t \cdot v \cdot OD_{600}} \geq 1$$

t = elapsed reaction time in min
v = volume of assayed culture in ml

an interaction between the proteins of interest can be assumed.

4.2.3 *Escherichia coli* and *Agrobacterium tumefaciens*

For propagation, maintenance and transformation to plants *Escherichia coli* and *Agrobacterium tumefaciens* were used. To make them taking up the plasmid of choice it is needed to make them competent. To transform them they need to be made either electro or chemical competent. In this thesis only electro competent cells were used.

4.2.3.1 Preparation of electro competent *Escherichia coli* and *Agrobacterium tumefaciens* cells

Reagents

- LB-media
- 10 % Glycerol sterile **Precool**
- Liquid nitrogen

The glycerol stock of the desired strain was streaked out to get single colonies. One colony was inoculated in 5 ml LB without antibiotics overnight. *E. coli* strains were grown at 37 °C, whereas *Agrobacterium* was cultured at 30 °C. While inoculating the pre-culture a one liter flask with 250 ml LB without antibiotics was kept overnight at 37 °C under agitation to check for putative contaminations. If the LB was ok 2.5 ml of the pre-culture were added and grown 2-3 h until they reached OD_{600}=0.3-0.4.
The following steps were done in the cold room only. The 250 ml culture was transfered to a pre-cooled big centrifuge bottle and chilled on ice for 20 min. Subsequently the culture was centrifuged (4500 g, 4 °C, 15 min), the supernatant

was discarded and the pellet got dissolved in 50 ml 10 % glycerol. After the pellet was dissolved, 200 ml of glycerol was added and centrifuged again. The pellet was washed 2 times more with first 125 ml and then with 20 ml glycerol after transferring the solution to small centrifuge bottles. Finally the pellet was dissolved in 2 ml glycerol and aliquoted at 60 µl in 1.5 ml reaction tubes.

4.2.3.2 Transformation of electro competent *Escherichia coli* and *Agrobacterium tumefaciens*

For transformation of electro competent *E. coli* cells, 0.5 µl of a ligation reaction or not more than 10 ng of purified plasmid were transformed. For electroporation 2000 V were used and the cells were taken up in 1 ml SOB immediately. After shaking 1h at 37 °C the cells were struck on two LB plates with selective media (250 µl and 750 µl) and incubated overnight.

For transformation of Agrobacteria only 1250 V were used and the cells were incubated 1 h at 30 °C. For selection LB plates with Rifampicin, Gentamycin plus the vector specific antibiotic was used and plates were incubated 48 h.

Glycerol Stocks Of each used or cloned plasmid a glycerol stock was prepared. For that purpose 1 ml of the Midi Prep culture were taken before centrifugation and added in a kryotube. 500 µl of 100 % glycerol were added, vortexed vigorously and kept for 10 min in liquid nitrogen. Afterwards the glycerol stock was transferred to −80 °C for long term storage.

4.2.4 DNA work

4.2.4.1 *Arabidopsis* genomic DNA isolation

Reagents

- CTAB-buffer (2 % CTAB, 1.42 M NaCl, 20 mM EDTA, 100 mM Tris-HCl pH 8)
- 10 mg/ml RNAseA
- 3 M NaOAc pH 5.2
- 100 % Isopropanol **Keep at -20 °C**
- 70 % Ethanol **Keep at -20 °C**

- Phenol
- Chloroform
- β-mercaptoethanol

Tissue from several plants (e.g. 1-2 healthy, green leaves) was collected in 2 ml tubes and immediately frozen in liquid nitrogen. Small plastic mortars were used to grind the tissue and the powder was resuspended in 1 ml preheated (65 °C) CTAB-buffer. 6.25 µl β-mercaptoethanol was added. The solution was incubated for 20 min at 65 °C and shaken strongly. Subsequently 200 µl of phenol + 400 µl chloroform was added and incubated for 5 min at room temperature while shaking. The mixture was centrifuged for 10 min, 13000 rpm at 4 °C. The supernatant was transferred to a fresh 2 ml tube and 2 µl RNAseA was added. After incubation for 30 min at 37 °C the phenol/chloroform step was repeated. Following 800 µl cold isopropanol + 80 µl NaOAc was added to the supernatant, mixed by inversion and spun down for 10 min (13000 rpm, 4 °C). The supernatant was discarded and the pellet was washed with 200 µl cold Ethanol. Be careful when discarding the supernatant as the pellet can move. After letting the pellet air dry it was dissolved in 50 µl dH_2O. To perform a PCR on the extracted genomic DNA a 1:20 dilution was used and 1 µl was taken as template. [Murray and Thompson, 1980]

4.2.4.2 Genotyping

Genotyping was done with the corresponding Left-Border (LB) and Right-Border (RB) primer and gene specific forward and reverse primers (GS_F and GS_R). To check if one plant carried the insertion and how the T-DNA was located in the gene, five different PCRs were carried out:

1st PCR: LB + GS_F
2nd PCR: LB + GS_R
3rd PCR: RB + GS_F
4th PCR: RB + GS_R
5th PCR: GS_F + GS_R

According to the amplified bands of PCR 1-4 the orientation of the T-DNA could be deduced. Depending on the result of the 5th PCR in combination with the other PCR reactions it could be concluded whether the plant is homo- or

heterozygote or even wildtype. The primers used in this thesis for genotyping can be found in table 4.2.

4.2.4.3 DNA isolation from agarose gel

If DNA was needed to be purified on gels, e.g. after PCR to exclude unspecific bands or after vector digestion for cloning, it was run on a TAE (Tris-acetate-EDTA buffer) gel. The band of interest was cut under low energetic UV light. DNA was then extracted using a kit (see table 4.5) which are based on the silica membrane technology.

4.2.4.4 Cloning

For investigation of genes it is essential to clone them into certain vectors which are capable for different purposes. An overview of the vectors, their area of application and resistance is given in table 4.9. After cloning them they could be propagated and transformed to other organisms like yeast or plants.

DNA Digestion with Restriction Endonucleases For cloning into an empty vector two times 1 µg of plasmid was taken. For cutting a vector which contained already an insert two times 2 µg were used. If a PCR construct was cut all the 50 µl which resulted after gel extraction were used. For cutting, 1 µl of each enzyme was used in 50 µl (vector) or 60 µl (PCR). To digest the vector completely it was kept two to four hours at the required temperature. For cutting the insert mostly two hours incubation time was applied. After cutting, the vector was purified on gel and if the insert was already gel purified, it was simply cleaned with the extraction kit which includes a protocol for cleaning samples of enzymes.

Polymerase Chain Reaction (PCR) To perform a PCR for cloning proof reading polymerases were used to cause as less mistakes as possible. In this thesis mostly Takara Primestar was used. The insert was amplified either out of genomic DNA, cDNA or plasmids using primers containing the needed restriction sites. For Primestar annealing temperature was always 55 °C. Final primer concentration was 0.3 µM in a 50 µl attempt. The template concentration should not exceed 200 ng as this would block the reaction. The product was purified on an agarose gel and used for ligation.

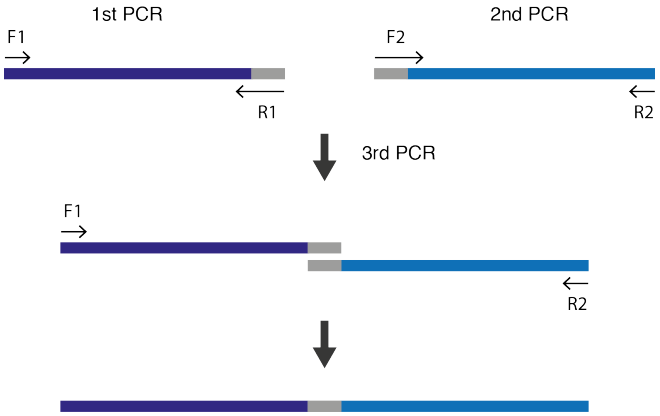

Figure 4.1: Overview of the overlapping PCR approach.

Overlapping PCR When performing an overlapping PCR the aim was to combine two independent amplified PCR products in one. For that purpose two pairs of primers were designed (F1 and R1, F2 and R2). The first pair amplifies the first sequence while the reverse primer (R1) includes some significant overlap with the 5' end of the second amplified piece. Vice versa the second sequence was amplified with another primer pair while the forward primer (F2) contains some significant overlap with the 3' end of the first sequence. The overlap should be between 8 to 20 nucleotides. In the third step 20-80 ng of sequence one and two got amplified in an independent PCR reaction using primer F1 and R2. The overlapping step is included in the third PCR and needs no special conditions. Like that a combination between both pieces was produced and could be used for further attempts. An overview of the technique can be found in picture 4.1.

Ligation reaction For ligation 50-150 ng of vector were taken. The amount of insert was calculated the following way

$$Insert(ng) = Vector(ng) \cdot \frac{Insert\ size(bp)}{Vector\ size(bp)} \cdot \frac{3}{1}$$

Plasmid Preps To check whether the selected *E.coli* carry the plasmid of choice one can perform the following Quick Prep Protocol.

Reagents

- lysis solution (7.55 ml dH_2O, 2 ml 50 % glucose, 0.2 ml 0.5 M EDTA pH 8, 0.25 ml 1 M Tris-HCl pH 8) **Prepare fresh**

- alkaline SDS (8.6 ml dH_2O, 1 ml 10 % SDS, 0.4 ml 5 M NaOH)
- 3 M NaOAc pH 5.2
- RNAseA (20 µg/ml in TE)

After growing a single colony overnight in 3 ml LB selective media at 37 °C, 1.5 ml of the culture were pelleted down in a tube (30 sec, 13000 rpm, RT). The supernatant was decanted and the pellet was resuspended in 100 µl lysis solution by vortexing. Then 200 µl alkaline SDS was added and the mixture was vortexed well. After incubation for 5 min on ice, 150 µl of 3 M NaOAc were added and mixed well. The solution was incubated for 10 min on ice and then centrifuged (10 min, 13000 rpm, RT). Meanwhile fresh 1.5 ml tubes were prepared and prefilled with 400 µl isopropanol. The supernatant was then transferred to the new tubes and mixed by inverting. The tubes were kept on ice for 10 min and again spun down (10 min, 13000 rpm, 4 °C). The pellet was washed with 200 µl 70 % Ethanol (5 min, 13000 rpm, 4 °C) and the supernatant was poured away. The pellet was vacuum dried for 5 min and taken up in 50 µl TE + 2 µl RNAseA. The tubes were incubated for 10 min at 65 °C while shaking. Normally 1-2 µl are enough for a digest of a high copy plasmid.
This protocol is not recommended if you want to send the plasmid immediately for sequencing or keep them for longer terms. For this intentions use the NucleoSpin Plasmid Kit (see table 4.5) instead.
If a clone of interest turns up after digestion of the plasmid prep, one can use the remained culture to inoculate a 100 ml culture for a midi prep. For this purpose the JetStar 2.0 Kit (see table 4.5) was used.

4.2.4.5 Sequencing

Sequencing was done by MWG and later by GATC. 1500 ng DNA was sent in a labeled tube together with 10 µM primer in a separate tube. Sequencing was done overnight.

4.2.5 RNA work

To check the transcript level in transgenic plant lines it is needed to extract the mRNA and reverse transcribe it to cDNA. How this was done in this thesis is described in the following points.

4.2.5.1 *Arabidopsis* RNA isolation

For RNA isolation the NucleoSpin RNA II Kit from Macherey Nagel was used. Not more than 100 mg of tissue was homogenized as the columns got easily overloaded. After following the protocol up to 250 ng/µl RNA could be achieved.

4.2.5.2 cDNA synthesis

cDNA was synthesized using the Revert Aid First Strand cDNA Synthesis kit (Fermentas). Between 500-1000 ng were reverse transcribed and used afterwards for RT-PCR.

4.2.5.3 RT-PCR

For RT-PCR 50 ng of cDNA was used in a 20 µl reaction. Normal Taq was used to amplify the transcript of choice. Between 30 and 40 cycles were used to amplify also low expressed transcripts. For semi-quantitative RT-PCR a 50 µl attempt was prepared and after at least 20 cycles 10 µl in intervals of 4 cycles was taken 3 times. The amount of volume and number of samples can be varied and depends strongly on the transcript to be amplified.

4.2.6 Protein work

To yield a decent amount of tagged protein that can be used in different attempts it is needed to express it recombinantly and purify it via a matrix. In this thesis a kinase assay was performed for which SRF4 and DLG protein was needed. The intracellular part of SRF4 ($SRF4_i$) was fused with a GST-tag while DLG had a His-tag. How those fusion proteins where induced, purified and the kinase assay was performed is explained in the following sections.

4.2.6.1 *E. coli* as expression system

The expression system of choice was the *E.coli* strain BL21 (DE3) pLysS. This strain encodes the T7 RNA polymerase which can be induced by IPTG due to the fact that the polymerase is controlled by a lac UV5 promoter. This polymerase acts very specific only on the so called T7 promoter and therefore transcribes only sequences which are under the control of this promoter. As SRF4 and DLG were independently transformed to this strain and as both are driven under a T7 promoter sequence, their expression could be guided by adding IPTG. For each

protein, the expression conditions need to be optimized for amount of IPTG, temperature and expression time.

4.2.6.2 Optimized conditions for induction of $SRF4_i$ and DLG

The optimal conditions for expression of $SRF4_i$ and DLG in BL21 were found by Eva Herold, a former master student in the lab. They were slightly modified and the conditions are summarized in the following paragraphs.

$SRF4_i$ $SRF4_i$ was induced after reaching an OD_{600} of 0.4-0.8 with 1 mM final concentration of IPTG. The cells were grown overnight at 25 °C. Also the kinase dead constructs $SRF4_i$ K $\rightarrow$ E and R $\rightarrow$ C were induced on the same way.

DLG DLG and ΔDLG (Y2H part of DLG) were induced after reaching an OD_{600} of 0.4-0.8 with 1mM IPTG as a final concentration. DLG was induced at 30 °C overnight and ΔDLG was induced for 3 hrs at 37 °C.

4.2.6.3 Purification of $SRF4_i$ and DLG

As $SRF4_i$ was fused with GST and DLG with a His-tag both proteins could be purified via those tags. For $SRF4_i$ sepharose beads were used as for DLG Nickel-TED columns were applied.

GST-tagged $SRF4_i$ To reach an adequate amount of $SRF4_i$ protein for a kinase assay, 500 ml of culture were pelleted (15 min, 4000 rpm, 4 °C) and kept at -20 °C or better directly purified.

Reagents

- Elution buffer pH 8.5 (50 mM Tris-Cl pH 8.5, 10 mM reduced glutathione)
- PBS buffer pH 7.4 (137 mM NaCl, 2.7 mM KCl, 10 mM Na_2HPO_4, 2 mM KH_2PO_4) **Store at 4 °C**
- Protease inhibitor cocktail tablets
- 10 mg/ml Lysozyme
- Glutathione Sepharose 4 Fast Flow

After centrifugation of the induced culture, the pellet was resuspended in 25 ml of cold PBS Buffer plus 1 protease inhibitor cocktail tablet. 10 µg/ml lysozyme (final concentration) was added and incubated on ice for 30 min. Subsequently the solution was shock cooled in liquid nitrogen and put to a sonicator bath for 5 min (until the cultures were thawed). Freezing and sonication was repeated. The solution was centrifuged at 15000 rpm, for 30 min at 4 °C. 300 µl sepharose beads were equilibrated by applying it with 3 ml cold PBS, mixing and centrifugation at 1000 rcf for 5 min at 4 °C. The supernatant was removed and the washing step repeated. Cold PBS (vol/vol = 1/1, here 150 µl) was added. The supernatant with the protein was applied and incubated at 4 °C for 2 hrs on the end-over-end rotator. After centrifugation (10 min, 1000 rcf, 4 °C) the beads were washed three times with 3 ml PBS + protease inhibitor (5 min, 1000 rcf, 4 °C). The protein was eluted with an adequate amount of elution buffer. For $SRF4_i$ 150 µl was used. The kinase dead versions showed in general a lower amount of expression and were therefore taken up in 50 µl. The pellet was kept as the beads fraction. All fractions were kept for analysis on SDS gel. The vast bulk of protein was found in the beads fraction.

His-tagged DLG As for $SRF4_i$ also for DLG 500 ml induced culture was pelleted.

Reagents

- Lysozyme (10 mg/ml)
- Protino Ni-TED 2000 (Macherey-Nagel)

The pellet was resuspended in supplied 15 ml LEW buffer and 10 µl/ml lysozyme. Cell lysis was done like for $SRF4_i$ in the sonicator waterbath and liquid nitrogen. The supernatant was loaded on the Nickel TED column and the provided protocol was followed. The first fraction was eluted in 3 ml and the second in 1.5 ml. All fractions were kept for analysis on SDS gels. Most protein was found in the second elution fraction.

4.2.6.4 SDS-PAGE

To check the expression level of the proteins SDS gels were prepared.

Reagents

- 10 % APS (Ammoniumpersulfat)
- Rotiphorese Gel 30
- TEMED (Tetramethylethylendiamin)
- 1 M DTT
- 2x Loading Buffer (100 mM Tris-HCl pH 6.8, 200 mM DTT, 4 % SDS, 0.2 % bromphenol blue, 20 % glycerol; DTT is added just before use from the 1 M stock)
- 10x Running Buffer (25 mM Tris, 192 mM glycine, 0.1 % SDS)
- Coomassie Blue Staining Solution (0.25 % Coomassie Brilliant Blue R-250, 45 % methanol, 10 % glacial acetic acid)
- Destaining solution (10 % glacial acetic acid, 10 % methanol)

The used percentage of the gel to check for $SRF4_i$ was 10 % and for DLG and ΔDLG 15 %. The molecular weight of GST:$SRF4_i$ is ∼69 kDa and of DLG and the Y2H part ΔDLG is ∼35 kDa and ∼19 kDa, respectively. The protein ladder used in this thesis was P7709 V from NEB. The samples were mixed with loading buffer, heated to 95 °C for 5 min. and snap cooled on ice for 2-3 min. The gels were placed into the Mini Protean Tetra Cell with running buffer and subsequently ran at 200 V for 50 min. Afterwards they were stained with the Coomassie Blue staining solution for 20-30 min under agitation, while destaining was done overnight.

4.2.6.5 Western Blot

Reagents

- 10x Transfer Buffer (25 mM Tris pH 7.4, 192 mM glycine, 10 % methanol)
- 10x TBST Buffer (20 mM Tris-HCl ph 7.6, 135 mM NaCl, 0.1 % (wt:vol) Tween-20)
- Dry milk powder
- Whatman® 3 mm Chromatography Paper
- Transfer Membrane

- According antibodies and their substrate

The identity of the expressed proteins was checked by doing a Western Blot and detection of SRF4 and DLG protein via a Anti-GST or Anti-His antibody (see section 4.1.1.4) . After running the SDS gel the gel was equilibrated in transfer buffer for 30 min. During this time the size of blotting membrane (see section 4.1.1.5) was adjusted and rinsed in methanol. Afterwards it was also equilibrated for 10 min in transfer buffer. The gel and the membrane were placed between two times 3 layers of Whatman paper, soaked in Transfer Buffer, in the Blotter. Do not forget to place the Blotting Membrane between the gel and the Whatman paper on side of the Anode. The blot was done at 10 V for 30 min. To avoid unspecific bindings the membrane was incubated for at least 1 h in TBST buffer containing 5 % dry milk powder. The according antibodies were added to the TBST-buffer (plus 3 % dry milk powder) in which the membrane was incubated overnight at 4 °C under agitation. The GST antibody was used as a 1:1000 dilution while the Anti-HisG antibody was diluted 1:50000. The membrane was washed twice with TBST buffer for 10 min. Subsequently the substrate (see section 4.1.1.4) was applied for 5 min according to manufacturers instructions. Signal detection was done with the LAS-4000 mini.

4.2.6.6 Kinase assay

Reagents

- 5x Kinase Buffer (20 mM Tris-HCl pH 7.5, 50 mM NaCl, 10 mM $MgCl_2$, 0.01 % Triton X-100, Phosphatase Inhibitor, Protease Inhibitor)
- 10x DTT (1 mM)
- 20x ATP (50 µM)
- 10 µci γ-^{32}p ATP
- 6x SDS Loading Buffer (300 mM Tris-HCl pH 6.8, 600 mM DTT, 12 % SDS, 0.6 % bromphenol blue, 60 % glycerol; DTT is added just before use from the 1 M stock)
- two SDS gels
- Developer

- Fixer

The kinase assay was performed with freshly induced and purified protein. A decent amount which is visible on a SDS gel was taken for the assay. A 25 µl reaction mixture was pipetted by adding the 5x Kinase Buffer, 10x DTT, 20x ATP, up to 15 µl of protein, 0.8-1 µl 10 µci γ-^{32}p ATP and dH_2O to fill up the reaction. The attempt was incubated for one hour at 28-30 °C. Afterwards the reaction was stopped by adding 6x SDS loading dye. The mixture was heated to 95 °C for 5 min, snap chilled on ice for 2-3 min and centrifuged down. Subsequently the two SDS gels were loaded, each with half of the reaction mixture (15 µl). One of the gels was exposed to a X-ray film while the other one was stained. The exposure time was between two to 48 hrs, depending on the signal strength. All work with radioactive material was done in a special isotope lab with increased caution.

4.2.6.7 *In vitro* GST-pulldown assay

The *in vitro* GST-pulldown was done by Eva Herold in the course of her diploma thesis. Here a short overview of the principle of the assay is given. A more detailed version can be found in her thesis [Herold, 2008].

In general the proteins GST:SRF4 and DLG-His were recombinantly expressed like described in the sections 4.2.6.2. GST:SRF4 was purified via equilibrated sepharose beads. 100 µl beads were washed twice with 1 ml ice cold PBS plus protease Inhibitor, containing 0.5 % Nonidet P-40 and 1 mM EDTA, pH 8.0 (10 seconds, 13000 rpm, 4 °C). The beads were mixed with this buffer 1:1. 50 µl equilibrated beads and 600 µl of the GST:SRF4 containing cell lysate were brought together. The volume was adjusted to 1 ml with the GST pull-down lysis buffer. The mixture was incubated for 2 hrs at 4 °C and centrifuged afterwards (10 sec, 13000 rpm, 4 °C) to get rid of unbound proteins. The supernatant was discarded and 200 µl cell lysate with DLG-His was added. The volume was again adjusted to 1 ml with the according buffer. Both proteins were incubated together on an end-over-end rotator at 4 °C overnight. Subsequently the samples were centrifuged (10sec, 13000 rpm, 4 °C) and washed four times with the buffer. The first supernatant of the first centrifugation step was kept as the flow through fraction (F) and the first and last supernatant of the washing step were also kept (W). For the elution of GST:SRF4 and the potentially bound DLG-His reduced glutathione buffer (20 mM reduced glutathione in 50 mM Tris-Cl, pH

8.0) was applied on the beads and incubated for 5 min. at room temperature. The samples were centrifuged (10 sec, 13000 rpm, RT) afterwards and the supernatant was collected as elution fraction (E). This step was repeated three times.

To detect the possible interaction between GST:SRF4 and DLG-His, the fractions F, final W, E and the beads (B) were applied with the same amount (50 µl) on two 15 % SDS gel (see section 4.2.6.4). 25 µl were subsequently loaded on each gel, except for the beads fraction where only 15 µl were applied. The proteins were separated for 50 min. at 200 V. One gel was stained and the other one was used for a Western Blot (see section 4.2.6.5). The detection of DLG-His was done with a Anti-HisG-HRP antibody.

4.2.7 Evolutionary analysis

Orthologous gene clusters (OGCs) were determined applying the orthoMCL software version 2.0 with its standard parameters. The protein sequence datasets of the genomes in table 4.15 were used. All splice variants in the protein sequence datasets were prior removed to avoid potential exclusive grouping of these identical or highly similar sequences. Table 4.15 provides an overview of the annotation release versions used in this analysis. OrthoMCL uses a Markov clustering algorithm on a precalculated sequence similarity matrix to group (putative) orthologs and paralogs [Li et al., 2003]. Each OGC was subject to the multiple sequence alignment software MAFFT [Katoh et al., 2009]. ProtTest [Abascal et al., 2005] was used to automatically select the best fitting model of protein evolution for each gene cluster. Based on that alignment, phylogenetic trees were calculated for relevant gene clusters using the bootstrap-based RAxML software tool [Stamatakis, 2006]. The analysis was done in corporation with the plant group of the MIPS at the Helmholtz Zentrum in Munich.

4.2.8 Microscopy and art work

4.2.8.1 Cell size analysis

For cell size analysis hypocotyl epidermis were prepared according to the Dried Gel method (see section 4.2.1.7) and checked under the microscope (BX61). Pictures of the cells were taken and measured with ImageJ Software (see table 4.12).

Genome	Version	Reference
Arabidopsis thaliana (mouse-ear cress)	TAIR10	[Swarbreck et al., 2008]
Brachypodium distachyon (purple false brome)	v1.2	[Vogel et al., 2010]
Brassica rapa (trunip rape)	v1.0	[Wang et al., 2011]
Carica papaya Linnaeus (papaya)	ASGPB 2008	[Ming et al., 2008]
Chlamydomonas reinhardtii (green algae)	v4.0	[Merchant et al., 2007]
Glycine max (soybean)	v1.0	[Schmutz et al., 2010]
Medicago truncatula (barrel clover)	v3.5	[Young et al., 2011]
Oryza sativa (rice)	RAP2	[Rice Genome, 2005]
Physcomitrella patens (moss)	v1.1	[Rensing et al., 2008]
Selaginella moellendorffii (spikemoss)	v1.0	[Banks et al., 2011]
Solanum lycopersicum (tomato)	v2.2	[Tomato Genome, 2011]
Sorghum bicolor (sorghum)	v1.4	[Paterson et al., 2009]
Vitis vinifera (grapevine)	v1.0	[Jaillon et al., 2007]
Zea mays (maize)	5b60	[Schnable et al., 2009]

Table 4.15: Versions of used genomes for evolutionary analysis of *SRF4*, *DLG* and *WIZ*.

4.2.8.2 Alexander stain

Reagents

- Alexander stain solution (10 ml Ethanol 95 %, 1 ml Malachite green (1 % in 95 % Ethanol), 5 ml Fuchsin acid (1 % in water), 0.5 ml Orange G (1 % in water), 5 g Phenol, 5 g Chloral hydrate, 2 ml Glacial acetic acid, 25 ml Glycerol, 50 ml dH_2O)

Pollen have, like all plant cells, a cell wall and a cytosol. Those parts can be stained with different dyes like Malachite green for the pollen wall, Fuchsin acid for the cytoplasm and mitochondria and Orange G for cytoplasm and nuclear staining. If the pollen architecture has some problems, it can be detected by staining the pollen and compare it to wildtype grains. To do so, pollen was put on a microscopy slide and a drop of Alexander stain solution was added. After incubation for 15 min the pollen grains were checked under the microscope. If the pollen is viable, the membrane should appear light green whereas the cytosol should turn violet (see figure 2.6) [Alexander, 1969].

4.2.8.3 Screening and imaging of transgenic EGFP lines

For screening of transgenic EGFP plants of *SRF4* and *DLG* the roots of 25 to 50 seven to ten day old T1 lines were screened under the CLSM and light emitting plants were kept for further analysis in T2. The constructs were not only

transformed to plants but also directly transformed to mesophyll protoplasts. EGFP fusion proteins can be visualized by exciting them at a wavelength of 488 nm and subsequently an emission at 509 nm at the lower green spectra can be observed.

4.2.8.4 Plasmolysis

To get an idea if the spotted signal is appearing in the cell wall or in the plasma membrane of the cell, a Plasmolysis should be performed. For that purpose a hypertone solution, here 1 M Sorbitol, is added to the root tissue and after five to ten minutes a shrinkage of the plasma membrane of the cell can be observed whereas the cell wall stays stable. The extent of shrinkage depends on the applied concentration of sorbitol and the time.

4.2.8.5 FM4-64 staining

FM4-64 stains the plasma membrane and later also endosomes. To check the EGFP signal it is helpful to stain emitting roots also with 2 µM FM4-64 by simply adding the solution on the slide. After 5 min a strong red staining of the membrane should be visible, after around 15 min a staining of the endosomes can be observed. Using it in parallel to plasmolysis supports the finding of the localization.

Chapter 5

Appendix

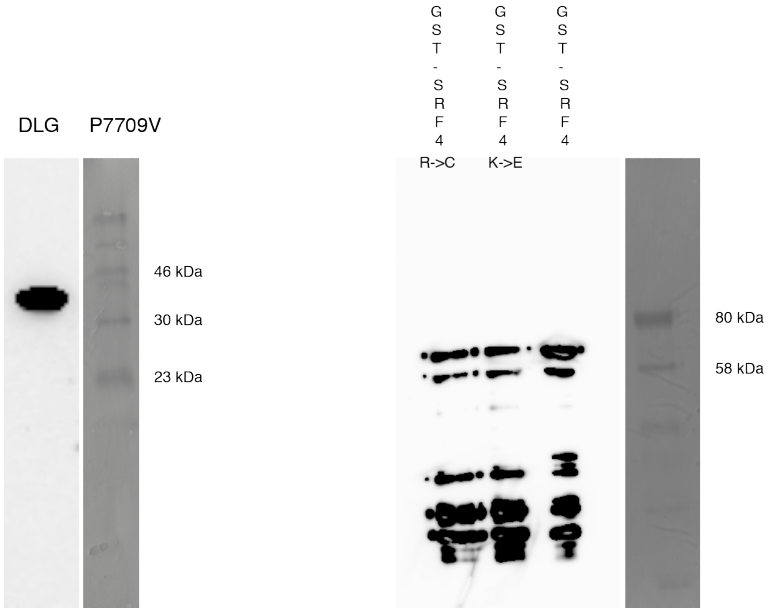

Figure 5.1: Results for the Western Blot of GST-SRF4 and DLG. The kinase dead versions K→E and R→C of SRF4 are also shown.

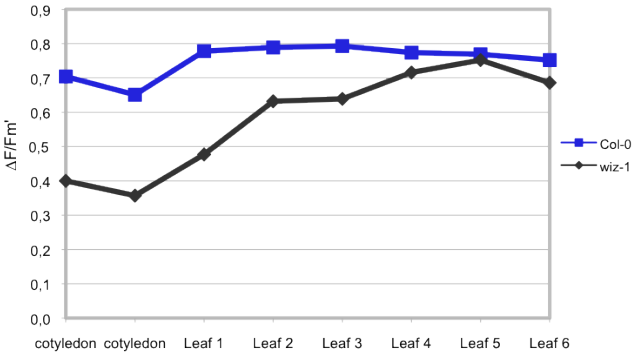

Figure 5.2: Photosynthetic Yield of a single, 16 d old *wiz-1* plant. An obvious increase in photosynthetic yield can be observed the younger the leaves get.

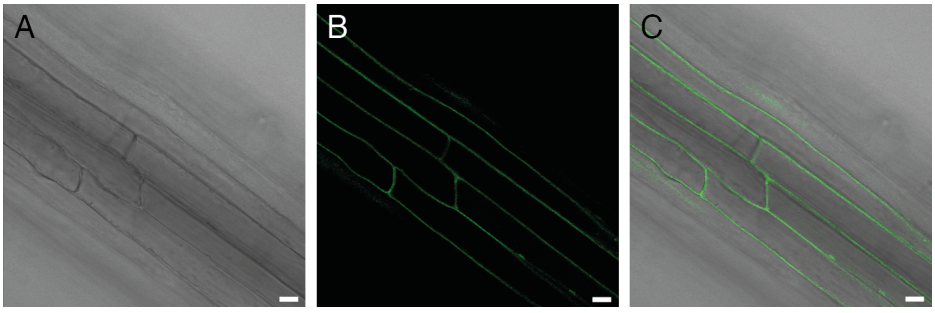

Figure 5.3: *35S::SRF4:EGFP* in *wiz-1* background. A: Bright field, B: EGFP, C: overlay. Scale Bar: 10 µm

pGADT7 \ **pGBKT7**	empty	EGFP	$SRF4_{intra}$	*DLG*	Δ*DLG*	*WIZ*	Δ*WIZ*
empty	-		-	-	+	-	-
EGFP		-	-	-		-	
$SRF4_{intra}$	-	-	-	-	+	-	-
DLG	-	-	-	+		-	-
Δ*DLG*	-	-	-			-	
WIZ	-	-	-	-	+	-	
Δ*WIZ*	+	-	+	-			

Table 5.1: Overview of the tested Y2H interactions. - corresponds to no interaction, + confirmed interaction, empty boxes represent untested combinations.

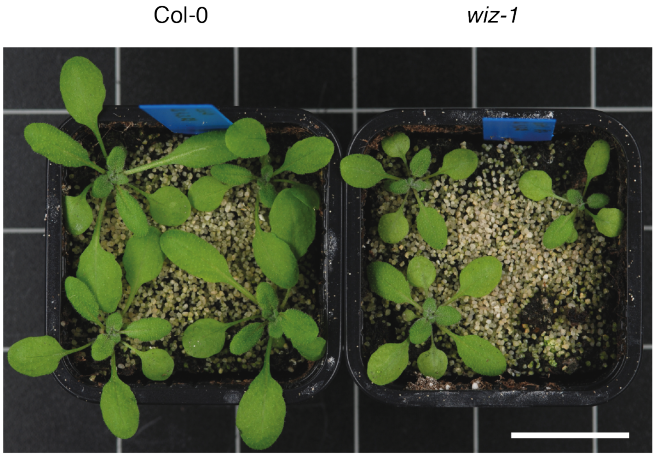

Figure 5.4: *wiz-1* shows no rescue of its growth phenotype under high CO2. Bleaching is less due to very bad light conditions in the phytochamber (72 $\mu m^{-2}s^{-1}$).

Pos.	Sequence of Target	miRNA	Sequence of miRNA	Free Energy
2031	AATGTGGTGGAGGCATTGAAGAGGCTAGTGTA	ath-miR408	augcacugccucuucccuggc	-33.09
1984	TTTCCATCTGCGTAATGACGGAGCCTGGACTT	ath-miR826	uaguccgguuuuggauacgug	-31.93
444	GGCCGTAACAACCTCAATGGTGAACTCAGTGA	ath-miR397b	ucauugagugcaucguugaug	-31.21
444	GGCCGTAACAACCTCAATGGTGAACTCAGTGA	ath-miR397a	ucauugagugcagcguugaug	-31.21
149	CTGGTCTTCAAGCGGAGGCGATCCTTGTGGCG	ath-miR399c	ugccaaaggagaguugcccug	-31.05
149	CTGGTCTTCAAGCGGAGGCGATCCTTGTGGCG	ath-miR399b	ugccaaaggagaguugcccug	-30.89
149	CTGGTCTTCAAGCGGAGGCGATCCTTGTGGCG	ath-miR399e	ugccaaaggagauuugccucg	-30.15
149	CTGGTCTTCAAGCGGAGGCGATCCTTGTGGCG	ath-miR399a	ugccaaaggagauuugcccug	-30.15
149	CTGGTCTTCAAGCGGAGGCGATCCTTGTGGCG	ath-miR399d	ugccaaaggagauuugccccg	-30.15
5	ACCAAATCTGCAGCGAATCGTACTTGTCTTCA	ath-miR447b	uuggggacgagauguuuuguug	-29.8

Table 5.2: Best 10 results of the miRNA prediction of SRF4. Prediction was done with MicroInspector.

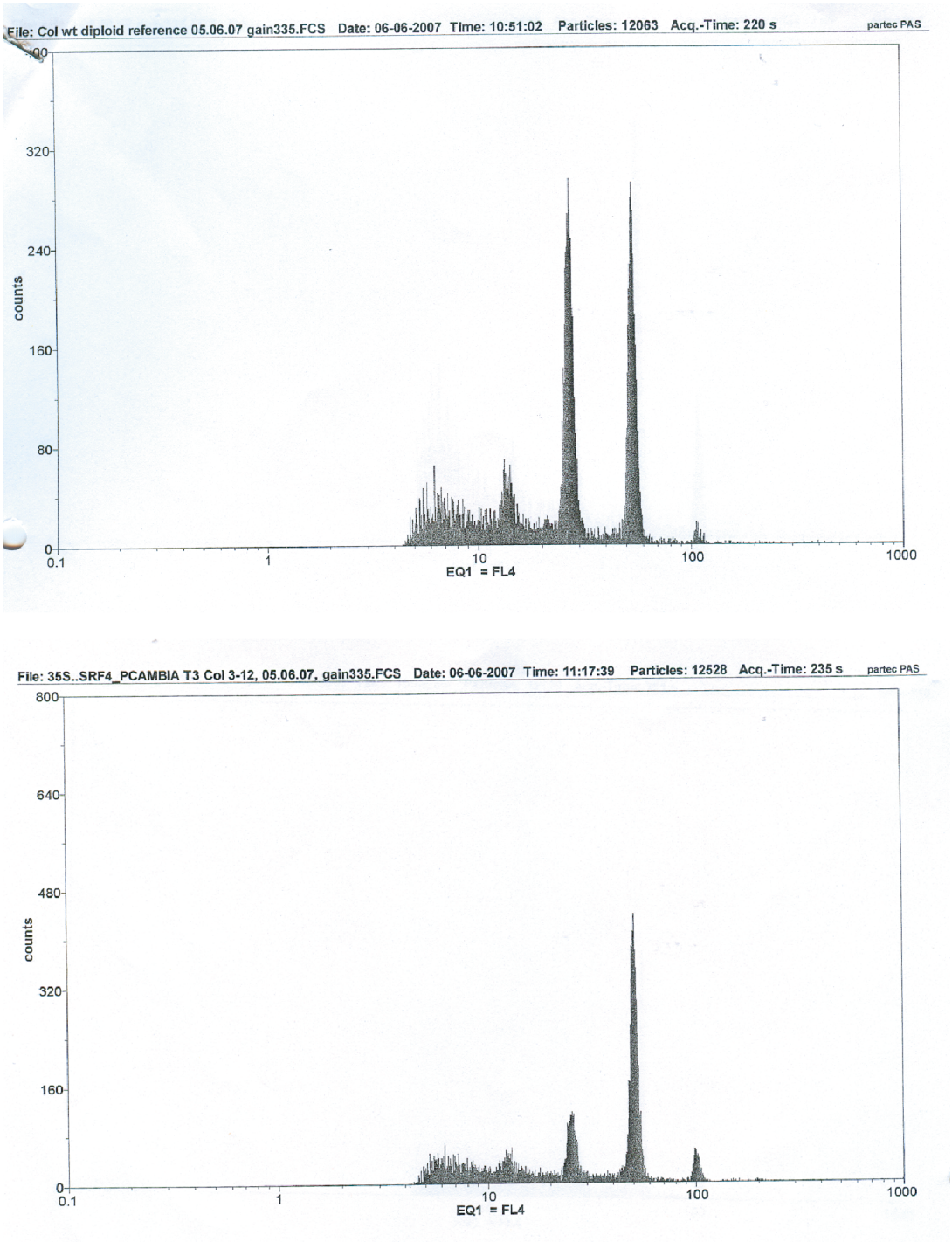

Figure 5.5: Polyploidy scan for *35S::SRF4* and Col-0 by flow cytometry, performed in the lab of Ramon Torres Riuz, TUM Genetics. The upper picture shows the results of *35S::SRF4* the lower one Col-0. No interesting shift of peaks could be observed.

Bibliography

[Abascal et al., 2005] Abascal, F., Zardoya, R., and Posada, D. (2005). ProtTest: selection of best-fit models of protein evolution. *Bioinformatics*, 21:2104–2105.

[Affolter and Basler, 2007] Affolter, M. and Basler, K. (2007). The Decapentaplegic morphogen gradient: from pattern formation to growth regulation. *Nat. Rev. Genet.*, 8:663–674.

[Afzal et al., 2008] Afzal, A. J., Wood, A. J., and Lightfoot, D. A. (2008). Plant receptor-like serine threonine kinases: roles in signaling and plant defense. *Mol. Plant Microbe Interact.*, 21:507–517.

[Ahn et al., 2006] Ahn, J. Y., Liu, X., Liu, Z., Pereira, L., Cheng, D., Peng, J., Wade, P. A., Hamburger, A. W., and Ye, K. (2006). Nuclear Akt associates with PKC-phosphorylated Ebp1, preventing DNA fragmentation by inhibition of caspase-activated DNase. *EMBO J.*, 25:2083–2095.

[Alcazar et al., 2010] Alcazar, R., Garcia, A. V., Kronholm, I., de Meaux, J., Koornneef, M., Parker, J. E., and Reymond, M. (2010). Natural variation at Strubbelig Receptor Kinase 3 drives immune-triggered incompatibilities between Arabidopsis thaliana accessions. *Nat. Genet.*, 42:1135–1139.

[Alexander, 1969] Alexander, M. P. (1969). Differential staining of aborted and non-aborted pollen. *Stain Technol*, 44:117–122.

[Altschul et al., 1990] Altschul, S. F., Gish, W., Miller, W., Myers, E. W., and Lipman, D. J. (1990). Basic local alignment search tool. *J. Mol. Biol.*, 215:403–410.

[Anastasiou et al., 2007] Anastasiou, E., Kenz, S., Gerstung, M., MacLean, D., Timmer, J., Fleck, C., and Lenhard, M. (2007). Control of plant organ size by KLUH/CYP78A5-dependent intercellular signaling. *Dev. Cell*, 13:843–856.

[Anastasiou and Lenhard, 2007] Anastasiou, E. and Lenhard, M. (2007). Growing up to one's standard. *Curr. Opin. Plant Biol.*, 10:63–69.

[Anderson and Hanson, 2005] Anderson, G. H. and Hanson, M. R. (2005). The Arabidopsis Mei2 homologue AML1 binds AtRaptor1B, the plant homologue of a major regulator of eukaryotic cell growth. *BMC Plant Biol.*, 5:2.

[Anderson, 1971a] Anderson, L. E. (1971a). Chloroplast and cytoplasmic enzymes. 3. Pea leaf ribose 5-phosphate isomerases. *Biochim. Biophys. Acta*, 235:245–249.

[Anderson, 1971b] Anderson, L. E. (1971b). Chloroplast and cytoplasmic enzymes. II. Pea leaf triose phosphate isomerases. *Biochim. Biophys. Acta*, 235:237–244.

[Anggono and Robinson, 2007] Anggono, V. and Robinson, P. J. (2007). Syndapin I and endophilin I bind overlapping proline-rich regions of dynamin I: role in synaptic vesicle endocytosis. *J. Neurochem.*, 102:931–943.

[Arnold et al., 2006] Arnold, K., Bordoli, L., Kopp, J., and Schwede, T. (2006). The SWISS-MODEL workspace: a web-based environment for protein structure homology modelling. *Bioinformatics*, 22:195–201.

[Arsham and Neufeld, 2006] Arsham, A. M. and Neufeld, T. P. (2006). Thinking globally and acting locally with TOR. *Curr. Opin. Cell Biol.*, 18:589–597.

[Banks et al., 2011] Banks, J. A., Nishiyama, T., Hasebe, M., Bowman, J. L., Gribskov, M., dePamphilis, C., Albert, V. A., Aono, N., Aoyama, T., Ambrose, B. A., Ashton, N. W., Axtell, M. J., Barker, E., Barker, M. S., Bennetzen, J. L., Bonawitz, N. D., Chapple, C., Cheng, C., Correa, L. G., Dacre, M., DeBarry, J., Dreyer, I., Elias, M., Engstrom, E. M., Estelle, M., Feng, L., Finet, C., Floyd, S. K., Frommer, W. B., Fujita, T., Gramzow, L., Gutensohn, M., Harholt, J., Hattori, M., Heyl, A., Hirai, T., Hiwatashi, Y., Ishikawa, M., Iwata, M., Karol, K. G., Koehler, B., Kolukisaoglu, U., Kubo, M., Kurata, T., Lalonde, S., Li, K., Li, Y., Litt, A., Lyons, E., Manning, G., Maruyama, T., Michael, T. P., Mikami, K., Miyazaki, S., Morinaga, S., Murata, T., Mueller-Roeber, B., Nelson, D. R., Obara, M., Oguri, Y., Olmstead, R. G., Onodera, N., Petersen, B. L., Pils, B., Prigge, M., Rensing, S. A., Riano-Pachon, D. M., Roberts, A. W., Sato, Y., Scheller, H. V., Schulz, B., Schulz, C., Shakirov, E. V., Shibagaki, N., Shinohara, N., Shippen, D. E., Srensen, I., Sotooka, R., Sugimoto, N., Sugita, M., Sumikawa, N., Tanurdzic, M., Theissen, G., Ulvskov, P., Wakazuki, S., Weng, J. K., Willats, W. W., Wipf, D., Wolf, P. G., Yang, L., Zimmer, A. D., Zhu, Q., Mitros, T., Hellsten, U., Loque, D., Otillar, R., Salamov, A., Schmutz, J., Shapiro, H., Lindquist, E., Lucas, S., Rokhsar, D., and Grigoriev, I. V. (2011). The Selaginella genome identifies genetic changes associated with the evolution of vascular plants. *Science*, 332:960–963.

[Bari et al., 2004] Bari, R., Kebeish, R., Kalamajka, R., Rademacher, T., and Peterhansel, C. (2004). A glycolate dehydrogenase in the mitochondria of Arabidopsis thaliana. *J. Exp. Bot.*, 55:623–630.

[Bauwe et al., 2010] Bauwe, H., Hagemann, M., and Fernie, A. R. (2010). Photorespiration: players, partners and origin. *Trends Plant Sci.*, 15:330–336.

[Berman et al., 2002] Berman, H. M., Battistuz, T., Bhat, T. N., Bluhm, W. F., Bourne, P. E., Burkhardt, K., Feng, Z., Gilliland, G. L., Iype, L., Jain, S., Fagan, P., Marvin, J., Padilla, D., Ravichandran, V., Schneider, B., Thanki, N., Weissig, H., Westbrook, J. D., and Zardecki, C. (2002). The Protein Data Bank. *Acta Crystallogr. D Biol. Crystallogr.*, 58:899–907.

[Bernhardt et al., 2010] Bernhardt, A., Mooney, S., and Hellmann, H. (2010). Arabidopsis DDB1a and DDB1b are critical for embryo development. *Planta*, 232:555–566.

[Bertani, 1951] Bertani, G. (1951). Studies on lysogenesis. I. The mode of phage liberation by lysogenic Escherichia coli. *J. Bacteriol.*, 62:293–300.

[Bertani, 2004] Bertani, G. (2004). Lysogeny at mid-twentieth century: P1, P2, and other experimental systems. *J. Bacteriol.*, 186:595–600.

[Bleckmann et al., 2010] Bleckmann, A., Weidtkamp-Peters, S., Seidel, C. A., and Simon, R. (2010). Stem cell signaling in Arabidopsis requires CRN to localize CLV2 to the plasma membrane. *Plant Physiol.*, 152:166–176.

[Brohawn et al., 2008] Brohawn, S. G., Leksa, N. C., Spear, E. D., Rajashankar, K. R., and Schwartz, T. U. (2008). Structural evidence for common ancestry of the nuclear pore complex and vesicle coats. *Science*, 322:1369–1373.

[Buchanan et al., 2000] Buchanan, B., Gruissem, W., and Jones, R. (2000). *Biochemistry & Molecular Biology of Plants.* American Society of Plant Physiologists, 2nd edition.

[Busov et al., 2008] Busov, V. B., Brunner, A. M., and Strauss, S. H. (2008). Genes for control of plant stature and form. *New Phytol.*, 177:589–607.

[Campell, 1998] Campell, N. (1998). *Biologie.* Spektrum Akademischer Verlag, Heidelberg, Berlin, Oxford.

[Cao et al., 2011] Cao, J., Schneeberger, K., Ossowski, S., Gnther, T., Bender, S., Fitz, J., Koenig, D., Lanz, C.and Stegle, O., Lippert, C., Wang, X., Ott, F., Mller, J., Alonso-Blanco, C., B., K., S., J., K., and Weigel, D. (2011). Whole-genome

sequencing of multiple arabidopsis thaliana populations. *Nat. Genet.*, accepted for publication.

[Carpita and Gibeaut, 1993] Carpita, N. C. and Gibeaut, D. M. (1993). Structural models of primary cell walls in flowering plants: consistency of molecular structure with the physical properties of the walls during growth. *Plant J.*, 3:1–30.

[Carrera et al., 1994] Carrera, A. C., Borlado, L. R., Roberts, T. M., and Martinez, C. (1994). Tyrosine kinase specific motif at subdomain VIII does not confer specificity for tyrosine. *Biochem. Biophys. Res. Commun.*, 205:1114–1120.

[Castells and Casacuberta, 2007] Castells, E. and Casacuberta, J. M. (2007). Signalling through kinase-defective domains: the prevalence of atypical receptor-like kinases in plants. *J. Exp. Bot.*, 58:3503–3511.

[Castells et al., 2006] Castells, E., Puigdomenech, P., and Casacuberta, J. M. (2006). Regulation of the kinase activity of the MIK GCK-like MAP4K by alternative splicing. *Plant Mol. Biol.*, 61:747–756.

[Cavalier et al., 2008] Cavalier, D. M., Lerouxel, O., Neumetzler, L., Yamauchi, K., Reinecke, A., Freshour, G., Zabotina, O. A., Hahn, M. G., Burgert, I., Pauly, M., Raikhel, N. V., and Keegstra, K. (2008). Disrupting two Arabidopsis thaliana xylosyltransferase genes results in plants deficient in xyloglucan, a major primary cell wall component. *Plant Cell*, 20:1519–1537.

[Cegelski and Schaefer, 2006] Cegelski, L. and Schaefer, J. (2006). NMR determination of photorespiration in intact leaves using in vivo 13CO2 labeling. *J. Magn. Reson.*, 178:1–10.

[Chen and Clarke, 2002] Chen, E. Y. and Clarke, D. M. (2002). The PEST sequence does not contribute to the stability of the cystic fibrosis transmembrane conductance regulator. *BMC Biochem.*, 3:29.

[Chevalier et al., 2005] Chevalier, D., Batoux, M., Fulton, L., Pfister, K., Yadav, R. K., Schellenberg, M., and Schneitz, K. (2005). STRUBBELIG defines a receptor kinase-mediated signaling pathway regulating organ development in Arabidopsis. *Proc. Natl. Acad. Sci. U.S.A.*, 102:9074–9079.

[Chinchilla et al., 2007] Chinchilla, D., Zipfel, C., Robatzek, S., Kemmerling, B., Nurnberger, T., Jones, J. D., Felix, G., and Boller, T. (2007). A flagellin-induced complex of the receptor FLS2 and BAK1 initiates plant defence. *Nature*, 448:497–500.

[Cho et al., 2006] Cho, S. K., Kim, J. E., Park, J. A., Eom, T. J., and Kim, W. T. (2006). Constitutive expression of abiotic stress-inducible hot pepper CaXTH3, which encodes a xyloglucan endotransglucosylase/hydrolase homolog, improves drought and salt tolerance in transgenic Arabidopsis plants. *FEBS Lett.*, 580:3136–3144.

[Citri et al., 2003] Citri, A., Skaria, K. B., and Yarden, Y. (2003). The deaf and the dumb: the biology of ErbB-2 and ErbB-3. *Exp. Cell Res.*, 284:54–65.

[Clark et al., 1997] Clark, S. E., Williams, R. W., and Meyerowitz, E. M. (1997). The CLAVATA1 gene encodes a putative receptor kinase that controls shoot and floral meristem size in Arabidopsis. *Cell*, 89:575–585.

[Clough and Bent, 1998] Clough, S. J. and Bent, A. F. (1998). Floral dip: a simplified method for Agrobacterium-mediated transformation of Arabidopsis thaliana. *Plant J.*, 16:735–743.

[Cock et al., 2002] Cock, J. M., Vanoosthuyse, V., and Gaude, T. (2002). Receptor kinase signalling in plants and animals: distinct molecular systems with mechanistic similarities. *Curr. Opin. Cell Biol.*, 14:230–236.

[Cosgrove, 2005] Cosgrove, D. J. (2005). Growth of the plant cell wall. *Nat. Rev. Mol. Cell Biol.*, 6:850–861.

[Davanloo et al., 1984] Davanloo, P., Rosenberg, A. H., Dunn, J. J., and Studier, F. W. (1984). Cloning and expression of the gene for bacteriophage T7 RNA polymerase. *Proc. Natl. Acad. Sci. U.S.A.*, 81:2035–2039.

[Deak et al., 1999] Deak, M., Casamayor, A., Currie, R. A., Downes, C. P., and Alessi, D. R. (1999). Characterisation of a plant 3-phosphoinositide-dependent protein kinase-1 homologue which contains a pleckstrin homology domain. *FEBS Lett.*, 451:220–226.

[Deprost et al., 2005] Deprost, D., Truong, H. N., Robaglia, C., and Meyer, C. (2005). An Arabidopsis homolog of RAPTOR/KOG1 is essential for early embryo development. *Biochem. Biophys. Res. Commun.*, 326:844–850.

[Deprost et al., 2007] Deprost, D., Yao, L., Sormani, R., Moreau, M., Leterreux, G., Nicolai, M., Bedu, M., Robaglia, C., and Meyer, C. (2007). The Arabidopsis TOR kinase links plant growth, yield, stress resistance and mRNA translation. *EMBO Rep.*, 8:864–870.

[Disch et al., 2006] Disch, S., Anastasiou, E., Sharma, V. K., Laux, T., Fletcher, J. C., and Lenhard, M. (2006). The E3 ubiquitin ligase BIG BROTHER controls arabidopsis organ size in a dosage-dependent manner. *Curr. Biol.*, 16:272–279.

[Drummond et al., 2010] Drummond, A., Ashton, B., Buxton, S., Cheung, M., Cooper, A., Heled, J., Kearse, M., Moir, R., Stones-Havas, S., Sturrock, S., Thierer, T., and Wilson, A. (2010). Geneious v5.3. `http://www.geneious.com`.

[Eisenhut et al., 2008] Eisenhut, M., Ruth, W., Haimovich, M., Bauwe, H., Kaplan, A., and Hagemann, M. (2008). The photorespiratory glycolate metabolism is essential for cyanobacteria and might have been conveyed endosymbiontically to plants. *Proc. Natl. Acad. Sci. U.S.A.*, 105:17199–17204.

[Eyuboglu, 2008] Eyuboglu, B. (2008). Molecular and Functional Analysis of the LRRV/SRF Family of Putative Leucine-Rich Repeat Receptor-Like Kinases in Arabidopsis thaliana. [PhD Thesis].

[Eyuboglu et al., 2007] Eyuboglu, B., Pfister, K., Haberer, G., Chevalier, D., Fuchs, A., Mayer, K. F., and Schneitz, K. (2007). Molecular characterisation of the STRUBBELIG-RECEPTOR FAMILY of genes encoding putative leucine-rich repeat receptor-like kinases in Arabidopsis thaliana. *BMC Plant Biol.*, 7:16.

[Fong et al., 1986] Fong, H. K., Hurley, J. B., Hopkins, R. S., Miake-Lye, R., Johnson, M. S., Doolittle, R. F., and Simon, M. I. (1986). Repetitive segmental structure of the transducin beta subunit: homology with the CDC4 gene and identification of related mRNAs. *Proc. Natl. Acad. Sci. U.S.A.*, 83:2162–2166.

[Fry, 1989] Fry, S. C. (1989). Cellulases, hemicelluloses and auxin-stimulated growth: A possible relationship. *Physiol. Plant*, 75:532–536.

[Fulton et al., 2009] Fulton, L., Batoux, M., Vaddepalli, P., Yadav, R. K., Busch, W., Andersen, S. U., Jeong, S., Lohmann, J. U., and Schneitz, K. (2009). DETORQUEO, QUIRKY, and ZERZAUST represent novel components involved in organ development mediated by the receptor-like kinase STRUBBELIG in Arabidopsis thaliana. *PLoS Genet.*, 5:e1000355.

[Gan and Amasino, 1995] Gan, S. and Amasino, R. M. (1995). Inhibition of leaf senescence by autoregulated production of cytokinin. *Science*, 270:1986–1988.

[Gasteiger et al., 2003] Gasteiger, E., Gattiker, A., Hoogland, C., Ivanyi, I., Appel, R. D., and Bairoch, A. (2003). ExPASy: The proteomics server for in-depth protein knowledge and analysis. *Nucleic Acids Res.*, 31:3784–3788.

[Gendreau et al., 1997] Gendreau, E., Traas, J., Desnos, T., Grandjean, O., Caboche, M., and Hofte, H. (1997). Cellular basis of hypocotyl growth in Arabidopsis thaliana. *Plant Physiol.*, 114:295–305.

[Georgiev et al., 2008] Georgiev, A., Leipus, A., Olsson, I., Berrez, J. M., and Mutvei, A. (2008). Characterization of MYR1, a dosage suppressor of YPT6 and RIC1 deficient mutants. *Curr. Genet.*, 53:235–247.

[Gietz et al., 1992] Gietz, D., St Jean, A., Woods, R. A., and Schiestl, R. H. (1992). Improved method for high efficiency transformation of intact yeast cells. *Nucleic Acids Res.*, 20:1425.

[Gilmartin and Bowler, 2002] Gilmartin, P. and Bowler, C. (2002). *Molecular plant biology: a practical approach*, volume 2, chapter 9. Oxford University Press.

[Gish and Clark, 2011] Gish, L. A. and Clark, S. E. (2011). The RLK/Pelle family of kinases. *Plant J.*, 66:117–127.

[Gomez-Gomez and Boller, 2000] Gomez-Gomez, L. and Boller, T. (2000). FLS2: an LRR receptor-like kinase involved in the perception of the bacterial elicitor flagellin in Arabidopsis. *Mol. Cell*, 5:1003–1011.

[Gomez-Gomez and Boller, 2002] Gomez-Gomez, L. and Boller, T. (2002). Flagellin perception: a paradigm for innate immunity. *Trends Plant Sci.*, 7:251–256.

[Grant et al., 1990] Grant, S. G., Jessee, J., Bloom, F. R., and Hanahan, D. (1990). Differential plasmid rescue from transgenic mouse DNAs into Escherichia coli methylation-restriction mutants. *Proc. Natl. Acad. Sci. U.S.A.*, 87:4645–4649.

[Guo et al., 2010] Guo, Y., Han, L., Hymes, M., Denver, R., and Clark, S. E. (2010). CLAVATA2 forms a distinct CLE-binding receptor complex regulating Arabidopsis stem cell specification. *Plant J.*, 63:889–900.

[Guy et al., 1994] Guy, P. M., Platko, J. V., Cantley, L. C., Cerione, R. A., and Carraway, K. L. (1994). Insect cell-expressed p180erbB3 possesses an impaired tyrosine kinase activity. *Proc. Natl. Acad. Sci. U.S.A.*, 91:8132–8136.

[Hanks and Hunter, 1995] Hanks, S. K. and Hunter, T. (1995). Protein kinases 6. The eukaryotic protein kinase superfamily: kinase (catalytic) domain structure and classification. *FASEB J.*, 9:576–596.

[Hanks et al., 1988] Hanks, S. K., Quinn, A. M., and Hunter, T. (1988). The protein kinase family: conserved features and deduced phylogeny of the catalytic domains. *Science*, 241:42–52.

[Hartati et al., 2008] Hartati, S., Sudarmonowati, E., Park, Y. W., Kaku, T., Kaida, R., Baba, K., and Hayashi, T. (2008). Overexpression of poplar cellulase accelerates growth and disturbs the closing movements of leaves in sengon. *Plant Physiol.*, 147:552–561.

[Hattendorf et al., 2007] Hattendorf, D. A., Andreeva, A., Gangar, A., Brennwald, P. J., and Weis, W. I. (2007). Structure of the yeast polarity protein Sro7 reveals a SNARE regulatory mechanism. *Nature*, 446:567–571.

[Hayashi, 1989] Hayashi, T. (1989). Xyloglucans in the primary cell wall. *Ann. Rev. Plant Physiol. Plant Mol. Biol.*, 40:139–168.

[Hayashi and Kaida, 2011] Hayashi, T. and Kaida, R. (2011). Functions of xyloglucan in plant cells. *Mol Plant*, 4:17–24.

[He et al., 2002] He, J. X., Gendron, J. M., Yang, Y., Li, J., and Wang, Z. Y. (2002). The GSK3-like kinase BIN2 phosphorylates and destabilizes BZR1, a positive regulator of the brassinosteroid signaling pathway in Arabidopsis. *Proc. Natl. Acad. Sci. U.S.A.*, 99:10185–10190.

[Heese et al., 2007] Heese, A., Hann, D. R., Gimenez-Ibanez, S., Jones, A. M., He, K., Li, J., Schroeder, J. I., Peck, S. C., and Rathjen, J. P. (2007). The receptor-like kinase SERK3/BAK1 is a central regulator of innate immunity in plants. *Proc. Natl. Acad. Sci. U.S.A.*, 104:12217–12222.

[Herold, 2008] Herold, E. (2008). *In vitro* interaction studies between the LRR-RLK SRF4 and a putative interaction partner DAEUMLING. *Master Thesis at the Technical University of Munich, Department of Plant Developmental Biology*, page unpublished data.

[Heupel et al., 1991] Heupel, R., Markgraf, T., Robinson, D. G., and Heldt, H. W. (1991). Compartmentation studies on spinach leaf peroxisomes : evidence for channeling of photorespiratory metabolites in peroxisomes devoid of intact boundary membrane. *Plant Physiol.*, 96:971–979.

[Horiguchi et al., 2005] Horiguchi, G., Kim, G. T., and Tsukaya, H. (2005). The transcription factor AtGRF5 and the transcription coactivator AN3 regulate cell proliferation in leaf primordia of Arabidopsis thaliana. *Plant J.*, 43:68–78.

[Hortensteiner, 2004] Hortensteiner, S. (2004). The loss of green color during chlorophyll degradation–a prerequisite to prevent cell death? *Planta*, 219:191–194.

[Hortensteiner and Krautler, 2011] Hortensteiner, S. and Krautler, B. (2011). Chlorophyll breakdown in higher plants. *Biochim. Biophys. Acta*, 1807:977–988.

[Horvath et al., 2006] Horvath, B. M., Magyar, Z., Zhang, Y., Hamburger, A. W., Bako, L., Visser, R. G., Bachem, C. W., and Bogre, L. (2006). EBP1 regulates organ size through cell growth and proliferation in plants. *EMBO J.*, 25:4909–4920.

[Hruz et al., 2008] Hruz, T., Laule, O., Szabo, G., Wessendorp, F., Bleuler, S., Oertle, L., Widmayer, P., Gruissem, W., and Zimmermann, P. (2008). Genevestigator v3: a reference expression database for the meta-analysis of transcriptomes. *Adv Bioinformatics*, 2008:420747.

[Hsia et al., 2007] Hsia, K. C., Stavropoulos, P., Blobel, G., and Hoelz, A. (2007). Architecture of a coat for the nuclear pore membrane. *Cell*, 131:1313–1326.

[Hu et al., 2011] Hu, T. T., Pattyn, P., Bakker, E. G., Cao, J., Cheng, J. F., Clark, R. M., Fahlgren, N., Fawcett, J. A., Grimwood, J., Gundlach, H., Haberer, G., Hollister, J. D., Ossowski, S., Ottilar, R. P., Salamov, A. A., Schneeberger, K., Spannagl, M., Wang, X., Yang, L., Nasrallah, M. E., Bergelson, J., Carrington, J. C., Gaut, B. S., Schmutz, J., Mayer, K. F., Van de Peer, Y., Grigoriev, I. V., Nordborg, M., Weigel, D., and Guo, Y. L. (2011). The Arabidopsis lyrata genome sequence and the basis of rapid genome size change. *Nat. Genet.*, 43:476–481.

[Hu et al., 2003] Hu, Y., Xie, Q., and Chua, N. H. (2003). The Arabidopsis auxin-inducible gene ARGOS controls lateral organ size. *Plant Cell*, 15:1951–1961.

[Huala et al., 2001] Huala, E., Dickerman, A. W., Garcia-Hernandez, M., Weems, D., Reiser, L., LaFond, F., Hanley, D., Kiphart, D., Zhuang, M., Huang, W., Mueller, L. A., Bhattacharyya, D., Bhaya, D., Sobral, B. W., Beavis, W., Meinke, D. W., Town, C. D., Somerville, C., and Rhee, S. Y. (2001). The Arabidopsis Information Resource (TAIR): a comprehensive database and web-based information retrieval, analysis, and visualization system for a model plant. *Nucleic Acids Res.*, 29:102–105.

[Huang and Madan, 1999] Huang, X. and Madan, A. (1999). CAP3: A DNA sequence assembly program. *Genome Res.*, 9:868–877.

[Hunter et al., 2009] Hunter, S., Apweiler, R., Attwood, T. K., Bairoch, A., Bateman, A., Binns, D., Bork, P., Das, U., Daugherty, L., Duquenne, L., Finn, R. D., Gough, J., Haft, D., Hulo, N., Kahn, D., Kelly, E., Laugraud, A., Letunic, I., Lonsdale, D., Lopez, R., Madera, M., Maslen, J., McAnulla, C., McDowall, J., Mistry, J., Mitchell, A., Mulder, N., Natale, D., Orengo, C., Quinn, A. F., Selengut, J. D., Sigrist, C. J., Thimma, M., Thomas, P. D., Valentin, F., Wilson, D., Wu, C. H., and Yeats, C. (2009). InterPro: the integrative protein signature database. *Nucleic Acids Res.*, 37:D211–215.

[Huse and Kuriyan, 2002] Huse, M. and Kuriyan, J. (2002). The conformational plasticity of protein kinases. *Cell*, 109:275–282.

[ImageJ, 2010] ImageJ (2010). Image Processing and Analysis in Java. `http://rsb.info.nih.gov/ij/`. [Online; accessed 16-November-2010].

[Imaishi et al., 2000] Imaishi, H., Matsuo, S., Swai, E., and Ohkawa, H. (2000). CYP78A1 preferentially expressed in developing inflorescences of Zea mays encoded a cytochrome P450-dependent lauric acid 12-monooxygenase. *Biosci. Biotechnol. Biochem.*, 64:1696–1701.

[Inskeep and Bloom, 1985] Inskeep, W. P. and Bloom, P. R. (1985). Extinction coefficients of chlorophyll a and b in N,N-dimethylformamide and 80 % acetone. *Plant Physiol.*, 77:483–485.

[Ito et al., 2006] Ito, Y., Nakanomyo, I., Motose, H., Iwamoto, K., Sawa, S., Dohmae, N., and Fukuda, H. (2006). Dodeca-CLE peptides as suppressors of plant stem cell differentiation. *Science*, 313:842–845.

[Iwai et al., 2002] Iwai, H., Masaoka, N., Ishii, T., and Satoh, S. (2002). A pectin glucuronyltransferase gene is essential for intercellular attachment in the plant meristem. *Proc. Natl. Acad. Sci. U.S.A.*, 99:16319–16324.

[Jaillon et al., 2007] Jaillon, O., Aury, J. M., Noel, B., Policriti, A., Clepet, C., Casagrande, A., Choisne, N., Aubourg, S., Vitulo, N., Jubin, C., Vezzi, A., Legeai, F., Hugueney, P., Dasilva, C., Horner, D., Mica, E., Jublot, D., Poulain, J., Bruyere, C., Billault, A., Segurens, B., Gouyvenoux, M., Ugarte, E., Cattonaro, F., Anthouard, V., Vico, V., Del Fabbro, C., Alaux, M., Di Gaspero, G., Dumas, V., Felice, N., Paillard, S., Juman, I., Moroldo, M., Scalabrin, S., Canaguier, A., Le Clainche, I., Malacrida, G., Durand, E., Pesole, G., Laucou, V., Chatelet, P., Merdinoglu, D., Delledonne, M., Pezzotti, M., Lecharny, A., Scarpelli, C., Artiguenave, F., Pe, M. E., Valle, G., Morgante, M., Caboche, M., Adam-Blondon, A. F., Weissenbach, J., Quetier, F., and Wincker, P. (2007). The grapevine genome sequence suggests ancestral hexaploidization in major angiosperm phyla. *Nature*, 449:463–467.

[James et al., 1996] James, P., Halladay, J., and Craig, E. A. (1996). Genomic libraries and a host strain designed for highly efficient two-hybrid selection in yeast. *Genetics*, 144:1425–1436.

[Jefferson et al., 1987] Jefferson, R. A., Kavanagh, T. A., and Bevan, M. W. (1987). GUS fusions: beta-glucuronidase as a sensitive and versatile gene fusion marker in higher plants. *EMBO J.*, 6:3901–3907.

[Johnson et al., 1996] Johnson, L. N., Noble, M. E., and Owen, D. J. (1996). Active and inactive protein kinases: structural basis for regulation. *Cell*, 85:149–158.

[Jordan and Ogren, 1984] Jordan, D. and Ogren, W. (1984). The CO2Ø2 specificity of ribulose 1,5-bisphosphate carboxylase/oxygenase. *Planta*, 161:308–313.

[Kaida et al., 2010] Kaida, R., Sugawara, S., Negoro, K., Maki, H., Hayashi, T., and Kaneko, T. S. (2010). Acceleration of cell growth by xyloglucan oligosaccharides in suspension-cultured tobacco cells. *Mol Plant*, 3:549–554.

[Katoh et al., 2009] Katoh, K., Asimenos, G., and Toh, H. (2009). Multiple alignment of DNA sequences with MAFFT. *Methods Mol. Biol.*, 537:39–64.

[Kawade et al., 2010] Kawade, K., Horiguchi, G., and Tsukaya, H. (2010). Non-cell-autonomously coordinated organ size regulation in leaf development. *Development*, 137:4221–4227.

[Kayes and Clark, 1998] Kayes, J. M. and Clark, S. E. (1998). CLAVATA2, a regulator of meristem and organ development in Arabidopsis. *Development*, 125:3843–3851.

[Kebeish et al., 2007] Kebeish, R., Niessen, M., Thiruveedhi, K., Bari, R., Hirsch, H. J., Rosenkranz, R., Stabler, N., Schonfeld, B., Kreuzaler, F., and Peterhansel, C. (2007). Chloroplastic photorespiratory bypass increases photosynthesis and biomass production in Arabidopsis thaliana. *Nat. Biotechnol.*, 25:593–599.

[Kelly and Latzko, 1976] Kelly, G. J. and Latzko, E. (1976). Inhibition of spinach-leaf phosphofructokinase by 2-phosphoglycollate. *FEBS Lett.*, 68:55–58.

[Kilian et al., 2007] Kilian, J., Whitehead, D., Horak, J., Wanke, D., Weinl, S., Batistic, O., D'Angelo, C., Bornberg-Bauer, E., Kudla, J., and Harter, K. (2007). The AtGenExpress global stress expression data set: protocols, evaluation and model data analysis of UV-B light, drought and cold stress responses. *Plant J.*, 50:347–363.

[Kim et al., 1998a] Kim, G. T., Tsukaya, H., and Uchimiya, H. (1998a). The ROTUNDIFOLIA3 gene of Arabidopsis thaliana encodes a new member of the cytochrome P-450 family that is required for the regulated polar elongation of leaf cells. *Genes Dev.*, 12:2381–2391.

[Kim et al., 1998b] Kim, H. H., Vijapurkar, U., Hellyer, N. J., Bravo, D., and Koland, J. G. (1998b). Signal transduction by epidermal growth factor and heregulin via the kinase-deficient ErbB3 protein. *Biochem. J.*, 334 (Pt 1):189–195.

[Kinoshita et al., 2010] Kinoshita, N., Berr, A., Belin, C., Chappuis, R., Nishizawa, N. K., and Lopez-Molina, L. (2010). Identification of growth insensitive to ABA3 (gia3), a recessive mutation affecting ABA Signaling for the control of early post-germination growth in Arabidopsis thaliana. *Plant Cell Physiol.*, 51:239–251.

[Kleczkowski and Randall, 1988] Kleczkowski, L. A. and Randall, D. D. (1988). Purification and characterization of a novel NADPH(NADH)-dependent hydroxypyruvate reductase from spinach leaves. Comparison of immunological properties of leaf hydroxypyruvate reductases. *Biochem. J.*, 250:145–152.

[Kobe and Kajava, 2001] Kobe, B. and Kajava, A. V. (2001). The leucine-rich repeat as a protein recognition motif. *Curr. Opin. Struct. Biol.*, 11:725–732.

[Koncz and Schell, 1986] Koncz, C. and Schell, J. (1986). The promoter of the tl-dna gene 5 controls the tissue-specific expression of chimeric genes carried by a novel type of agrobacterium binary vector. *Mol. Gen. Genet.*, 204:383–396.

[Kondo et al., 2008] Kondo, T., Nakamura, T., Yokomine, K., and Sakagami, Y. (2008). Dual assay for MCLV3 activity reveals structure-activity relationship of CLE peptides. *Biochem. Biophys. Res. Commun.*, 377:312–316.

[Krizek, 1999] Krizek, B. A. (1999). Ectopic expression of AINTEGUMENTA in Arabidopsis plants results in increased growth of floral organs. *Dev. Genet.*, 25:224–236.

[Krizek, 2009] Krizek, B. A. (2009). Making bigger plants: key regulators of final organ size. *Curr. Opin. Plant Biol.*, 12:17–22.

[Krizek and Sulli, 2006] Krizek, B. A. and Sulli, C. (2006). Mapping sequences required for nuclear localization and the transcriptional activation function of the Arabidopsis protein AINTEGUMENTA. *Planta*, 224:612–621.

[Krogh et al., 2001] Krogh, A., Larsson, B., von Heijne, G., and Sonnhammer, E. L. (2001). Predicting transmembrane protein topology with a hidden Markov model: application to complete genomes. *J. Mol. Biol.*, 305:567–580.

[Ku and Edwards, 1977] Ku, S. and Edwards, G. (1977). Oxygen Inhibition of Photosynthesis: I. Temperature Dependence and Relation to O(2)/CO(2) Solubility Ratio. *Plant Physiol.*, 59:986–90.

[Kwak and Schiefelbein, 2007] Kwak, S. H. and Schiefelbein, J. (2007). The role of the SCRAMBLED receptor-like kinase in patterning the Arabidopsis root epidermis. *Dev. Biol.*, 302:118–131.

[Kwak et al., 2005] Kwak, S. H., Shen, R., and Schiefelbein, J. (2005). Positional signaling mediated by a receptor-like kinase in Arabidopsis. *Science*, 307:1111–1113.

[Labavitch and Ray, 1974] Labavitch, J. M. and Ray, P. M. (1974). Relationship between Promotion of Xyloglucan Metabolism and Induction of Elongation by Indoleacetic Acid. *Plant Physiol.*, 54:499–502.

[Lambright et al., 1996] Lambright, D. G., Sondek, J., Bohm, A., Skiba, N. P., Hamm, H. E., and Sigler, P. B. (1996). The 2.0 A crystal structure of a heterotrimeric G protein. *Nature*, 379:311–319.

[Lee and Schiefelbein, 1999] Lee, M. M. and Schiefelbein, J. (1999). WEREWOLF, a MYB-related protein in Arabidopsis, is a position-dependent regulator of epidermal cell patterning. *Cell*, 99:473–483.

[Lehti-Shiu et al., 2009] Lehti-Shiu, M. D., Zou, C., Hanada, K., and Shiu, S. H. (2009). Evolutionary history and stress regulation of plant receptor-like kinase/pelle genes. *Plant Physiol.*, 150:12–26.

[Leishman, 2001] Leishman, M. (2001). Does the seed size/number trade-off model determine plant community structure? An assessment of the model mechanisms and their generality. *OIKOS*, 93:294–302.

[Li and Chory, 1997] Li, J. and Chory, J. (1997). A putative leucine-rich repeat receptor kinase involved in brassinosteroid signal transduction. *Cell*, 90:929–938.

[Li and Nam, 2002] Li, J. and Nam, K. H. (2002). Regulation of brassinosteroid signaling by a GSK3/SHAGGY-like kinase. *Science*, 295:1299–1301.

[Li et al., 2002] Li, J., Wen, J., Lease, K. A., Doke, J. T., Tax, F. E., and Walker, J. C. (2002). BAK1, an Arabidopsis LRR receptor-like protein kinase, interacts with BRI1 and modulates brassinosteroid signaling. *Cell*, 110:213–222.

[Li et al., 2003] Li, L., Stoeckert, C. J., and Roos, D. S. (2003). OrthoMCL: identification of ortholog groups for eukaryotic genomes. *Genome Res.*, 13:2178–2189.

[Li and Wurtzel, 1998] Li, Z. and Wurtzel, E. T. (1998). The ltk gene family encodes novel receptor-like kinases with temporal expression in developing maize endosperm. *Plant Mol. Biol.*, 37:749–761.

[Llompart et al., 2003] Llompart, B., Castells, E., Rio, A., Roca, R., Ferrando, A., Stiefel, V., Puigdomenech, P., and Casacuberta, J. M. (2003). The direct activation

of MIK, a germinal center kinase (GCK)-like kinase, by MARK, a maize atypical receptor kinase, suggests a new mechanism for signaling through kinase-dead receptors. *J. Biol. Chem.*, 278:48105–48111.

[Ma et al., 2010] Ma, Y., Sugiura, R., Zhang, L., Zhou, X., Takeuchi, M., He, Y., and Kuno, T. (2010). Isolation of a fission yeast mutant that is sensitive to valproic acid and defective in the gene encoding Ric1, a putative component of Ypt/Rab-specific GEF for Ryh1 GTPase. *Mol. Genet. Genomics*, 284:161–171.

[Mahfouz et al., 2006] Mahfouz, M. M., Kim, S., Delauney, A. J., and Verma, D. P. (2006). Arabidopsis TARGET OF RAPAMYCIN interacts with RAPTOR, which regulates the activity of S6 kinase in response to osmotic stress signals. *Plant Cell*, 18:477–490.

[Marchler-Bauer et al., 2009] Marchler-Bauer, A., Anderson, J. B., Chitsaz, F., Derbyshire, M. K., DeWeese-Scott, C., Fong, J. H., Geer, L. Y., Geer, R. C., Gonzales, N. R., Gwadz, M., He, S., Hurwitz, D. I., Jackson, J. D., Ke, Z., Lanczycki, C. J., Liebert, C. A., Liu, C., Lu, F., Lu, S., Marchler, G. H., Mullokandov, M., Song, J. S., Tasneem, A., Thanki, N., Yamashita, R. A., Zhang, D., Zhang, N., and Bryant, S. H. (2009). CDD: specific functional annotation with the Conserved Domain Database. *Nucleic Acids Res.*, 37:D205–210.

[Mayer et al., 1998] Mayer, K. F., Schoof, H., Haecker, A., Lenhard, M., Jurgens, G., and Laux, T. (1998). Role of WUSCHEL in regulating stem cell fate in the Arabidopsis shoot meristem. *Cell*, 95:805–815.

[Menand et al., 2002] Menand, B., Desnos, T., Nussaume, L., Berger, F., Bouchez, D., Meyer, C., and Robaglia, C. (2002). Expression and disruption of the Arabidopsis TOR (target of rapamycin) gene. *Proc. Natl. Acad. Sci. U.S.A.*, 99:6422–6427.

[Merchant et al., 2007] Merchant, S. S., Prochnik, S. E., Vallon, O., Harris, E. H., Karpowicz, S. J., Witman, G. B., Terry, A., Salamov, A., Fritz-Laylin, L. K., Marechal-Drouard, L., Marshall, W. F., Qu, L. H., Nelson, D. R., Sanderfoot, A. A., Spalding, M. H., Kapitonov, V. V., Ren, Q., Ferris, P., Lindquist, E., Shapiro, H., Lucas, S. M., Grimwood, J., Schmutz, J., Cardol, P., Cerutti, H., Chanfreau, G., Chen, C. L., Cognat, V., Croft, M. T., Dent, R., Dutcher, S., Fernandez, E., Fukuzawa, H., Gonzalez-Ballester, D., Gonzalez-Halphen, D., Hallmann, A., Hanikenne, M., Hippler, M., Inwood, W., Jabbari, K., Kalanon, M., Kuras, R., Lefebvre, P. A., Lemaire, S. D., Lobanov, A. V., Lohr, M., Manuell, A., Meier, I., Mets, L., Mittag, M., Mittelmeier, T., Moroney, J. V., Moseley, J., Napoli, C., Nedelcu, A. M., Niyogi, K., Novoselov, S. V., Paulsen, I. T., Pazour, G., Purton, S.,

Ral, J. P., Riano-Pachon, D. M., Riekhof, W., Rymarquis, L., Schroda, M., Stern, D., Umen, J., Willows, R., Wilson, N., Zimmer, S. L., Allmer, J., Balk, J., Bisova, K., Chen, C. J., Elias, M., Gendler, K., Hauser, C., Lamb, M. R., Ledford, H., Long, J. C., Minagawa, J., Page, M. D., Pan, J., Pootakham, W., Roje, S., Rose, A., Stahlberg, E., Terauchi, A. M., Yang, P., Ball, S., Bowler, C., Dieckmann, C. L., Gladyshev, V. N., Green, P., Jorgensen, R., Mayfield, S., Mueller-Roeber, B., Rajamani, S., Sayre, R. T., Brokstein, P., Dubchak, I., Goodstein, D., Hornick, L., Huang, Y. W., Jhaveri, J., Luo, Y., Martinez, D., Ngau, W. C., Otillar, B., Poliakov, A., Porter, A., Szajkowski, L., Werner, G., Zhou, K., Grigoriev, I. V., Rokhsar, D. S., and Grossman, A. R. (2007). The Chlamydomonas genome reveals the evolution of key animal and plant functions. *Science*, 318:245–250.

[Meylan and Tschopp, 2008] Meylan, E. and Tschopp, J. (2008). IRAK2 takes its place in TLR signaling. *Nat. Immunol.*, 9:581–582.

[Ming et al., 2008] Ming, R., Hou, S., Feng, Y., Yu, Q., Dionne-Laporte, A., Saw, J. H., Senin, P., Wang, W., Ly, B. V., Lewis, K. L., Salzberg, S. L., Feng, L., Jones, M. R., Skelton, R. L., Murray, J. E., Chen, C., Qian, W., Shen, J., Du, P., Eustice, M., Tong, E., Tang, H., Lyons, E., Paull, R. E., Michael, T. P., Wall, K., Rice, D. W., Albert, H., Wang, M. L., Zhu, Y. J., Schatz, M., Nagarajan, N., Acob, R. A., Guan, P., Blas, A., Wai, C. M., Ackerman, C. M., Ren, Y., Liu, C., Wang, J., Wang, J., Na, J. K., Shakirov, E. V., Haas, B., Thimmapuram, J., Nelson, D., Wang, X., Bowers, J. E., Gschwend, A. R., Delcher, A. L., Singh, R., Suzuki, J. Y., Tripathi, S., Neupane, K., Wei, H., Irikura, B., Paidi, M., Jiang, N., Zhang, W., Presting, G., Windsor, A., Navajas-Perez, R., Torres, M. J., Feltus, F. A., Porter, B., Li, Y., Burroughs, A. M., Luo, M. C., Liu, L., Christopher, D. A., Mount, S. M., Moore, P. H., Sugimura, T., Jiang, J., Schuler, M. A., Friedman, V., Mitchell-Olds, T., Shippen, D. E., dePamphilis, C. W., Palmer, J. D., Freeling, M., Paterson, A. H., Gonsalves, D., Wang, L., and Alam, M. (2008). The draft genome of the transgenic tropical fruit tree papaya (Carica papaya Linnaeus). *Nature*, 452:991–996.

[Mizukami and Fischer, 2000] Mizukami, Y. and Fischer, R. L. (2000). Plant organ size control: AINTEGUMENTA regulates growth and cell numbers during organogenesis. *Proc. Natl. Acad. Sci. U.S.A.*, 97:942–947.

[Mizuta et al., 1997] Mizuta, K., Park, J. S., Sugiyama, M., Nishiyama, M., and Warner, J. R. (1997). RIC1, a novel gene required for ribosome synthesis in Saccharomyces cerevisiae. *Gene*, 187:171–178.

[Mizuta and Warner, 1994] Mizuta, K. and Warner, J. R. (1994). Continued functioning of the secretory pathway is essential for ribosome synthesis. *Mol. Cell. Biol.*, 14:2493–2502.

[Molinier et al., 2006] Molinier, J., Ries, G., Zipfel, C., and Hohn, B. (2006). Transgeneration memory of stress in plants. *Nature*, 442:1046–1049.

[Mossie et al., 1995] Mossie, K., Jallal, B., Alves, F., Sures, I., Plowman, G. D., and Ullrich, A. (1995). Colon carcinoma kinase-4 defines a new subclass of the receptor tyrosine kinase family. *Oncogene*, 11:2179–2184.

[Muller and Sheen, 2007] Muller, B. and Sheen, J. (2007). Arabidopsis cytokinin signaling pathway. *Sci. STKE*, 2007:cm5.

[Muller et al., 2008] Muller, R., Bleckmann, A., and Simon, R. (2008). The receptor kinase CORYNE of Arabidopsis transmits the stem cell-limiting signal CLAVATA3 independently of CLAVATA1. *Plant Cell*, 20:934–946.

[Murashige and Skoog, 1962] Murashige, T. and Skoog, F. (1962). A revised medium for rapid growth and bio assays with tobacco tissue cultures. *Physiologia Plantarum*, 15(3):473–497.

[Murray and Thompson, 1980] Murray, M. G. and Thompson, W. F. (1980). Rapid isolation of high molecular weight plant DNA. *Nucleic Acids Res.*, 8:4321–4325.

[Murzin, 1992] Murzin, A. G. (1992). Structural principles for the propeller assembly of beta-sheets: the preference for seven-fold symmetry. *Proteins*, 14:191–201.

[Narita et al., 2004] Narita, N. N., Moore, S., Horiguchi, G., Kubo, M., Demura, T., Fukuda, H., Goodrich, J., and Tsukaya, H. (2004). Overexpression of a novel small peptide ROTUNDIFOLIA4 decreases cell proliferation and alters leaf shape in Arabidopsis thaliana. *Plant J.*, 38:699–713.

[NASC, 2010] NASC (2010). Crossing Arabidopsis. `http://arabidopsis.info/InfoPages?template=crossing;web_section=arabidopsis`. [Online; accessed 15-November-2010].

[NASC, 2011] NASC (2011). Nottingham Arabidopsis Stock Centre. `http://arabidopsis.info`. [Online; accessed 24-June-2011].

[NCBI, 2011] NCBI (2011). The National Center for Biotechnology Information. `http://www.ncbi.nlm.nih.gov/`. [Online; accessed 24-June-2011].

[Neer et al., 1994] Neer, E. J., Schmidt, C. J., Nambudripad, R., and Smith, T. F. (1994). The ancient regulatory-protein family of WD-repeat proteins. *Nature*, 371:297–300.

[Ni et al., 2011] Ni, J., Guo, Y., Jin, H., Hartsell, J., and Clark, S. E. (2011). Characterization of a CLE processing activity. *Plant Mol. Biol.*, 75:67–75.

[Nishitani and Masuda, 1981] Nishitani, K. and Masuda, Y. (1981). Auxin-induced changes in the cell wall structure: changes in the sugar compositions, intrinsic viscosity and molecular weight distributions of matrix polysaccharides of the epicotyl cell wall of Vigna angularis. *Physiol. Plant.*, 52:482–494.

[Nishiyama et al., 2011] Nishiyama, R., Watanabe, Y., Fujita, Y., Le, D. T., Kojima, M., Werner, T., Vankova, R., Yamaguchi-Shinozaki, K., Shinozaki, K., Kakimoto, T., Sakakibara, H., Schmulling, T., and Tran, L. S. (2011). Analysis of cytokinin mutants and regulation of cytokinin metabolic genes reveals important regulatory roles of cytokinins in drought, salt and abscisic Acid responses, and abscisic Acid biosynthesis. *Plant Cell*, 23:2169–2183.

[Nooden et al., 1979] Nooden, L. D., Kahanak, G. M., and Okatan, Y. (1979). Prevention of monocarpic senescence in soybeans with auxin and cytokinin: an antidote for self-destruction. *Science*, 206:841–843.

[Ogawa et al., 2008] Ogawa, M., Shinohara, H., Sakagami, Y., and Matsubayashi, Y. (2008). Arabidopsis CLV3 peptide directly binds CLV1 ectodomain. *Science*, 319:294.

[Okushima et al., 2005] Okushima, Y., Mitina, I., Quach, H. L., and Theologis, A. (2005). AUXIN RESPONSE FACTOR 2 (ARF2): a pleiotropic developmental regulator. *Plant J.*, 43:29–46.

[Paoli, 2001] Paoli, M. (2001). Protein folds propelled by diversity. *Prog. Biophys. Mol. Biol.*, 76:103–130.

[Park et al., 2004] Park, Y. W., Baba, K., Furuta, Y., Iida, I., Sameshima, K., Arai, M., and Hayashi, T. (2004). Enhancement of growth and cellulose accumulation by overexpression of xyloglucanase in poplar. *FEBS Lett.*, 564:183–187.

[Park et al., 2003] Park, Y. W., Tominaga, R., Sugiyama, J., Furuta, Y., Tanimoto, E., Samejima, M., Sakai, F., and Hayashi, T. (2003). Enhancement of growth by expression of poplar cellulase in Arabidopsis thaliana. *Plant J.*, 33:1099–1106.

[Paterson et al., 2009] Paterson, A. H., Bowers, J. E., Bruggmann, R., Dubchak, I., Grimwood, J., Gundlach, H., Haberer, G., Hellsten, U., Mitros, T., Poliakov, A.,

Schmutz, J., Spannagl, M., Tang, H., Wang, X., Wicker, T., Bharti, A. K., Chapman, J., Feltus, F. A., Gowik, U., Grigoriev, I. V., Lyons, E., Maher, C. A., Martis, M., Narechania, A., Otillar, R. P., Penning, B. W., Salamov, A. A., Wang, Y., Zhang, L., Carpita, N. C., Freeling, M., Gingle, A. R., Hash, C. T., Keller, B., Klein, P., Kresovich, S., McCann, M. C., Ming, R., Peterson, D. G., ur Rahman, M., Ware, D., Westhoff, P., Mayer, K. F., Messing, J., and Rokhsar, D. S. (2009). The Sorghum bicolor genome and the diversification of grasses. *Nature*, 457:551–556.

[Peterhansel and Maurino, 2011] Peterhansel, C. and Maurino, V. G. (2011). Photorespiration redesigned. *Plant Physiol.*, 155:49–55.

[Pettersen et al., 2004] Pettersen, E. F., Goddard, T. D., Huang, C. C., Couch, G. S., Greenblatt, D. M., Meng, E. C., and Ferrin, T. E. (2004). UCSF Chimera–a visualization system for exploratory research and analysis. *J Comput Chem*, 25:1605–1612.

[Pfleger and Kirschner, 2000] Pfleger, C. M. and Kirschner, M. W. (2000). The KEN box: an APC recognition signal distinct from the D box targeted by Cdh1. *Genes Dev.*, 14:655–665.

[Prigent and Gullick, 1994] Prigent, S. A. and Gullick, W. J. (1994). Identification of c-erbB-3 binding sites for phosphatidylinositol 3'-kinase and SHC using an EGF receptor/c-erbB-3 chimera. *EMBO J.*, 13:2831–2841.

[Rattei et al., 2010] Rattei, T., Tischler, P., Gotz, S., Jehl, M. A., Hoser, J., Arnold, R., Conesa, A., and Mewes, H. W. (2010). SIMAP–a comprehensive database of pre-calculated protein sequence similarities, domains, annotations and clusters. *Nucleic Acids Res.*, 38:D223–226.

[Rechsteiner and Rogers, 1996] Rechsteiner, M. and Rogers, S. W. (1996). PEST sequences and regulation by proteolysis. *Trends Biochem. Sci.*, 21:267–271.

[Rensing et al., 2008] Rensing, S. A., Lang, D., Zimmer, A. D., Terry, A., Salamov, A., Shapiro, H., Nishiyama, T., Perroud, P. F., Lindquist, E. A., Kamisugi, Y., Tanahashi, T., Sakakibara, K., Fujita, T., Oishi, K., Shin-I, T., Kuroki, Y., Toyoda, A., Suzuki, Y., Hashimoto, S., Yamaguchi, K., Sugano, S., Kohara, Y., Fujiyama, A., Anterola, A., Aoki, S., Ashton, N., Barbazuk, W. B., Barker, E., Bennetzen, J. L., Blankenship, R., Cho, S. H., Dutcher, S. K., Estelle, M., Fawcett, J. A., Gundlach, H., Hanada, K., Heyl, A., Hicks, K. A., Hughes, J., Lohr, M., Mayer, K., Melkozernov, A., Murata, T., Nelson, D. R., Pils, B., Prigge, M., Reiss, B., Renner, T., Rombauts, S., Rushton, P. J., Sanderfoot, A., Schween, G., Shiu, S. H., Stueber, K., Theodoulou, F. L., Tu, H., Van de Peer, Y., Verrier, P. J., Waters, E., Wood, A., Yang, L., Cove, D., Cuming, A. C., Hasebe, M., Lucas, S., Mishler,

B. D., Reski, R., Grigoriev, I. V., Quatrano, R. S., and Boore, J. L. (2008). The Physcomitrella genome reveals evolutionary insights into the conquest of land by plants. *Science*, 319:64–69.

[Reumann et al., 1994] Reumann, S., Heupel, R., and Heldt, H. (1994). Compartmentation studies on spinach leaf peroxisomes. 2. Evidence for the transfer of reductant from the cytosol to the peroxisomal compartment via a malate shuttle. *Planta*.

[Reumann and Weber, 2006] Reumann, S. and Weber, A. P. (2006). Plant peroxisomes respire in the light: some gaps of the photorespiratory C2 cycle have become filled–others remain. *Biochim. Biophys. Acta*, 1763:1496–1510.

[Rice Genome, 2005] Rice Genome (2005). International Rice Genome Sequencing Project: The map-based sequence of the rice genome. *Nature*, 436:793–800.

[Riethmacher et al., 1997] Riethmacher, D., Sonnenberg-Riethmacher, E., Brinkmann, V., Yamaai, T., Lewin, G. R., and Birchmeier, C. (1997). Severe neuropathies in mice with targeted mutations in the ErbB3 receptor. *Nature*, 389:725–730.

[RIKEN, 2011] RIKEN (2011). Japanese Research Institute. `http://www.riken.jp/engn/index.html`. [Online; accessed 24-June-2011].

[Rocca-Serra et al., 2003] Rocca-Serra, P., Brazma, A., Parkinson, H., Sarkans, U., Shojatalab, M., Contrino, S., Vilo, J., Abeygunawardena, N., Mukherjee, G., Holloway, E., Kapushesky, M., Kemmeren, P., Lara, G. G., Oezcimen, A., and Sansone, S. A. (2003). ArrayExpress: a public database of gene expression data at EBI. *C. R. Biol.*, 326:1075–1078.

[Rogers et al., 1986] Rogers, S., Wells, R., and Rechsteiner, M. (1986). Amino acid sequences common to rapidly degraded proteins: the PEST hypothesis. *Science*, 234:364–368.

[Rusinov et al., 2005] Rusinov, V., Baev, V., Minkov, I. N., and Tabler, M. (2005). MicroInspector: a web tool for detection of miRNA binding sites in an RNA sequence. *Nucleic Acids Res.*, 33:696–700.

[Saibo et al., 2003] Saibo, N. J., Vriezen, W. H., Beemster, G. T., and Van Der Straeten, D. (2003). Growth and stomata development of Arabidopsis hypocotyls are controlled by gibberellins and modulated by ethylene and auxins. *Plant J.*, 33:989–1000.

[Sambrook and Russel, 2001] Sambrook, J. and Russel, D. W. (2001). *Molecular Cloning*, volume 1-3. Cold Spring Harbor Laboratory Press, Cold Spring Harbor, third edition.

[Sargent et al., 2007] Sargent, R. D., Goodwillie, C., Kalisz, S., and Ree, R. H. (2007). Phylogenetic evidence for a flower size and number trade-off. *Am. J. Bot.*, 94:2059–2062.

[Savant-Bhonsale et al., 1999] Savant-Bhonsale, S., Friese, M., McCoon, P., and Montell, D. J. (1999). A Drosophila derailed homolog, doughnut, expressed in invaginating cells during embryogenesis. *Gene*, 231:155–161.

[Scheibe et al., 2005] Scheibe, R., Backhausen, J. E., Emmerlich, V., and Holtgrefe, S. (2005). Strategies to maintain redox homeostasis during photosynthesis under changing conditions. *J. Exp. Bot.*, 56:1481–1489.

[Schiestl and Gietz, 1989] Schiestl, R. H. and Gietz, R. D. (1989). High efficiency transformation of intact yeast cells using single stranded nucleic acids as a carrier. *Curr. Genet.*, 16:339–346.

[Schmid et al., 2005] Schmid, M., Davison, T. S., Henz, S. R., Pape, U. J., Demar, M., Vingron, M., Scholkopf, B., Weigel, D., and Lohmann, J. U. (2005). A gene expression map of Arabidopsis thaliana development. *Nat. Genet.*, 37:501–506.

[Schmutz et al., 2010] Schmutz, J., Cannon, S. B., Schlueter, J., Ma, J., Mitros, T., Nelson, W., Hyten, D. L., Song, Q., Thelen, J. J., Cheng, J., Xu, D., Hellsten, U., May, G. D., Yu, Y., Sakurai, T., Umezawa, T., Bhattacharyya, M. K., Sandhu, D., Valliyodan, B., Lindquist, E., Peto, M., Grant, D., Shu, S., Goodstein, D., Barry, K., Futrell-Griggs, M., Abernathy, B., Du, J., Tian, Z., Zhu, L., Gill, N., Joshi, T., Libault, M., Sethuraman, A., Zhang, X. C., Shinozaki, K., Nguyen, H. T., Wing, R. A., Cregan, P., Specht, J., Grimwood, J., Rokhsar, D., Stacey, G., Shoemaker, R. C., and Jackson, S. A. (2010). Genome sequence of the palaeopolyploid soybean. *Nature*, 463:178–183.

[Schnable et al., 2009] Schnable, P. S., Ware, D., Fulton, R. S., Stein, J. C., Wei, F., Pasternak, S., Liang, C., Zhang, J., Fulton, L., Graves, T. A., Minx, P., Reily, A. D., Courtney, L., Kruchowski, S. S., Tomlinson, C., Strong, C., Delehaunty, K., Fronick, C., Courtney, B., Rock, S. M., Belter, E., Du, F., Kim, K., Abbott, R. M., Cotton, M., Levy, A., Marchetto, P., Ochoa, K., Jackson, S. M., Gillam, B., Chen, W., Yan, L., Higginbotham, J., Cardenas, M., Waligorski, J., Applebaum, E., Phelps, L., Falcone, J., Kanchi, K., Thane, T., Scimone, A., Thane, N., Henke, J., Wang, T., Ruppert, J., Shah, N., Rotter, K., Hodges, J., Ingenthron, E., Cordes,

M., Kohlberg, S., Sgro, J., Delgado, B., Mead, K., Chinwalla, A., Leonard, S., Crouse, K., Collura, K., Kudrna, D., Currie, J., He, R., Angelova, A., Rajasekar, S., Mueller, T., Lomeli, R., Scara, G., Ko, A., Delaney, K., Wissotski, M., Lopez, G., Campos, D., Braidotti, M., Ashley, E., Golser, W., Kim, H., Lee, S., Lin, J., Dujmic, Z., Kim, W., Talag, J., Zuccolo, A., Fan, C., Sebastian, A., Kramer, M., Spiegel, L., Nascimento, L., Zutavern, T., Miller, B., Ambroise, C., Muller, S., Spooner, W., Narechania, A., Ren, L., Wei, S., Kumari, S., Faga, B., Levy, M. J., McMahan, L., Van Buren, P., Vaughn, M. W., Ying, K., Yeh, C. T., Emrich, S. J., Jia, Y., Kalyanaraman, A., Hsia, A. P., Barbazuk, W. B., Baucom, R. S., Brutnell, T. P., Carpita, N. C., Chaparro, C., Chia, J. M., Deragon, J. M., Estill, J. C., Fu, Y., Jeddeloh, J. A., Han, Y., Lee, H., Li, P., Lisch, D. R., Liu, S., Liu, Z., Nagel, D. H., McCann, M. C., SanMiguel, P., Myers, A. M., Nettleton, D., Nguyen, J., Penning, B. W., Ponnala, L., Schneider, K. L., Schwartz, D. C., Sharma, A., Soderlund, C., Springer, N. M., Sun, Q., Wang, H., Waterman, M., Westerman, R., Wolfgruber, T. K., Yang, L., Yu, Y., Zhang, L., Zhou, S., Zhu, Q., Bennetzen, J. L., Dawe, R. K., Jiang, J., Jiang, N., Presting, G. G., Wessler, S. R., Aluru, S., Martienssen, R. A., Clifton, S. W., McCombie, W. R., Wing, R. A., and Wilson, R. K. (2009). The B73 maize genome: complexity, diversity, and dynamics. *Science*, 326:1112–1115.

[Schneitz et al., 1997] Schneitz, K., Hulskamp, M., Kopczak, S. D., and Pruitt, R. E. (1997). Dissection of sexual organ ontogenesis: a genetic analysis of ovule development in Arabidopsis thaliana. *Development*, 124:1367–1376.

[Scholl et al., 2000] Scholl, R. L., May, S. T., and Ware, D. H. (2000). Seed and molecular resources for Arabidopsis. *Plant Physiol.*, 124:1477–1480.

[Schoof et al., 2000] Schoof, H., Lenhard, M., Haecker, A., Mayer, K. F., Jurgens, G., and Laux, T. (2000). The stem cell population of Arabidopsis shoot meristems in maintained by a regulatory loop between the CLAVATA and WUSCHEL genes. *Cell*, 100:635–644.

[Schoof et al., 2002] Schoof, H., Zaccaria, P., Gundlach, H., Lemcke, K., Rudd, S., Kolesov, G., Arnold, R., Mewes, H. W., and Mayer, K. F. (2002). MIPS Arabidopsis thaliana Database (MAtDB): an integrated biological knowledge resource based on the first complete plant genome. *Nucleic Acids Res.*, 30:91–93.

[Schruff et al., 2006] Schruff, M. C., Spielman, M., Tiwari, S., Adams, S., Fenby, N., and Scott, R. J. (2006). The AUXIN RESPONSE FACTOR 2 gene of Arabidopsis links auxin signalling, cell division, and the size of seeds and other organs. *Development*, 133:251–261.

[Schwede et al., 2003] Schwede, T., Kopp, J., Guex, N., and Peitsch, M. C. (2003). SWISS-MODEL: An automated protein homology-modeling server. *Nucleic Acids Res.*, 31:3381–3385.

[Scrima et al., 2008] Scrima, A., Konickova, R., Czyzewski, B. K., Kawasaki, Y., Jeffrey, P. D., Groisman, R., Nakatani, Y., Iwai, S., Pavletich, N. P., and Thoma, N. H. (2008). Structural basis of UV DNA-damage recognition by the DDB1-DDB2 complex. *Cell*, 135:1213–1223.

[Shani et al., 2004] Shani, Z., Dekel, M., Tzbary, G., Goren, R., and Shoseyov, O. (2004). Growth enhancement of transgenic poplar plants by overexpression of Arabidopsis thaliana endo-1,4-β-glucanase (cel1). *Mol. Breed*, 14:321–330.

[Shiu and Bleecker, 2001] Shiu, S. H. and Bleecker, A. B. (2001). Receptor-like kinases from Arabidopsis form a monophyletic gene family related to animal receptor kinases. *Proc. Natl. Acad. Sci. U.S.A.*, 98:10763–10768.

[Shiu et al., 2004] Shiu, S. H., Karlowski, W. M., Pan, R., Tzeng, Y. H., Mayer, K. F., and Li, W. H. (2004). Comparative analysis of the receptor-like kinase family in Arabidopsis and rice. *Plant Cell*, 16:1220–1234.

[Sierke et al., 1997] Sierke, S. L., Cheng, K., Kim, H. H., and Koland, J. G. (1997). Biochemical characterization of the protein tyrosine kinase homology domain of the ErbB3 (HER3) receptor protein. *Biochem. J.*, 322 (Pt 3):757–763.

[Siniossoglou et al., 2000] Siniossoglou, S., Peak-Chew, S. Y., and Pelham, H. R. (2000). Ric1p and Rgp1p form a complex that catalyses nucleotide exchange on Ypt6p. *EMBO J.*, 19:4885–4894.

[Siniossoglou and Pelham, 2001] Siniossoglou, S. and Pelham, H. R. (2001). An effector of Ypt6p binds the SNARE Tlg1p and mediates selective fusion of vesicles with late Golgi membranes. *EMBO J.*, 20:5991–5998.

[Smith et al., 1999] Smith, T. F., Gaitatzes, C., Saxena, K., and Neer, E. J. (1999). The WD repeat: a common architecture for diverse functions. *Trends Biochem. Sci.*, 24:181–185.

[Somerville et al., 2004] Somerville, C., Bauer, S., Brininstool, G., Facette, M., Hamann, T., Milne, J., Osborne, E., Paredez, A., Persson, S., Raab, T., Vorwerk, S., and Youngs, H. (2004). Toward a systems approach to understanding plant cell walls. *Science*, 306:2206–2211.

[Sondek et al., 1996] Sondek, J., Bohm, A., Lambright, D. G., Hamm, H. E., and Sigler, P. B. (1996). Crystal structure of a G-protein beta gamma dimer at 2.1A resolution. *Nature*, 379:369–374.

[Song and Clark, 2005] Song, S. K. and Clark, S. E. (2005). POL and related phosphatases are dosage-sensitive regulators of meristem and organ development in Arabidopsis. *Dev. Biol.*, 285:272–284.

[Song et al., 2006] Song, S. K., Lee, M. M., and Clark, S. E. (2006). POL and PLL1 phosphatases are CLAVATA1 signaling intermediates required for Arabidopsis shoot and floral stem cells. *Development*, 133:4691–4698.

[Song et al., 1995] Song, W. Y., Wang, G. L., Chen, L. L., Kim, H. S., Pi, L. Y., Holsten, T., Gardner, J., Wang, B., Zhai, W. X., Zhu, L. H., Fauquet, C., and Ronald, P. (1995). A receptor kinase-like protein encoded by the rice disease resistance gene, Xa21. *Science*, 270:1804–1806.

[Soulard et al., 2009] Soulard, A., Cohen, A., and Hall, M. N. (2009). TOR signaling in invertebrates. *Curr. Opin. Cell Biol.*, 21:825–836.

[Squatrito et al., 2006] Squatrito, M., Mancino, M., Sala, L., and Draetta, G. F. (2006). Ebp1 is a dsRNA-binding protein associated with ribosomes that modulates eIF2alpha phosphorylation. *Biochem. Biophys. Res. Commun.*, 344:859–868.

[Stamatakis, 2006] Stamatakis, A. (2006). RAxML-VI-HPC: maximum likelihood-based phylogenetic analyses with thousands of taxa and mixed models. *Bioinformatics*, 22:2688–2690.

[Stein and Staros, 2000] Stein, R. A. and Staros, J. V. (2000). Evolutionary analysis of the ErbB receptor and ligand families. *J. Mol. Evol.*, 50:397–412.

[Stirnimann et al., 2010] Stirnimann, C. U., Petsalaki, E., Russell, R. B., and Muller, C. W. (2010). WD40 proteins propel cellular networks. *Trends Biochem. Sci.*, 35:565–574.

[Studier and Moffatt, 1986] Studier, F. and Moffatt, B. (1986). T7 RNA polymerase to direct selective high-level expression of cloned genes. *J Mol Biol.*, 189(1):113130. .

[Suganuma et al., 2008] Suganuma, T., Pattenden, S. G., and Workman, J. L. (2008). Diverse functions of WD40 repeat proteins in histone recognition. *Genes Dev.*, 22:1265–1268.

[Swarbreck et al., 2008] Swarbreck, D., Wilks, C., Lamesch, P., Berardini, T. Z., Garcia-Hernandez, M., Foerster, H., Li, D., Meyer, T., Muller, R., Ploetz, L., Radenbaugh, A., Singh, S., Swing, V., Tissier, C., Zhang, P., and Huala, E. (2008). The Arabidopsis Information Resource (TAIR): gene structure and function annotation. *Nucleic Acids Res.*, 36:D1009–1014.

[Takeda et al., 2002] Takeda, T., Furuta, Y., Awano, T., Mizuno, K., Mitsuishi, Y., and Hayashi, T. (2002). Suppression and acceleration of cell elongation by integration of xyloglucans in pea stem segments. *Proc. Natl. Acad. Sci. U.S.A.*, 99:9055–9060.

[Talbott and Ray, 1992] Talbott, L. D. and Ray, P. M. (1992). Molecular size and separability features of pea cell wall polysaccharides. Implications for models of primary wall structure. *Plant Physiol.*, 92:357–368.

[Tang et al., 2008] Tang, W., Kim, T. W., Oses-Prieto, J. A., Sun, Y., Deng, Z., Zhu, S., Wang, R., Burlingame, A. L., and Wang, Z. Y. (2008). BSKs mediate signal transduction from the receptor kinase BRI1 in Arabidopsis. *Science*, 321:557–560.

[Tcherkez et al., 2006] Tcherkez, G. G., Farquhar, G. D., and Andrews, T. J. (2006). Despite slow catalysis and confused substrate specificity, all ribulose bisphosphate carboxylases may be nearly perfectly optimized. *Proc. Natl. Acad. Sci. U.S.A.*, 103:7246–7251.

[Thompson et al., 1994] Thompson, J. D., Higgins, D. G., and Gibson, T. J. (1994). CLUSTAL W: improving the sensitivity of progressive multiple sequence alignment through sequence weighting, position-specific gap penalties and weight matrix choice. *Nucleic Acids Res.*, 22:4673–4680.

[Timm et al., 2011] Timm, S., Florian, A., Jahnke, K., Nunes-Nesi, A., Fernie, A. R., and Bauwe, H. (2011). The hydroxypyruvate-reducing system in Arabidopsis: multiple enzymes for the same end. *Plant Physiol.*, 155:694–705.

[Timm et al., 2008] Timm, S., Nunes-Nesi, A., Parnik, T., Morgenthal, K., Wienkoop, S., Keerberg, O., Weckwerth, W., Kleczkowski, L. A., Fernie, A. R., and Bauwe, H. (2008). A cytosolic pathway for the conversion of hydroxypyruvate to glycerate during photorespiration in Arabidopsis. *Plant Cell*, 20:2848–2859.

[Tomato Genome, 2011] Tomato Genome (2011). The International Tomato Genome Sequencing Consortium. `http://solgenomics.net/organism/Solanum_lycopersicum/genome`. [Online; accessed 22-November-2011].

[Trotochaud et al., 2000] Trotochaud, A. E., Jeong, S., and Clark, S. E. (2000). CLAVATA3, a multimeric ligand for the CLAVATA1 receptor-kinase. *Science*, 289:613–617.

[Tsukaya, 2005] Tsukaya, H. (2005). Leaf shape: genetic controls and environmental factors. *Int. J. Dev. Biol.*, 49:547–555.

[Tsukaya, 2006] Tsukaya, H. (2006). Mechanism of leaf-shape determination. *Annu Rev Plant Biol*, 57:477–496.

[Vaddepalli et al., 2011] Vaddepalli, P., Fulton, L., Batoux, M., Yadav, R. K., and Schneitz, K. (2011). Structure-function analysis of STRUBBELIG, an Arabidopsis atypical receptor-like kinase involved in tissue morphogenesis. *PLoS ONE*, 6:e19730.

[Vincken et al., 2003] Vincken, J. P., Schols, H. A., Oomen, R. J., McCann, M. C., Ulvskov, P., Voragen, A. G., and Visser, R. G. (2003). If homogalacturonan were a side chain of rhamnogalacturonan I. Implications for cell wall architecture. *Plant Physiol.*, 132:1781–1789.

[Vogel et al., 2010] Vogel, J. P., Garvin, D. F., Mockler, T. C., Schmutz, J., Rokhsar, D., Bevan, M. W., Barry, K., Lucas, S., Harmon-Smith, M., Lail, K., Tice, H., Schmutz, J., Grimwood, J., McKenzie, N., Bevan, M. W., Huo, N., Gu, Y. Q., Lazo, G. R., Anderson, O. D., Vogel, J. P., You, F. M., Luo, M. C., Dvorak, J., Wright, J., Febrer, M., Bevan, M. W., Idziak, D., Hasterok, R., Garvin, D. F., Lindquist, E., Wang, M., Fox, S. E., Priest, H. D., Filichkin, S. A., Givan, S. A., Bryant, D. W., Chang, J. H., Mockler, T. C., Wu, H., Wu, W., Hsia, A. P., Schnable, P. S., Kalyanaraman, A., Barbazuk, B., Michael, T. P., Hazen, S. P., Bragg, J. N., Laudencia-Chingcuanco, D., Vogel, J. P., Garvin, D. F., Weng, Y., McKenzie, N., Bevan, M. W., Haberer, G., Spannagl, M., Mayer, K., Rattei, T., Mitros, T., Rokhsar, D., Lee, S. J., Rose, J. K., Mueller, L. A., York, T. L., Wicker, T., Buchmann, J. P., Tanskanen, J., Schulman, A. H., Gundlach, H., Wright, J., Bevan, M., de Oliveira, A. C., Maia, L. d. a. C., Belknap, W., Gu, Y. Q., Jiang, N., Lai, J., Zhu, L., Ma, J., Sun, C., Pritham, E., Salse, J., Murat, F., Abrouk, M., Haberer, G., Spannagl, M., Mayer, K., Bruggmann, R., Messing, J., You, F. M., Luo, M. C., Dvorak, J., Fahlgren, N., Fox, S. E., Sullivan, C. M., Mockler, T. C., Carrington, J. C., Chapman, E. J., May, G. D., Zhai, J., Ganssmann, M., Gurazada, S. G., German, M., Meyers, B. C., Green, P. J., Bragg, J. N., Tyler, L., Wu, J., Gu, Y. Q., Lazo, G. R., Laudencia-Chingcuanco, D., Thomson, J., Vogel, J. P., Hazen, S. P., Chen, S., Scheller, H. V., Harholt, J., Ulvskov, P., Fox, S. E., Filichkin, S. A., Fahlgren, N., Kimbrel, J. A., Chang, J. H., Sullivan, C. M., Chapman, E. J., Carrington,

J. C., Mockler, T. C., Bartley, L. E., Cao, P., Jung, K. H., Sharma, M. K., Vega-Sanchez, M., Ronald, P., Dardick, C. D., De Bodt, S., Verelst, W., Inze, D., Heese, M., Schnittger, A., Yang, X., Kalluri, U. C., Tuskan, G. A., Hua, Z., Vierstra, R. D., Garvin, D. F., Cui, Y., Ouyang, S., Sun, Q., Liu, Z., Yilmaz, A., Grotewold, E., Sibout, R., Hematy, K., Mouille, G., Hofte, H., Michael, T., Pelloux, J., O'Connor, D., Schnable, J., Rowe, S., Harmon, F., Cass, C. L., Sedbrook, J. C., Byrne, M. E., Walsh, S., Higgins, J., Bevan, M., Li, P., Brutnell, T., Unver, T., Budak, H., Belcram, H., Charles, M., Chalhoub, B., and Baxter, I. (2010). Genome sequencing and analysis of the model grass Brachypodium distachyon. *Nature*, 463:763–768.

[Walker and Zhang, 1990] Walker, J. C. and Zhang, R. (1990). Relationship of a putative receptor protein kinase from maize to the S-locus glycoproteins of Brassica. *Nature*, 345:743–746.

[Wall et al., 1995] Wall, M. A., Coleman, D. E., Lee, E., Iniguez-Lluhi, J. A., Posner, B. A., Gilman, A. G., and Sprang, S. R. (1995). The structure of the G protein heterotrimer Gi alpha 1 beta 1 gamma 2. *Cell*, 83:1047–1058.

[Walter et al., 2004] Walter, M., Chaban, C., Schutze, K., Batistic, O., Weckermann, K., Nake, C., Blazevic, D., Grefen, C., Schumacher, K., Oecking, C., Harter, K., and Kudla, J. (2004). Visualization of protein interactions in living plant cells using bimolecular fluorescence complementation. *Plant J.*, 40:428–438.

[WALZ, 2011] WALZ (2011). WALZ Mess- und Regeltechnik PAM-2000 user manual. `http://www.walz.com/products/chl_p700/pam-2500/downloads.html`. [Online; accessed 1-June-2011].

[Wang et al., 2008] Wang, J. W., Schwab, R., Czech, B., Mica, E., and Weigel, D. (2008). Dual effects of miR156-targeted SPL genes and CYP78A5/KLUH on plastochron length and organ size in Arabidopsis thaliana. *Plant Cell*, 20:1231–1243.

[Wang et al., 2003] Wang, N., Chen, W., Linsel-Nitschke, P., Martinez, L. O., Agerholm-Larsen, B., Silver, D. L., and Tall, A. R. (2003). A PEST sequence in ABCA1 regulates degradation by calpain protease and stabilization of ABCA1 by apoA-I. *J. Clin. Invest.*, 111:99–107.

[Wang and Chory, 2006] Wang, X. and Chory, J. (2006). Brassinosteroids regulate dissociation of BKI1, a negative regulator of BRI1 signaling, from the plasma membrane. *Science*, 313:1118–1122.

[Wang et al., 2005] Wang, X., Li, X., Meisenhelder, J., Hunter, T., Yoshida, S., Asami, T., and Chory, J. (2005). Autoregulation and homodimerization are involved in the activation of the plant steroid receptor BRI1. *Dev. Cell*, 8:855–865.

[Wang et al., 2011] Wang, X., Wang, H., Wang, J., Sun, R., Wu, J., Liu, S., Bai, Y., Mun, J. H., Bancroft, I., Cheng, F., Huang, S., Li, X., Hua, W., Wang, J., Wang, X., Freeling, M., Pires, J. C., Paterson, A. H., Chalhoub, B., Wang, B., Hayward, A., Sharpe, A. G., Park, B. S., Weisshaar, B., Liu, B., Li, B., Liu, B., Tong, C., Song, C., Duran, C., Peng, C., Geng, C., Koh, C., Lin, C., Edwards, D., Mu, D., Shen, D., Soumpourou, E., Li, F., Fraser, F., Conant, G., Lassalle, G., King, G. J., Bonnema, G., Tang, H., Wang, H., Belcram, H., Zhou, H., Hirakawa, H., Abe, H., Guo, H., Wang, H., Jin, H., Parkin, I. A., Batley, J., Kim, J. S., Just, J., Li, J., Xu, J., Deng, J., Kim, J. A., Li, J., Yu, J., Meng, J., Wang, J., Min, J., Poulain, J., Wang, J., Hatakeyama, K., Wu, K., Wang, L., Fang, L., Trick, M., Links, M. G., Zhao, M., Jin, M., Ramchiary, N., Drou, N., Berkman, P. J., Cai, Q., Huang, Q., Li, R., Tabata, S., Cheng, S., Zhang, S., Zhang, S., Huang, S., Sato, S., Sun, S., Kwon, S. J., Choi, S. R., Lee, T. H., Fan, W., Zhao, X., Tan, X., Xu, X., Wang, Y., Qiu, Y., Yin, Y., Li, Y., Du, Y., Liao, Y., Lim, Y., Narusaka, Y., Wang, Y., Wang, Z., Li, Z., Wang, Z., Xiong, Z., Zhang, Z., Wang, X., Wang, H., Wang, J., Sun, R., Wu, J., Liu, S., Bai, Y., Mun, J. H., Bancroft, I., Cheng, F., Huang, S., Li, X., Hua, W., Wang, J., Wang, X., Freeling, M., Chris Pires, J., Paterson, A. H., Chalhoub, B., Wang, B., Hayward, A., Sharpe, A. G., Park, B. S., Weisshaar, B., Liu, B., Li, B., Liu, B., Tong, C., Song, C., Duran, C., Peng, C., Geng, C., Koh, C., Lin, C., Edwards, D., Mu, D., Shen, D., Soumpourou, E., Li, F., Fraser, F., Conant, G., Lassalle, G., King, G. J., Bonnema, G., Tang, H., Wang, H., Belcram, H., Zhou, H., Hirakawa, H., Abe, H., Guo, H., Wang, H., Jin, H., Parkin, I. A., Batley, J., Kim, J. S., Just, J., Li, J., Xu, J., Deng, J., Kim, J. A., Li, J., Yu, J., Meng, J., Wang, J., Min, J., Poulain, J., Wang, J., Hatakeyama, K., Wu, K., Wang, L., Fang, L., Trick, M., Links, M. G., Zhao, M., Jin, M., Ramchiary, N., Drou, N., Berkman, P. J., Cai, Q., Huang, Q., Li, R., Tabata, S., Cheng, S., Zhang, S., Zhang, S., Huang, S., Sato, S., Sun, S., Kwon, S. J., Choi, S. R., Lee, T. H., Fan, W., Zhao, X., Tan, X., Xu, X., Wang, Y., Qiu, Y., Yin, Y., Li, Y., Du, Y., Liao, Y., Lim, Y., Narusaka, Y., Wang, Y., Wang, Z., Li, Z., Wang, Z., Xiong, Z., and Zhang, Z. (2011). The genome of the mesopolyploid crop species Brassica rapa. *Nat. Genet.*, 43:1035–1039.

[Willats et al., 2001] Willats, W. G., McCartney, L., Mackie, W., and Knox, J. P. (2001). Pectin: cell biology and prospects for functional analysis. *Plant Mol. Biol.*, 47:9–27.

[Xu and Min, 2011] Xu, C. and Min, J. (2011). Structure and function of WD40 domain proteins. *Protein Cell*, 2:202–214.

[Yadav et al., 2008] Yadav, R. K., Fulton, L., Batoux, M., and Schneitz, K. (2008). The Arabidopsis receptor-like kinase STRUBBELIG mediates inter-cell-layer sig-

naling during floral development. *Dev. Biol.*, 323:261–270.

[Yin et al., 2002] Yin, Y., Wang, Z. Y., Mora-Garcia, S., Li, J., Yoshida, S., Asami, T., and Chory, J. (2002). BES1 accumulates in the nucleus in response to brassinosteroids to regulate gene expression and promote stem elongation. *Cell*, 109:181–191.

[Yokoyama et al., 2007] Yokoyama, A., Yamashino, T., Amano, Y., Tajima, Y., Imamura, A., Sakakibara, H., and Mizuno, T. (2007). Type-B ARR transcription factors, ARR10 and ARR12, are implicated in cytokinin-mediated regulation of protoxylem differentiation in roots of Arabidopsis thaliana. *Plant Cell Physiol.*, 48:84–96.

[Yoo et al., 2007] Yoo, S. D., Cho, Y. H., and Sheen, J. (2007). Arabidopsis mesophyll protoplasts: a versatile cell system for transient gene expression analysis. *Nat Protoc*, 2:1565–1572.

[Young et al., 2011] Young, N. D., Debelle, F., Oldroyd, G. E., Geurts, R., Cannon, S. B., Udvardi, M. K., Benedito, V. A., Mayer, K. F., Gouzy, J., Schoof, H., Van de Peer, Y., Proost, S., Cook, D. R., Meyers, B. C., Spannagl, M., Cheung, F., De Mita, S., Krishnakumar, V., Gundlach, H., Zhou, S., Mudge, J., Bharti, A. K., Murray, J. D., Naoumkina, M. A., Rosen, B., Silverstein, K. A., Tang, H., Rombauts, S., Zhao, P. X., Zhou, P., Barbe, V., Bardou, P., Bechner, M., Bellec, A., Berger, A., Berges, H., Bidwell, S., Bisseling, T., Choisne, N., Couloux, A., Denny, R., Deshpande, S., Dai, X., Doyle, J. J., Dudez, A. M., Farmer, A. D., Fouteau, S., Franken, C., Gibelin, C., Gish, J., Goldstein, S., Gonzalez, A. J., Green, P. J., Hallab, A., Hartog, M., Hua, A., Humphray, S. J., Jeong, D. H., Jing, Y., Jocker, A., Kenton, S. M., Kim, D. J., Klee, K., Lai, H., Lang, C., Lin, S., Macmil, S. L., Magdelenat, G., Matthews, L., McCorrison, J., Monaghan, E. L., Mun, J. H., Najar, F. Z., Nicholson, C., Noirot, C., O'Bleness, M., Paule, C. R., Poulain, J., Prion, F., Qin, B., Qu, C., Retzel, E. F., Riddle, C., Sallet, E., Samain, S., Samson, N., Sanders, I., Saurat, O., Scarpelli, C., Schiex, T., Segurens, B., Severin, A. J., Sherrier, D. J., Shi, R., Sims, S., Singer, S. R., Sinharoy, S., Sterck, L., Viollet, A., Wang, B. B., Wang, K., Wang, M., Wang, X., Warfsmann, J., Weissenbach, J., White, D. D., White, J. D., Wiley, G. B., Wincker, P., Xing, Y., Yang, L., Yao, Z., Ying, F., Zhai, J., Zhou, L., Zuber, A., Denarie, J., Dixon, R. A., May, G. D., Schwartz, D. C., Rogers, J., Quetier, F., Town, C. D., and Roe, B. A. (2011). The Medicago genome provides insight into the evolution of rhizobial symbioses. *Nature*.

[Yu et al., 2003] Yu, L. P., Miller, A. K., and Clark, S. E. (2003). POLTERGEIST encodes a protein phosphatase 2C that regulates CLAVATA pathways controlling

stem cell identity at Arabidopsis shoot and flower meristems. *Curr. Biol.*, 13:179–188.

[Zabotina et al., 2008] Zabotina, O. A., van de Ven, W. T., Freshour, G., Drakakaki, G., Cavalier, D., Mouille, G., Hahn, M. G., Keegstra, K., and Raikhel, N. V. (2008). Arabidopsis XXT5 gene encodes a putative alpha-1,6-xylosyltransferase that is involved in xyloglucan biosynthesis. *Plant J.*, 56:101–115.

[Zelitch, 1992] Zelitch, I. (1992). Control of plant productivity by regulation of photorespiration. *Bioscience*, 42:510–516.

[Zelitch et al., 2009] Zelitch, I., Schultes, N. P., Peterson, R. B., Brown, P., and Brutnell, T. P. (2009). High glycolate oxidase activity is required for survival of maize in normal air. *Plant Physiol.*, 149:195–204.

[Zhang and Gaut, 2003] Zhang, L. and Gaut, B. S. (2003). Does recombination shape the distribution and evolution of tandemly arrayed genes (TAGs) in the Arabidopsis thaliana genome? *Genome Res.*, 13:2533–2540.

[Zhang et al., 2005] Zhang, Y., Akinmade, D., and Hamburger, A. W. (2005). The ErbB3 binding protein Ebp1 interacts with Sin3A to repress E2F1 and AR-mediated transcription. *Nucleic Acids Res.*, 33:6024–6033.

[Zhao et al., 2002] Zhao, J., Peng, P., Schmitz, R. J., Decker, A. D., Tax, F. E., and Li, J. (2002). Two putative BIN2 substrates are nuclear components of brassinosteroid signaling. *Plant Physiol.*, 130:1221–1229.

[Zhu et al., 2010] Zhu, Y., Wang, Y., Li, R., Song, X., Wang, Q., Huang, S., Jin, J. B., Liu, C. M., and Lin, J. (2010). Analysis of interactions among the CLAVATA3 receptors reveals a direct interaction between CLAVATA2 and CORYNE in Arabidopsis. *Plant J.*, 61:223–233.

[Zipfel et al., 2006] Zipfel, C., Kunze, G., Chinchilla, D., Caniard, A., Jones, J. D., Boller, T., and Felix, G. (2006). Perception of the bacterial PAMP EF-Tu by the receptor EFR restricts Agrobacterium-mediated transformation. *Cell*, 125:749–760.

List of Figures

List of Tables

Danksagung

Zuallererst muss ich Prof. Dr. Kay Schneitz für die Möglichkeit in seinem Labor zu promovieren danken. Es ist nicht selbstverständlich, als Bioinformatiker, die Chance zu bekommen ein Labor zu erkunden. Durch diese Erfahrung habe ich viele Dinge gelernt, die mir sicherlich mein Leben lang im Gedächtnis bleiben und mir in schwierigen Situationen weiterhelfen werden. Mir wurde das benötigte Vertrauen entgegen gebracht um unabhängig und eigenverantwortlich zu arbeiten. Dadurch habe ich die Grundlagen wissenschaftlicher Forschung erlernt.

Mein zweiter Dank geht an Dr. Banu Eyueboglu, die sich mit dem unerfahrenen Computer-Mädchen, das noch nicht einmal wusste wie man eine Pipette richtig hält, herumschlagen musste. Deine Geduld war unglaublich und ich kann Dir nicht oft genug dafür danken, dass Du Dein Wissen bezüglich der Molekularbiologie und Pflanzenarbeit mit mir geteilt hast. Du hast mich nie für dumm abgestempelt, auch wenn ich es vielleicht war.

Vielen Dank auch an Colin Ruprecht aus der Pflanzen Zellwand Gruppe von Staffan Persson am MPI für molekulare Pflanzen Physiologie in Golm. Alle Zellwand Experimente der SRF4, DLG und WIZ Mutanten wurden von ihm ausgeführt. Danke für die Zeit, Ratschläge und neue Ideen.

Ich möchte auch den Leuten, mit denen ich im Laufe der Zeit zusammenarbeiten durfte, danken. Martine Batoux und Ram Yadav die mich am Anfang meiner Promotion unterstützt haben, Carina Müller für all den Spaß den wir hatten, Balaji Enugutti und Prasad Vaddepalli die mir halfen wenn mein biologischen Wissen nicht ausreichte und für den ein oder anderen Rat, Eva Herold für die harte Arbeit die sie in dieses Projekt gesteckt hat, Pamela Korte für die Organisation im Labor und Hong Dengfeng und so mancherlei Studenten die mich durch ihre erfrischende Art neu motiviert haben. Mein größter Dank geht in diesem Kontext an Maxi Oelschner die mein Leben um so Vieles leichter machte nachdem sie im Labor anfing. Sie kümmerte sich um die Bestellungen, das Autoklavieren, Schädlingsbekämpfung und allerlei anderes organisatorisches Zeug und hatte trotzdem immer noch eine helfende Hand frei wenn diese gebraucht wurde. Für mich warst und bist Du unbezahlbar!

Des weiteren schulde ich Caroline Klaus meinen ausdrücklichen Dank für Ihre Anleitung bezüglich Pflanzenpflege, Schädlingsbekämpfung und die amüsanten Unterhaltungen während des Erntens. Josef Reischenbeck half mir immer wenn verschiedenste Dinge kaputt waren oder etwas neu aufgebaut werden musste. Danke dafür! Ich möchte auch gerne Beate Seeliger für die Bewältigung der Bürokratie danken und allen anderen Menschen im Grill- und Schwechheimer-

Labor die mir mit ihrem Rat, ihrer Geduld und erfrischenden Pausen geholfen haben.

Vielen Dank an das Gietl Labor, die unsere neuen Nachbarn wurden, nachdem Prof. Dr. Höll in Ruhestand ging. Durch Prof. Dr. Gietls Einsatz wurde eine Gel Doc, eine große Zentrifuge und ein nano drop Photometer auf unserem Gang angeschafft, welche unser Leben enorm erleichtert haben. Auch Dr. Georg Hierl und Dr. Esther Dolze danke ich für ihre Hilfe in allen wissenschaftlichen Fragen und natürlich für Elvis!

Mein spezieller Dank geht an meine Mittags-Truppe, die zumindest im letzten Jahr meine Pausen mit mir verbracht haben: Sophie Brameyer, Charlotte Kirchhelle, Esther Dolze und Maxi Oelschner. Danke für die unterhaltsame Zeit, die guten Ratschläge, fürs Zuhören und die aufbauenden Worte. Esther und Maxi erwähne ich nicht ohne guten Grund zweimal: in der Zeit waren sie nicht nur Kollegen sondern auch gute Freunde für mich. Menschen wie sie gibt es wenige und ich bin stolz, dass sie ihre Zeit mit mir verbringen wollten.

Ich möchte auch meinen Geschwistern Christoph Skornia und Birgit Holzner danken. Sie haben mich immer inspiriert und mir gezeigt was wirklich wichtig ist im Leben. Sie und ihre Familien zerstreuten meine Gedanken wenn es nötig war. Außerdem möchte ich noch Christian und Franziska Spannagl dafür danken, dass ich mich bei ihnen wie zu Hause fühlen durfte, wenn meine Familie nicht in der Nähe war.

Der Mensch der mich in dieser ganzen Zeit am meisten unterstützt hat, ist zweifelsohne Manuel Spannagl. Manuel, Deine Hingabe ist unglaublich und Deine Unterstützung grenzenlos. Du hast mit mir meine Sorgen und Freude, meine Verzweiflung und Begeisterung geteilt. Durch Deine unendliche Liebe konnte ich über mich hinaus wachsen. Du bringst mich jeden Tag zum lächeln und ich bin so glücklich Dich gefunden zu haben.

Mein letzter, aber wichtigster, Dank geht an meine Eltern. Ihr unbezahlbarer Einsatz und ihre harte Arbeit, eröffneten mir alle Möglichkeiten, um es bis hierher zu schaffen. Ich konnte immer auf sie zählen und sie unterstützten mich auf jede erdenkliche Art und Weise. Danke Mama und Papa, ich weiß es ist nicht selbstverständlich solche Eltern zu haben.